SOFIA Observer's Handbook for Cycle 4

Change Log

- October 19, 2015 - v4.2.0.
  - Section 4.2.3 - Clarified discussion of EXES overheads
  - Section 7.1.4 - Added a table of updated FORCAST imaging sensitivities.
  - Figure 7-4 - Updated the plot of FORCAST sensitivities.
  - Figure 10-1 - Updated the table of HAWC+ instrument characteristics to reflect the newest performance measurements
  - Section 9.1 - Added discussion of upGREAT and GREAT configurations for Cycle 4
  - Section 7.1.6 - Clarified discussion of FORCAST spectroscopic sensitivities
  - Section 7.1.6 - Updated chop angle and amplitude restrictions for asymmetric modes

- June 29, 2015 - v4.1.4.
  - Table 10.1 SPT replaces SITE.
  - Section 10.1.5 SPT replaces SITE.

- June 16, 2015 - v4.1.3.
  - Section 7.1.6 Outdated description of extended source exposure time calculation removed.

- June 4, 2015 - v4.1.2.
  - Section 4.2.2 Description of exposure time calculation for EXES telluric calibrators added.

- June 1, 2015 - v4.1.1.
  - Section 7.1.3 - FORCAST - Links to ASCII tables of FORCAST filter transmission curves added.
  - Section 10.1.2 - HAWC+ - Links to ASCII tables of HAWC+ filter transmission curves added.

- May 13, 2015 - v4.1.0.
  - Section 5.2.2 - FIFI-LS - Updated the link to the FIFI-LS on-line exposure time estimator.
  - Section 7 - FORCAST - Included notes throughout reminding users that the FORCAST XD modes will not be available during Cycle 4.

- May 5, 2015 - v4.0.2.
  - Section 10 - HAWC+ - Corrected a number of minor typographical and formatting issues.

- May 4, 2015 - v4.0.1.
  - Table 6-2 - FLITECAM - Updated with corrected Coverage values.

- May 1, 2015 - v4.0.0
  - Cycle 4 Observer's Handbook v4.0.0 released

1. Introduction

1. Introduction

The Stratospheric Observatory for Infrared Astronomy (SOFIA) is a telescope with an effective diameter of 2.5 meters, carried aboard a Boeing 747-SP aircraft. It is the successor to the smaller Kuiper Airborne Observatory, which was operated by NASA from 1974 to 1996. The observing altitudes for SOFIA are between 37,000 and 45,000 feet, above 99% of the water vapor in the Earth's atmosphere. Once the observatory has achieved Full Operational Capability, the telescope and scientific instruments will provide imaging and spectroscopic capabilities across the 0.3 - 1600 μm wavelength range, making it one of the premier facilities for astronomical observations at infrared and sub-millimeter wavelengths. The first generation instrument suite provides coverage from 0.3 - 240 μm and will be fully operational within the next few years.

SOFIA is a joint project of NASA and the Deutsches Zentrum für Luft und Raumfahrt (DLR). The SOFIA Science Center (SSC), responsible for overseeing the scientific aspects of the mission, is located at the NASA Ames Research Center in Moffett Field, CA. Flight operations are conducted out of the NASA Armstrong Flight Research Center in Palmdale, CA. The Science Mission Operations are jointly managed by the Universities Space Research Association (USRA) for NASA and by the Deutsches SOFIA Institut (DSI), in Stuttgart, for DLR. Aircraft operations are managed by NASA Armstrong.

Most of the observing time on SOFIA is open to the international astronomical community via General Investigator (GI) proposal calls, which are issued on a yearly basis. The first of these proposal calls was for "Early Science,'" for which observations were obtained in a series of flights from May - July, September, and November 2011. The first open call for proposals, Cycle 1, covered the period from late 2012 to the end of 2013. The current proposal call is for Cycle 4 observations, which will take place between 1 February, 2016 and 31 January, 2017.

1.1 Intended Readership

This document, "SOFIA Observer's Handbook for Cycle 4" (hereafter the Observer's Handbook), provides information about SOFIA operations and the instruments that will be available for observations during Cycle 4, nominally scheduled for 1 February, 2016 - 31 January, 2017. The Observer's Handbook is the primary technical reference for astronomers who wish to submit a proposal for SOFIA Cycle 4. The information contained herein, and in documents and websites explicitly referred to, should be sufficient to allow proposers to plan viable SOFIA observations.

1.2 Updates to the Observer's Handbook

This version of the handbook is applicable to for Cycle 4. Between the time of writing and the start of Cycle 4 observations, the analysis of data obtained as part of the Instrument Commissioning process are likely to provide more empirical information regarding telescope and instrument performance. The Observer's Handbook will be updated as necessary and the list of changes will be included at the beginning of the document. Critical updates will also be published on the Cycle 4 web page. Any information that

supersedes what is given in this document will be explicitly indicated.

1.3 Other Documents and Resources

The following additional documents are available on the SOFIA Information for Researchers web pages.

- The "**SOFIA Cycle 4 Call for Proposals**" describes how to prepare and submit proposals. It includes details on how proposals will be evaluated. It formally establishes the policies for all matters concerned with the rules governing SOFIA Cycle 4 for guest investigators.
- The "**FORCAST Observation Modes**" document provides an explanation of the basic FORCAST observing modes for imaging observations. It is referred to explicitly in Section 7 below.
- The "**Guide to Observation Planning with GREAT**" is a tutorial for estimating exposure times for observations using GREAT. It is referred to explicitly in Section 9 below.
- The **HIPO Throughput/Sensitivity Spreadsheet** provides tools to estimate the signal-to-noise for HIPO observations.
- The **Science Instrument Suite** web pages provide a brief overview of the suite of instruments that will be available on SOFIA once it reaches full operational capability.
- "**The Science Vision for the Stratospheric Observatory for Infrared Astronomy**" presents many compelling science questions that SOFIA is uniquely positioned to address. The complementarity among several astronomical facilities (current and future, particularly in the IR/mm wavelength regime) are discussed where relevant. *Please note, that any information regarding the performance of the telescope and instruments contained within the "Science Vision" is superseded by this document and the SOFIA web sites.*

2. Overview

2.1 The Observatory

The telescope for SOFIA was supplied by the DLR as the major part of the German contribution to the observatory. It is a bent Cassegrain with 2.7-m parabolic primary mirror (2.5-m effective aperture) and a 0.35-m diameter hyperbolic secondary mirror. The telescope is mounted in an open cavity in the aft section of the aircraft and views the sky through a port-side door. The telescope is articulated by magnetic torque motors around a spherical bearing through which the Nasmyth beam passes. The unvignetted elevation range of the telescope is 20° – 60°. The cross-elevation travel is only ± 3°, and therefore most of the azimuthal telescope movement required for tracking is provided by steering the airplane. The flight plan is thus determined by the list of targets to be observed during the flight.

The telescope feeds two f/19.6 Nasmyth foci, an IR focus for the science instruments and a visible light focus for guiding, using a dichroic and an aluminum flat. The secondary mirror provides chop amplitudes of up to ± 5' (at chopping rates ≤ 10 Hz) and up to ± 10' (at a rate of ≤ 2 Hz). The visible beam is fed into the Focal Plane Imager (FPI+), which is an optical focal plane guiding camera. Independent of the FPI are two other optical imaging and guiding cameras, the Wide Field Imager (WFI) and the Fine Field Imager (FFI), both of which are installed on the front ring of the telescope.

Eight instruments, covering a wide range of wavelengths and resolving powers, will be used on SOFIA. Three of the instruments are Facility-class Science Instruments (FSIs), which will be maintained and operated by the Science Mission Operations (SMO) staff.

- Far Infrared Field-Imaging Line Spectrometer (FIFI-LS)
- First Light Infrared Test Experiment Camera (FLITECAM)
- Faint Object InfraRed Camera for the SOFIA Telescope (FORCAST)
- Focal Plane Imager (FPI+)
- High-resolution Airborne Wideband Camera + Polarimeter (HAWC+)

Two instruments are Principal Investigator-class Science Instruments (PSIs), which will be maintained and operated by the Instrument Principal Investigator (PI) teams.

- Echelon-Cross-Echelle Spectrograph (EXES)
- German Receiver for Astronomy at Terahertz Frequencies (GREAT)

One instrument is a Special Purpose, Principal Investigator-class Science Instrument (SSI).

- High-speed Imaging Photometer for Occultations (HIPO)

3. Cycle 4

Cycle 4 observations will take place between 1 February, 2016 and 31 January 2017. The observations will take place in a number of Science Flight Campaigns over the duration of the cycle. The campaigns will be interspersed with aircraft maintenance and instrument commissioning. Commissioning of upGREAT, the multi-beam heterodyne receiver, and the far infrared camera and polarimeter HAWC+ are ongoing in 2015 and 2016. These new capabilities are offered in Cycle 4, contingent on the success of commissioning activities. A single Southern Hemisphere observing series with up to two instruments is under consideration for the Cycle 4 time period, nominally in the summer of 2017.

For Cycle 4, the available instruments will be the mid-infrared high-resolution spectrograph EXES, the integral-field far-infrared spectrometer FIFI-LS, the near-IR camera FLITECAM, including its grism modes, the mid-infrared camera FORCAST, including its grism modes, the focal plane CCD imager FPI, in science mode, the heterodyne spectrometer GREAT, including the seven-beam receiver array upGREAT, the high-speed optical photometer HIPO, and the far-IR camera and polarimeter HAWC+. The instrument capabilities, the available modes, and the resulting performance specifications of the telescope are described in later sections.

Proposals are being solicited for the Cycle 4 SOFIA flights by USRA on behalf of NASA.

3.1 Observing with SOFIA during Cycle 4

The duration of each SOFIA Cycle 4 flight is expected to be between 9 – 10 hours, 8 – 9 hours of which will be available for observing at altitudes of 37,000 – 45,000 feet. FPI+ is always available. Among the other instruments, only one will be installed on the telescope at any time, with the exception of the FLIPO configuration (FLITECAM + HIPO). The SMO director will determine the total number of flights dedicated to each instrument, after consideration of the number of TAC-approved proposals for each.

Proposals should request observing time in units of hours. Once a proposal has been approved, the first stage is complete and the GI is then expected to carry out the detailed planning of their observations in consultation with a support scientist or, for PI instruments, with the instrument team. This second stage of observation planning is known as Phase II. The GIs will be informed who their SMO support scientists are and how to contact them.

On each SOFIA Cycle 4 flight, there will be one or more seats available for GIs or designated CoIs of the proposals scheduled for that flight. Since there are a limited number of seats available on each flight, the choice of GIs given the opportunity to fly on SOFIA will be made by the SMO director according to a number of considerations, including the duration of science observations for each program on the flight and the proposal rank.

The observations will be carried out either by members of the instrument team along with SOFIA personnel, or solely by SOFIA personnel. The GIs on board SOFIA will participate in the observing, and monitor the data as it is received, but will have limited decision making abilities. For example, the GI will be allowed to make real-time changes to exposure times for different filters or channels. However, changing targets or any modifications that alter the durations of flight-legs will not be allowed.

Those GIs or CoIs chosen to fly aboard SOFIA will be required to complete a flight participation form, a medical release form, and documentation related to badging. In addition, they will be required to participate in an Egress Training course prior to being allowed on board the aircraft. Full details will be provided to GIs of approved proposals during the Phase II process.

3.2 Scheduling and Flight Planning

Scheduling and flight planning will be handled by the SMO staff and is not the responsibility of the GI. However, an understanding of the flight planning process and the restrictions inherent to airborne astronomy may be useful in preparing a successful proposal.

The most distinctive aspect of SOFIA flight planning is the interdependency of the targets observed in a flight. Because the azimuthal pointing is controlled primarily by the aircraft heading and because, in normal operations, the take-off and landing air fields are the same, efficient flight plans must generally balance East-bound with West-bound flight legs and South-bound with North-bound legs. This also means that for any flight only a limited fraction of the observing can be performed in a given region of the sky. An example of a flight plan flown during Basic Science in May 2011 is shown in Figure 3-1 below. Several more examples of flight plans flown during Basic Science can be found on the Information for Researchers Flight Plans web page.
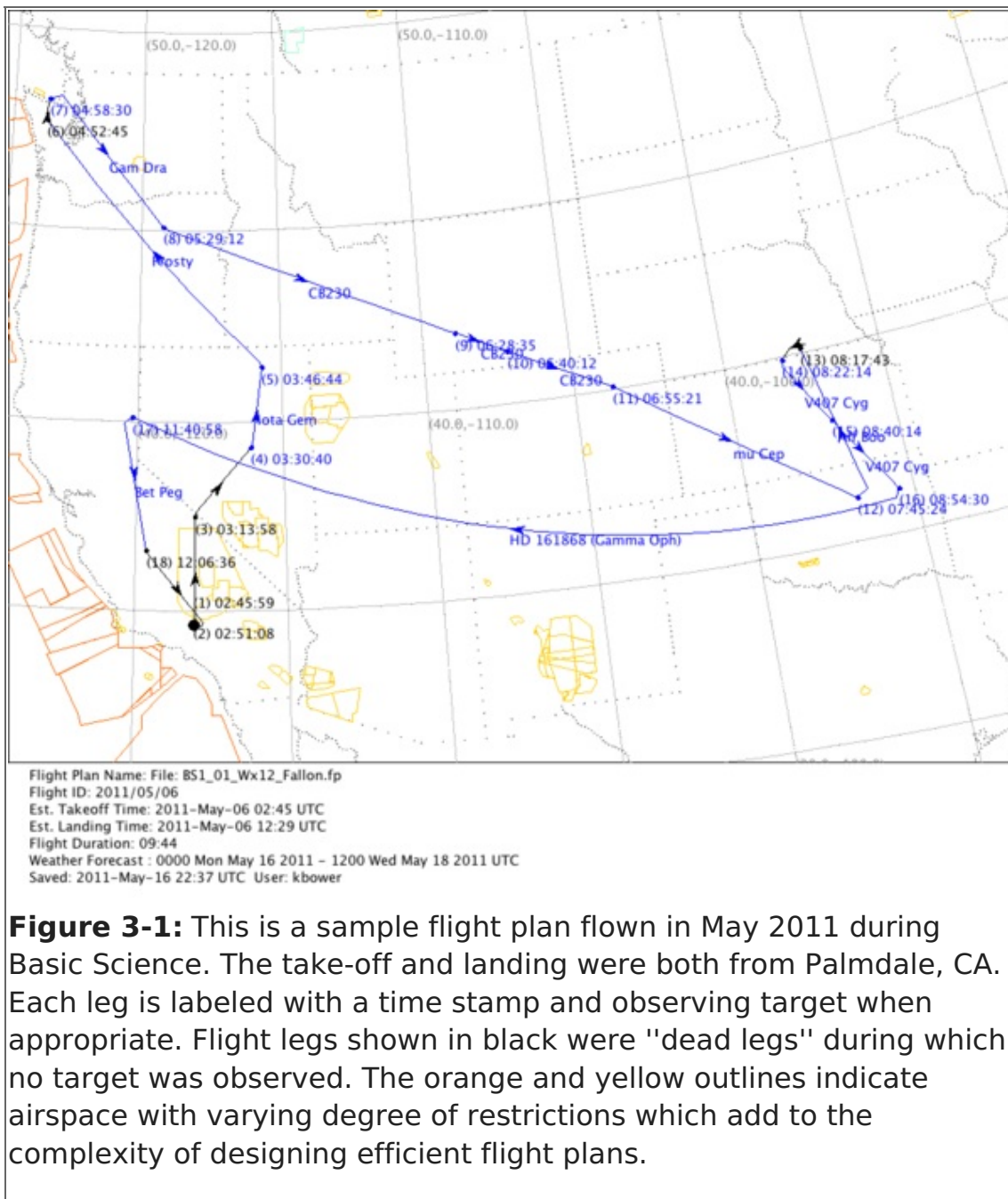
Figure 3-1: This is a sample flight plan flown in May 2011 during Basic Science. The take-off and landing were both from Palmdale, CA. Each leg is labeled with a time stamp and observing target when appropriate. Flight legs shown in black were "dead legs" during which no target was observed. The orange and yellow outlines indicate airspace with varying degree of restrictions which add to the complexity of designing efficient flight plans.

For the proposer this leads to several considerations:

- A strong scientific case must be made for observations with rigid time constraints or strict cadences in order to justify the restrictions they will impose on flight planning.
- Because the sky distribution of targets typically proposed for SOFIA observations (centered on the Galactic plane and certain regions of star formation, including Orion) is highly inhomogeneous, targets in areas that complement these high-target-density regions will allow more efficient flight planning and will likely have a higher chance – for a given scientific rating – to be scheduled. Consequently, it may be advantageous for those who can choose between targets from a large source pool for their SOFIA proposals and for those who plan to submit survey proposals to emphasize sources from complementary regions.
- For example, objects that complement the potentially popular Orion molecular clouds include circumpolar targets or targets north of about 40° with a right ascension in a roughly 6 to 8 hour wide window centered about 6 hours before or after the right ascension of Orion.
- The maximum length of flight legs will be determined by the need for efficient flight

plans as well as the typical requirement that SOFIA take-off and land in Palmdale, California. In most cases, the longest possible observing leg on a given target is ~ 4 hours. Therefore, observations of targets requiring long integrations may have to be done over multiple flights and flight legs.

- GIs may propose for observations for which the flight does not originate or end in Palmdale, CA, for example, in order to conduct observations under time constraints that require a specific flight path or that require a single flight leg in excess of ~ 4 hours. Such proposals would be equivalent to a deployment and due to resource requirements and the impact that this would have on flight planning, the scientific justification must be strong. The final decision on whether to allow programs with such a high impact on scheduling and flight planning will be made at the Director's discretion.

GIs are encouraged to review the Flight Planning presentation delivered by Dr. Randolf Klein at the SOFIA User's Workshop in November, 2011. The full list of presentations can be found on the SOFIA web site. In addition, a much more detailed discussion of target scheduling and flight planning can be found in the Observation Scheduling and Flight Planning White Paper.

3.3 Acquisition and Guiding

SOFIA has three optical cameras for acquisition, guiding and tracking. The Wide Field Imager (WFI) and Fine Field Imager (FFI) are mounted on the telescope head ring. The upgraded Focal Plane Imager (FPI+) images the focal plane of the telescope via a dichroic and a tertiary mirror. All three imagers use ''High Speed Slow Scan'' CCD cameras.

The WFI has a 6°x6° field of view, and is expected to achieve a centroid precision of ~8'' for stars brighter than R = 9. The field of view of the FFI is 1°x1°. It is expected to achieve a centroid precision of ~1'' for R = 11 or brighter stars. **The FPI+ has an 8' diameter and is expected to provide a centroid precision of 0.05'' for R = 16 or brighter stars.**

Most observers do not need to select guide stars as they will be chosen by the SMO staff. However proposers should be aware that the guiding cannot be done on IR sources unless they are optically bright.

3.4 Observing Moving Targets during Cycle 4

Once SOFIA achieves its nominal operating capabilities, it will be able to observe solar system targets by (i) guiding on the object itself, (ii) offset guiding from field stars, or (iii) predictive tracking based on accurate ephemerides. As of this writing, the non-sidereal tracking capabilities have been implemented, but have not been fully tested. Consequently, programs requesting non-sidereal tracking will inherently involve greater risk. Nevertheless, the SOFIA project will make every attempt to observe Solar System targets in highly ranked proposals.

Successful guiding on a moving target requires it to be bright at visible wavelengths, where the guider cameras operate. Our current estimate is that we will be able to guide on solar system targets with R ≤ 10 and that have a non-sidereal angular speed of 1'/s or less. The minimum acceptable solar elongation for a target is limited by the lower elevation limit of the telescope and the rule that no observations can be acquired before

sunset or after sunrise. For Cycle 4, the minimum solar elongation is 25 degrees.

Identification of solar system targets will be done manually by the Telescope Operator by inspecting images obtained with the FPI. The ephemerides of the proposed target must be accurate enough to allow for unambiguous identification. While the required accuracy could vary somewhat based on the complexity of the background star field, it should in general be better than about 30\arcsec.

3.5 Line-of-Sight (LOS) Rewinds

In many respects, the design of the SOFIA telescope is similar to that of a typical altitude-azimuth telescope. One such similarity is that as the telescope tracks a target it must rotate in order for the sky to remain at the same orientation on the detectors. The range of free rotation by the telescope is limited, however, to ± ~3°. Hence, the telescope must periodically undergo a ''Line-of-Sight (LOS) rewind'', or de-rotation. The required frequency of LOS rewinds depends on rate of field rotation experienced by the target, which is a complex function of the position of the target in the sky relative to that of the aircraft heading. Since the relative target position is not known *a priori* , but is only determined during flight planning, it is not possible to determine precisely the field rotation rate until after the observations have been scheduled. However, one can estimate either the rate of field rotation using Figure 3-2 or the time it takes for a field of view to rotate by six degrees using Figure 3-3.
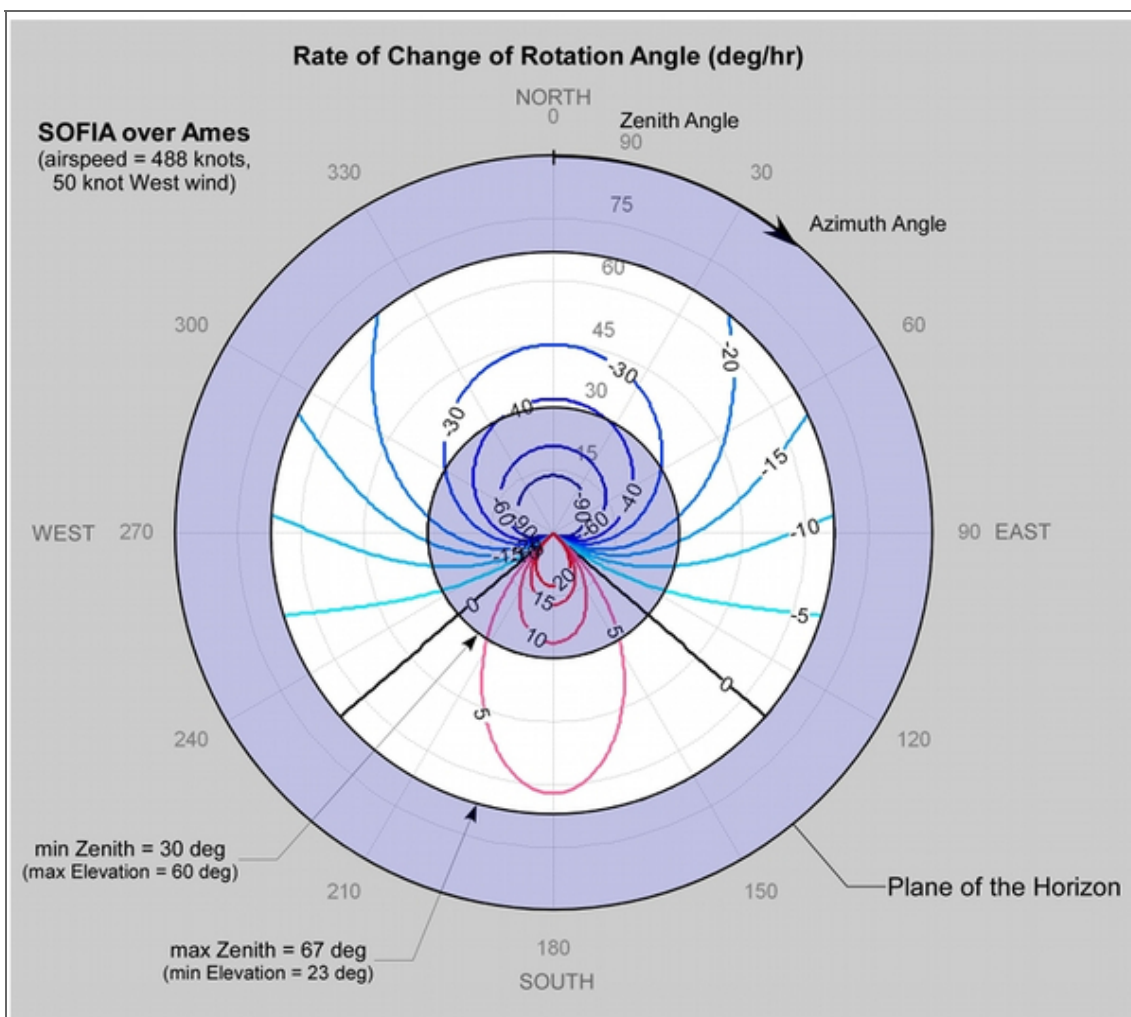

Figure 3-2: This plot shows the rate of change in the rotation angle (degrees/hour) as a function of target zenith angle and azimuth angle. The rates are calculated assuming an aircraft latitude of 37.415° N.

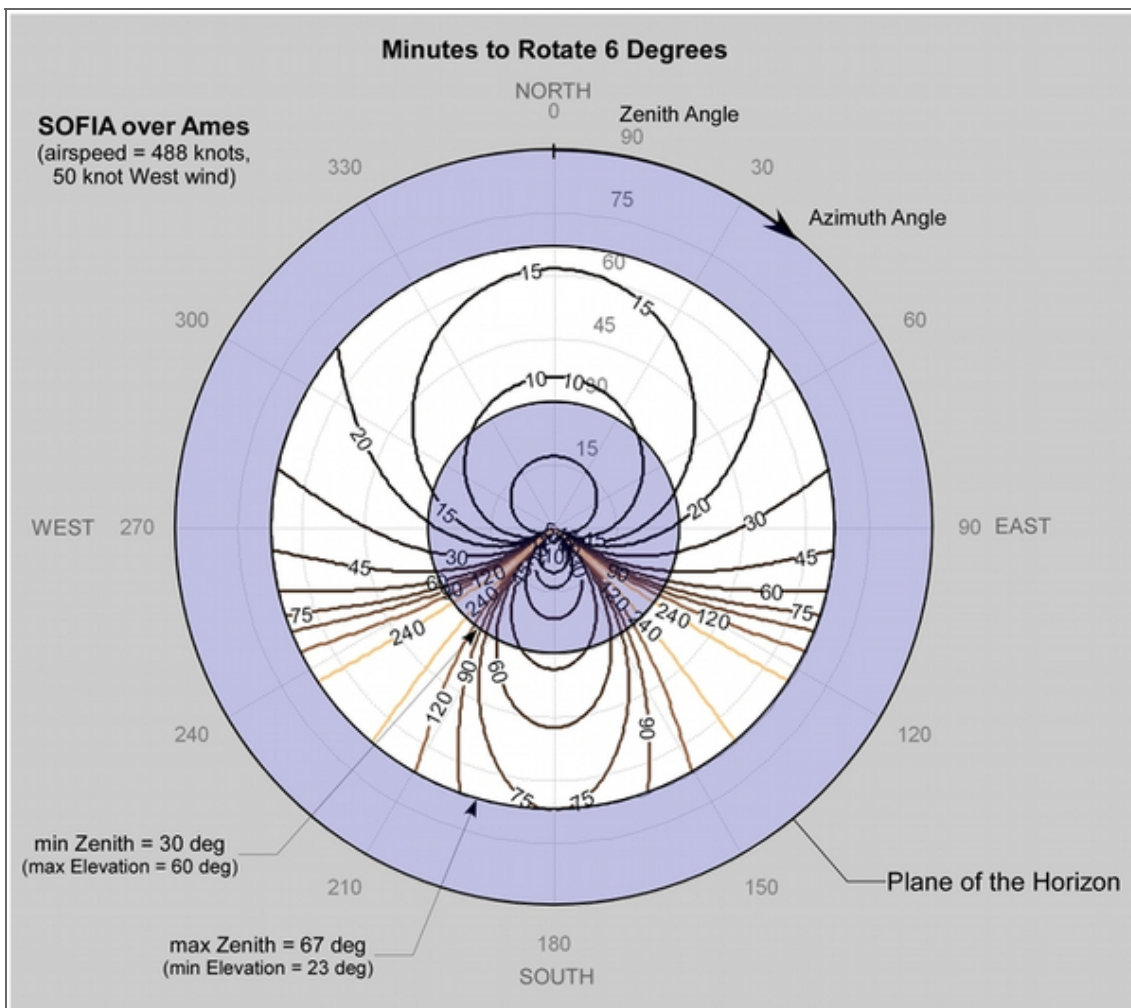The unvignetted range of zenith angles is shown in white.

Figure 3-3: This plot shows the time it takes for the field of view to rotate by 6 degrees as a function of target zenith angle and azimuth angle. The times are calculated assuming an aircraft latitude of 37.415° N. The unvignetted range of zenith angles is shown in white.

In order to use the plots effectively, one must first use the SOFIA Target Visibility Tool or similar visibility planning tool to determine the airplane heading (*AH*) and the target elevation (*El*) at the desired date of observation. Since the telescope is situated in the port side (i.e. the left side as seen by a person on board, facing the front of the aircraft), the target azimuth angle (*Az*) is calculated according to, *Az = AH - 90°* . The zenith angle (*ZA*) is calculated according to, *ZA = 90° – El* . Once the *ZA* and *Az* of the target have been determined for a sample observation date, then the LOS plots provide an estimate of the rotation of field for the target.

For example, according to the SOFIA Target Visibility Tool, during the month of August, the W3 star forming region, is at an elevation that ranges from between about 20° and 60° throughout the evening. The aircraft heading would be ~130°. Hence, *ZA = 70° – 30°* for an average of ~50° and *Az ≅ 40°* . On Figure 3-2, these coordinates correspond to a field rotation rate of approximately -25° per hour, or roughly 6 degrees every 15 minutes as indicated on Figure 3-3.

When using Figures 3-2 and 3-3 to estimate the rotation of field, it is important to bear in

mind the associated caveats. First, the plots were calculated assuming that the aircraft position was at 37.415°, the latitude of NASA Ames. In practice, the latitude of the aircraft may deviate significantly from this. In addition, in the example, we made the estimates using the average *ZA* of the target, but in practice, neither the *ZA* at the time of observation nor the actual observation date will be known until flight planning is complete. This means that one should consider the estimates of the rotation of field as being only approximate. Finally, in flight, the LOS rewinds are performed after a field rotation of ~3° rather than the maximum possible range of 6°, in order to account for slight deviations in the airplane heading.

Special care must be taken when designing spectroscopic observations. GIs should bear in mind that the orientation of the slit on their targets will change with each LOS rewind. For point sources, this should not cause problems, but for extended sources, this means that after each rewind the slit will be sampling a slightly different region of the source. In addition, there is no way to choose the orientation of the slit on the target.

3.6 Atmospheric Transmission

SOFIA operates at altitudes above 99% of the water vapor in the atmosphere. The average atmospheric transmission across the SOFIA bandpasses is about 80% at these altitudes. There are however a number of strong absorption features which, even at these altitudes, make the atmosphere nearly opaque. Broad band filters, such as those on FORCAST, account for the presence of such features. However, when using high-resolution tunable instruments such as GREAT and EXES, it is necessary to examine the atmospheric transmission at the wavelengths of interest in detail. This may be done using the web interface to the ATRAN program that was developed and kindly provided to the SOFIA program by Steve Lord. A plot of the atmospheric transmission seen by SOFIA in comparison to that achieved at Mauna Kea is shown in Figure 3-4 below.

In addition to its dependence on wavelength due to the presence of absorption features, the atmospheric transmission varies with latitude and with time of year, primarily due to differences in the amount of water vapor. It also exhibits variations on smaller time scales due to changes in the location of the tropopause. Full discussions of these issues may be found in Haas & Phister 1998 (PASP, 110, 339) and Horn & Becklin 2001 (PASP, 113, 997).

The variations in atmospheric water vapor could have a significant impact on some observations, particularly when using GREAT and EXES or grism modes with FLITECAM and FORCAST. For example, GREAT observations of a line situated on the shoulder of an atmospheric water feature could be strongly affected by water vapor variability. SITE allows the user to specify the water vapor overburden and adjusts the time estimates appropriately. The water vapor monitor has been installed and is currently undergoing testing, but may not be fully functional during Cycle 4.
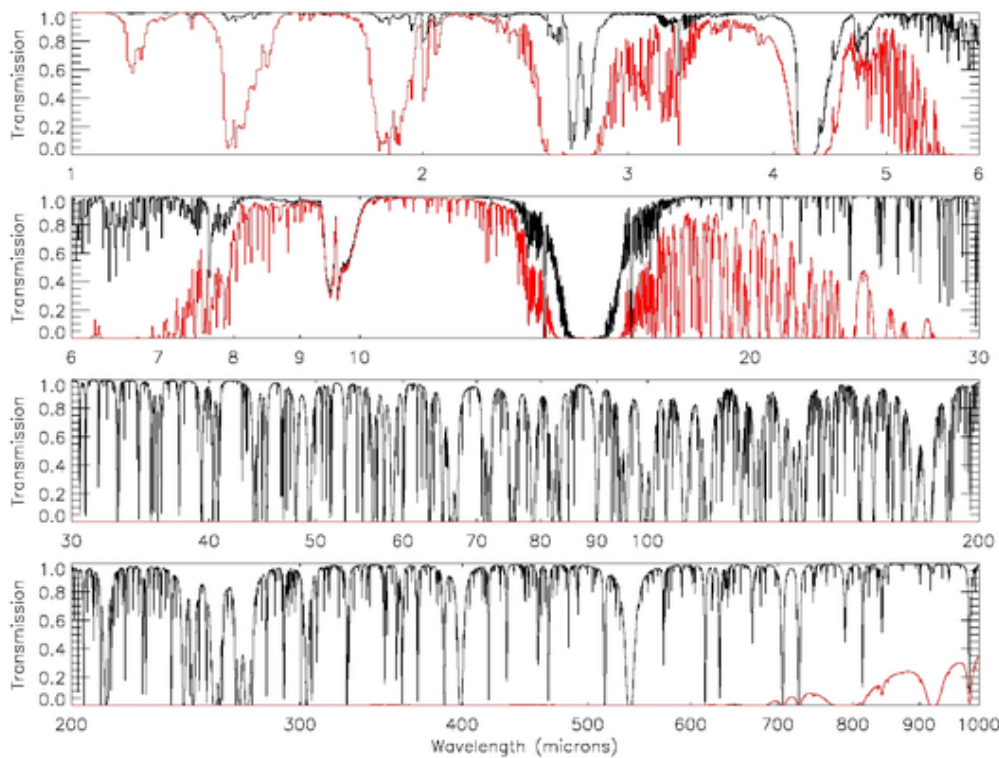
Figure 3-4: This is a plot showing the atmospheric transmission for SOFIA (black) at an altitude of 41K feet and 7.3 µm of precipitable water vapor compared to Mauna Kea (red) at an altitude of 13.8K feet and 3.4 mm water vapor over the range of 1 – 1000 µm. The transmission was calculated using the ATRAN code with a telescope zenith angle of 45°. and the data were smoothed to a resolution of R=2000.

3.7 Flux and Telluric Calibration

Flux and telluric calibration observations will be planned by the SMO staff and instrument scientists using standard stars, asteroids, and planets. Calibration plans will be specific to each instrument. In all cases, **except EXES**, the time used for calibration observations are considered part of the general overhead and will not be charged against the GI program time. GIs should look at the calibration details provided in each instrument chapter below for specific calibration plans.

The calibration accuracy will depend on the instrument and observation mode, but an accuracy of 20% is expected to be obtained, even in "Shared Risk" modes. Unless the proposer requires more accurate calibration, there is no need to request time for calibration or to choose calibration targets. If the GI has such requirements for more accurate calibration, they must be justified in the proposal, and the time required for the calibration observations should be included in the total time request. The only exception to this is EXES, for which all calibration observations must be specified in the proposal and will be charged to the science program time.

4. Instruments I: EXES

4.1 EXES Instrument Overview

The **E**chelon-**cross**-**E**chelle **S**pectrograph (EXES) operates in the 4.5 – 28.3 µm

wavelength region, at high (R ≈ 50,000 – 100,000), medium (R ≈ 5000 – 20,000) and low (R ≈ 1000 – 3000) spectral resolution. The instrument uses a 1024x1024 Si:As detector array. High resolution is provided by an echelon – a coarsely-ruled, steeply-blazed aluminum reflection grating – along with an echelle grating to cross-disperse the spectrum. The echelon can be bypassed so that the echelle acts as the sole dispersive element. This results in single order spectra at medium- or low-resolution depending on the incident angle.

4.1.1 Design

EXES is a liquid helium cooled instrument. The cryostat is approximately 24 inches in diameter and 72 inches long. There are two cryogen reservoirs, one for liquid nitrogen and one for liquid helium. These are at the forward end, as mounted on SOFIA, with the entrance window on the aft end toward the telescope. There are three layers of radiation shielding within EXES - a vapor cooled shield tied only to the cryogen fill tubes, one attached to the liquid nitrogen reservoir, and the third attached to the liquid helium reservoir. All optics except for the entrance window/lens are attached to the liquid helium level. Baffling tubes connected to the liquid nitrogen level reduce thermal emission impinging on the internal optics. Within the liquid helium level, the optics are all tied to a rigid optics box constructed out of aluminum, and the detector headerboard is isolated with G10 fiberglass and actively maintained at a uniform temperature.

4.1.2 Optics

The optics consist of an entrance window/lens, fore-optics, three wheels housing the slits, deckers and filters, an echelon chamber, and a cross-dispersion chamber. The entrance window/lens (2 inches diameter) forms an image of the SOFIA telescope secondary at the liquid helium cold stop within the fore-optics. The fore-optics, including the entrance window, changes the incoming f/19 beam to f/10. After coming to a focus, the beam expands through a pupil (at the cold stop) to an ellipsoidal mirror. The light is redirected off two flat mirrors to a focus at the slit plane.

As the beam comes to a focus, it passes through the slit/filter cassette. This consists of three wheels on a common axle containing (i) filters to isolate grating orders, (ii) deckers to determine the length of the slit, and (iii) slits of different widths. The filter wheel has 12 slots, and these will be loaded with specific filters for each cooldown cycle based on the planned observations. Broader Filters for use in the low-resolution configuration are included in 4 of the decker wheel slots. The decker wheel has a total of 11 features, which include continuously variable length slits, fixed length slits, pinholes, and an open position. The continuously variable slit length is provided by a cutout on the decker wheel that gets larger as a function of angle. The smallest size is about 4.5'' and the largest about 45''. The slit length depends on the wavelength and the instrument configuration. With that caveat, slit lengths can range from 1'' to 180'' on SOFIA.The slit wheel contains six slits. On SOFIA, EXES will typically use four of them (Table 4). There is also a wide 9.400 slit intended for flux calibration.

Table 4: EXES observing configurations, modes, slits and spectral resolutions

EXES observing configurations, modes, slits and spectral resolutions

Configuration	Available Modes	Available Slit Widths[a] arcseconds	Resolving Power [b]
High_Medium	nod on slit[c], nod off slit, map	1.4	112,000
		1.9	86,000
		2.4	67,000
		3.2	50,000
High_Low	nod off slit, map	1.4	112,000
		1.9	86,000
		2.4	67,000
		3.2	50,000
Medium	nod on slit, nod off slit, map	1.4, 1.9, 2.4, 3.2	5,000-20,000[d]
Low	nod on slit, nod off slit, map	1.4, 1.9, 2.4, 3.2	1,000-3,000[d]

[a] 1.400 slit unavailable >12 µm, 1.900 slit unavailable >16 µm, 2.400 slit unavailable >21 µm

[b] Observers must check the most recent resolving powers as a function of slit width and wavelength at http://irastro.physics.ucdavis.edu/exes/etc/

[c] On-slit nodding not possible at all wavelengths. Observers must check this at http://irastro.physics.ucdavis.edu/exes/etc/

[d] Resolving power is a strong function of wavelength and slit width

After passing through the slit wheel, the beam hits a flip mirror mechanism, which is used to choose between instrument resolution configurations (Table 4) by either directing the beam into the echelon chamber (high-resolution) or into the cross-dispersion chamber (medium- and low-resolution). In the high-resolution configuration, the beam enters the echelon chamber and expands to an off-axis hyperboloid mirror that serves as both collimator and camera mirror for the echelon grating. The dispersed light, focused by the hyperboloid, bounces off a flat into the cross-disperson chamber.

The cross-dispersion chamber is conceptually similar to the echelon chamber. The light expands from the input to an off-axis paraboloid that again serves as both collimator and camera mirror. The collimated beam is sent to the cross-dispersion grating which disperses the light in the plane of the grating. The camera mirror sends the light to our detector. When operating in single-order, long-slit spectral configurations -- our medium

and low resolution science configurations -- the light never enters the high-resolution echelon chamber.

There is a wheel in front of the detector, which provides a lens for imaging the pupil through the instrument, and a dark slide for isolating the detector. The wheel would also be available for including transmissive optics to adjust the plate scale on the detector, if desired.

4.1.3 Detector

The detector is a Raytheon Vision Systems Si:As array with 1024x1024 pixels. The detector material is bonded to a SB 375 multiplexer. The array is mounted in a separate enclosure to reduce scattered light. The headerboard is thermally isolated from the rest of the optics box to permit active temperature control of the array. The photon fluxes in the low-resolution configuration ("Low") will be significantly above the level intended for the array. This prevents observations at longer wavelengths and/or with wider slits. When photon fluxes allow, only a subsection of the array will be clocked out in this configuration for a faster read-out (as well as in any imaging configuration). It is expected that a quarter to half the array will be utilized in these configurations, so the effective slit length is about 60''. These limitations to the Low configuration are not reflected in the online ETC yet, and GIs are encouraged to contact the instrument team for more information.

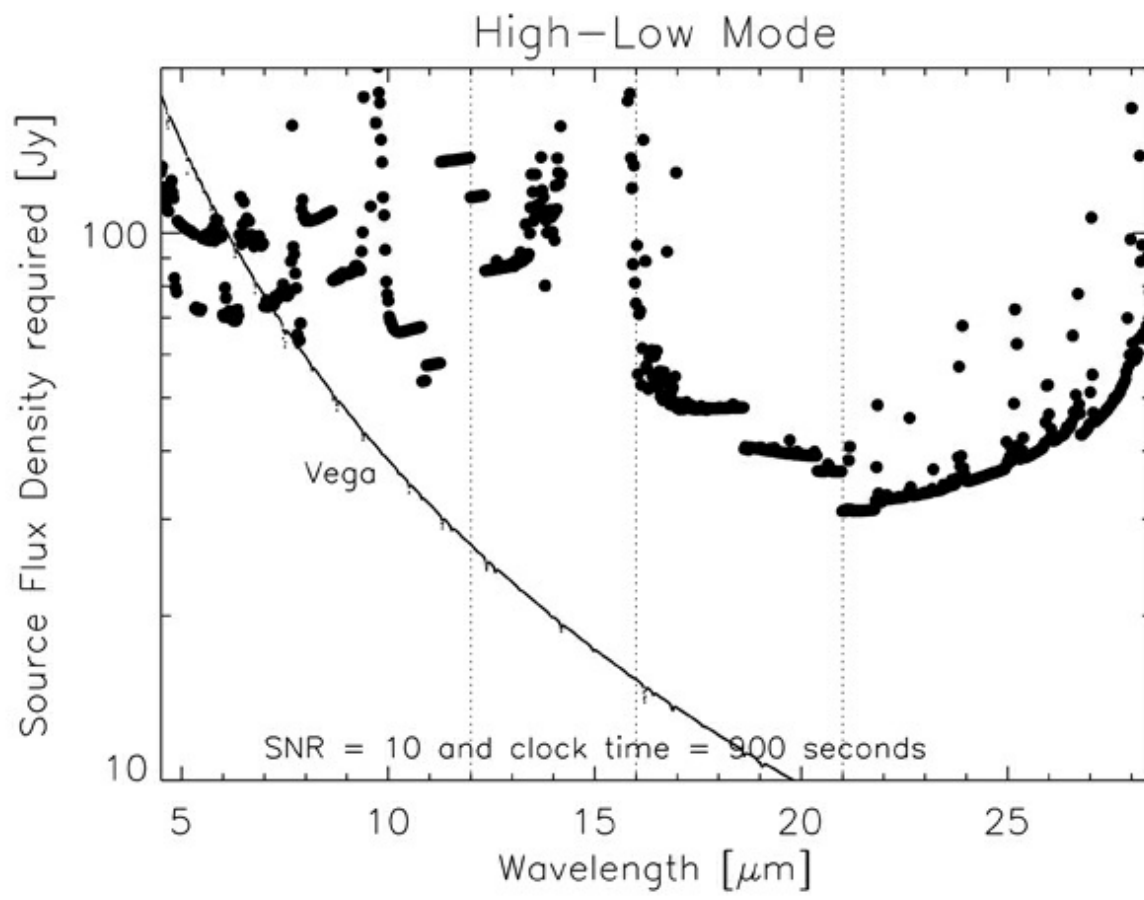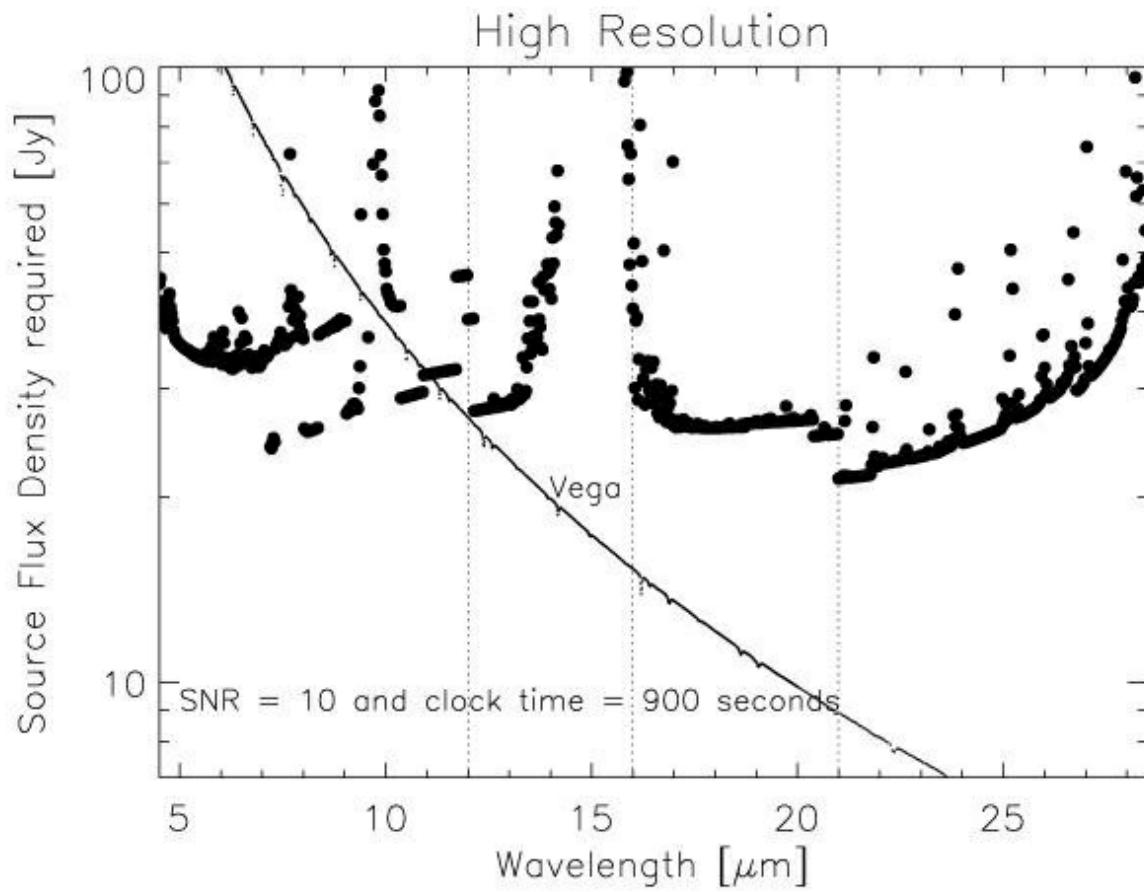### 4.1.4 Performance and Sensitivities

At the time of writing, the analysis of the EXES in-flight commissioning observations is ongoing. Many of the performance specifications quoted here are expectations, based on laboratory tests, and test runs on ground based telescopes. The angular resolution of EXES will match that achieved by the telescope. For the latest sensitivities, observers are recommended to consult the online Exposure Time Calculator (ETC) at http://irastro.physics.ucdavis.edu/exes/etc/. The ETC also provides the slit length as a function of wavelength and instrument configuration (and therefore whether on-slit nodding is possible or not), as well as the wavelength coverage in a single setting and echelon orders that can be targeted.

The wavelength coverage ranges from 4.5-28.3 μm. There are three resolution regimes -- high, medium and low -- with the exact resolving power depending on wavelength, grating angle and slit width. Generally, the resolution will be higher at shorter wavelengths in each regime. The high-resolution configurations will use the echelon grating and will achieve R = 50,000-100,000. If the cross disperser echelle angle is 35-65°, the configuration is called High_Medium and if 10-25° it is called High_Low. For these high-resolution configurations, there is non-continuous spectral coverage in high-resolution configuration for λ > 19 μm, but the central wavelength can be tuned so that lines of interest do not fall in the gaps. The Medium configuration will use high angles on the echelle grating to achieve R = 5,000-20,000, and the Low configuration will use low angles to achieve R = 1000-3000.

The High_Medium configuration slits are 4.5″-45″ long, and the High_Low slits are 1-12″ long. The shorter slits in High_Low allow for more orders to be packed onto the array, thus increasing the instantaneous wavelength coverage, while maintaining the high spectral resolution (see Fig. 4-6 for an example). In the Medium and Low configurations

the slit lengths vary from 25″ to 180″ depending on the number of rows to be read out.
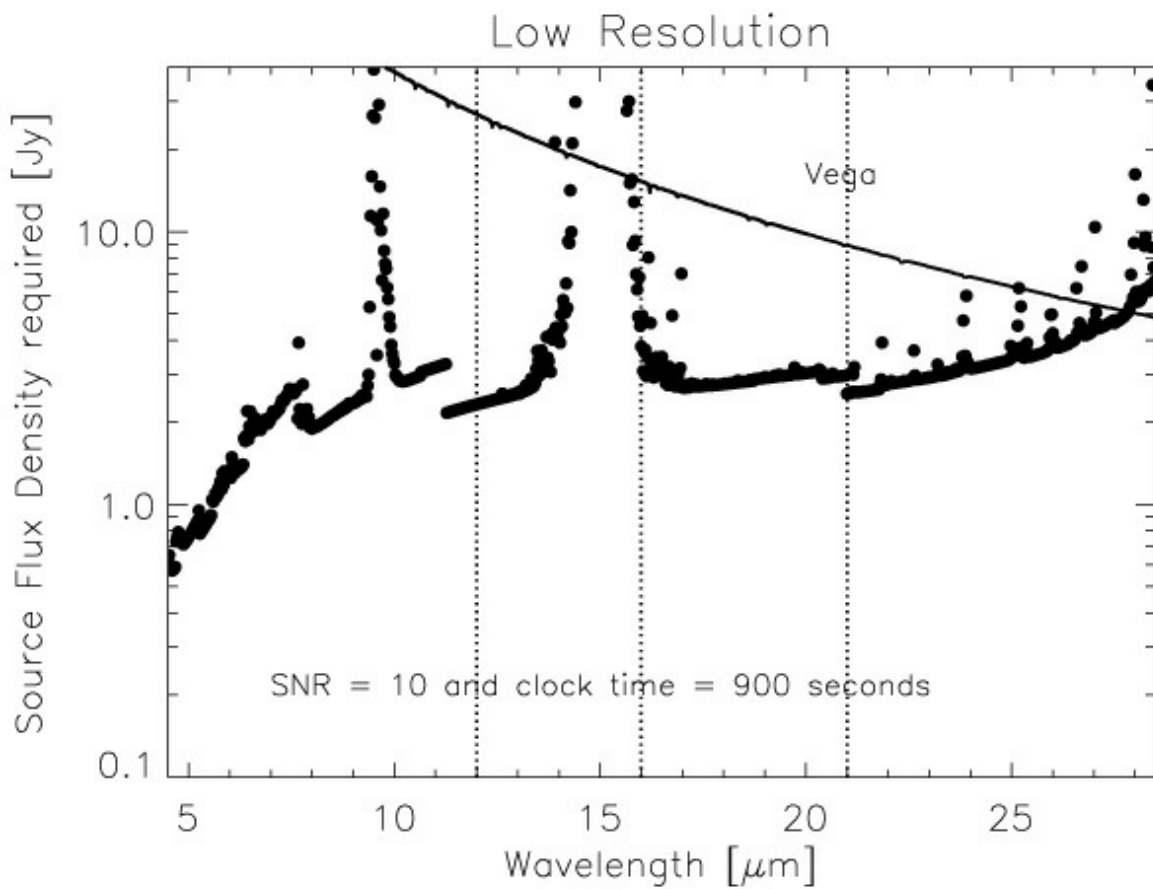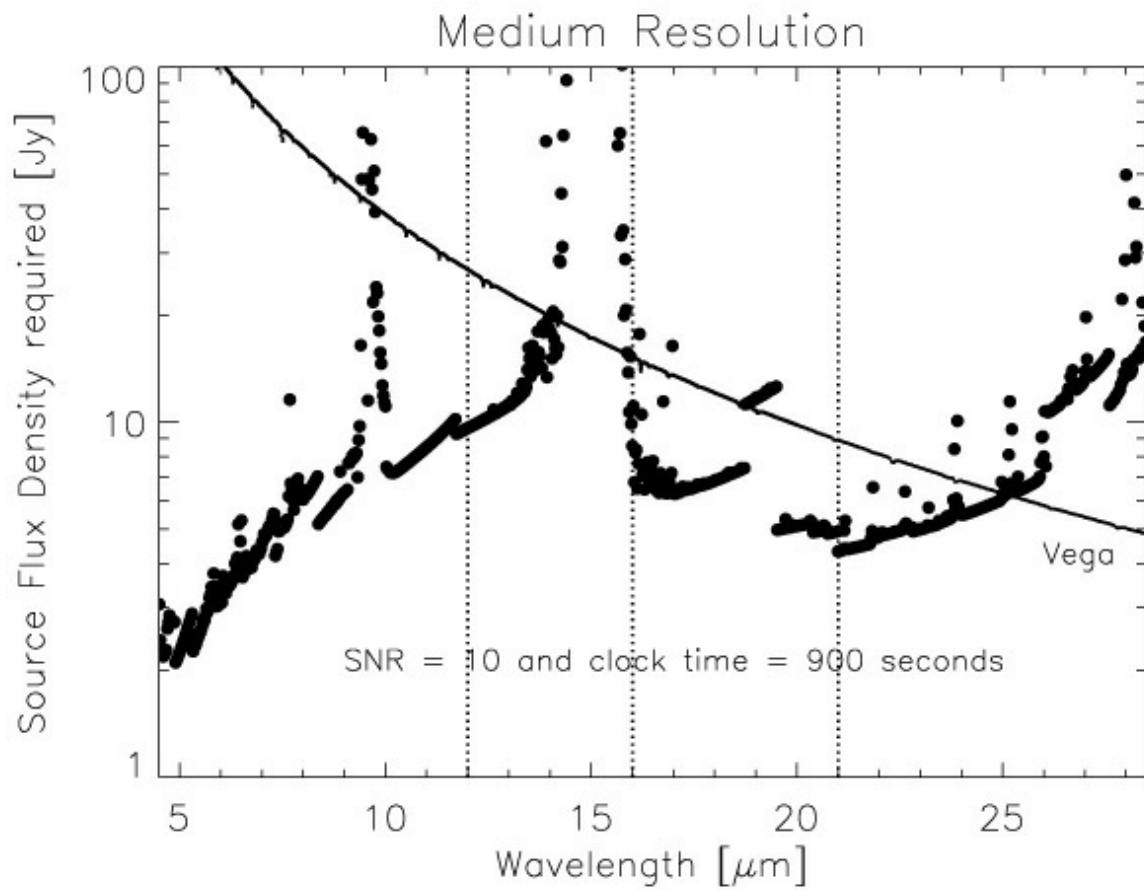
The sensitivity of the instrument is shown in Figures 4-1 through 4-4 for the High_Medium, Medium, and Low configurations for both point sources and extended sources. The Noise Equivalent Flux Density for S/N of 10σ in a clock-time (Note that the other instruments in this Handbook report sensitivities based on the total time on-source, not the clock-time. The latter includes the total time on-source + applicable overheads, excluding target acquisition and instrument set-up time.) of 900 seconds is plotted as a function of wavelength. These values have been calculated for a point source assuming image quality between 2" and 4" (FWHM) and the narrowest of the available 1.4" to 3.2" slits, both of which vary with wavelength, and take into account estimated instrument efficiency. They assume an altitude of 41,000 feet, 40° elevation, and 7 μm precipitable water vapor.

High Resolution

SNR = 10 and clock time = 900 seconds

Vega

High−Low Mode

SNR = 10 and clock time = 900 seconds

Vega

4.2 Planning EXES Observations

EXES commissioning observations were performed in April 2014 and February/March 2015. The analysis of these data is ongoing. The Low configuration will be offered in shared-risk mode.

The proposer needs to supply the central wavelength, the spectroscopic configuration, the slit width, and the observing mode for each observation (Table 4). These parameters define the default instrument set-up. Each central wavelength specified should count as a separate observation. In addition, the proposer should estimate the clock time necessary to reach the desired S/N.

Medium Resolution

SNR = 10 and clock time = 900 seconds

Vega

Low Resolution

SNR = 10 and clock time = 900 seconds

Vega

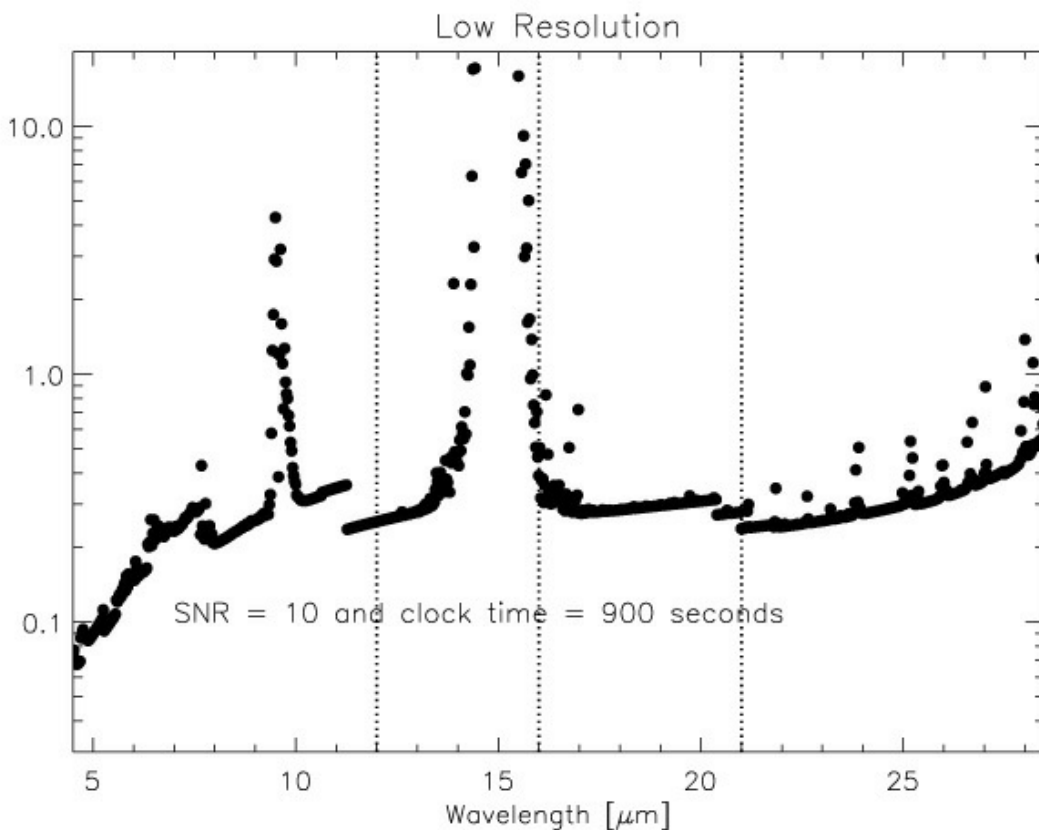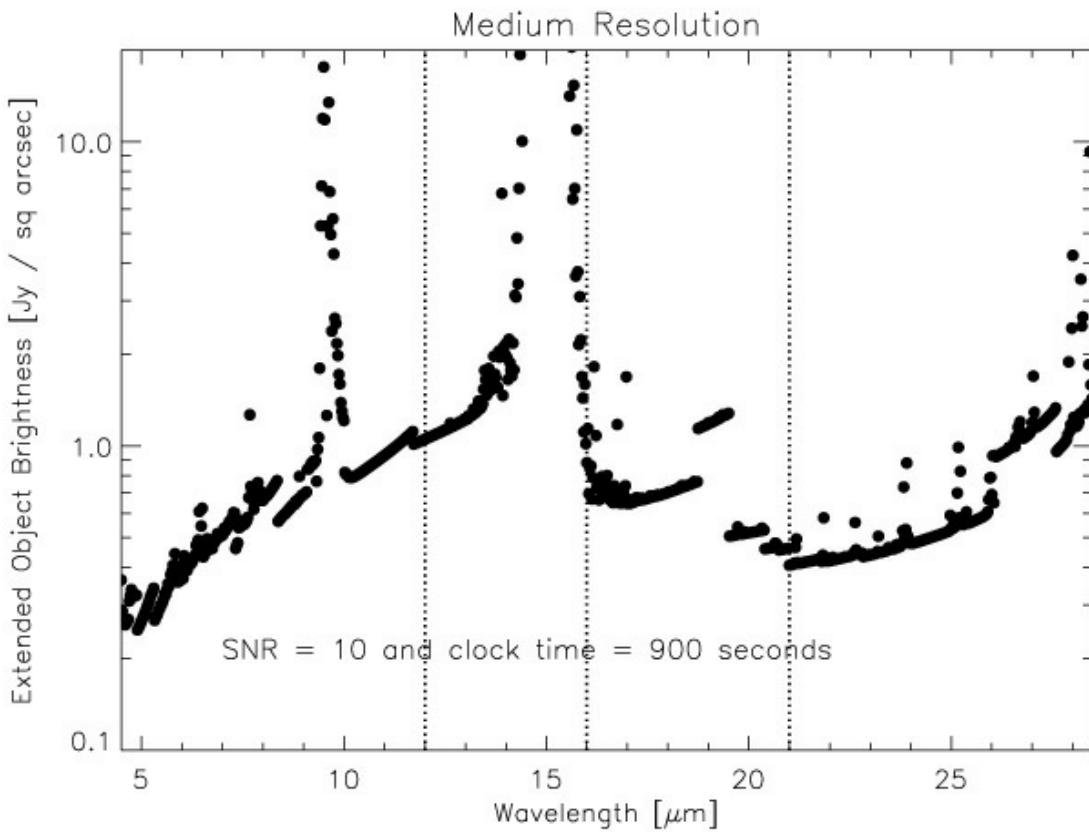The calculation may be based on Figure 4-1 or 4-2 for point sources and on Figure 4-3 and 4-4 for extended sources, noting that the minimum detectable flux ∝ (S/N) / $\sqrt{t_{exp}}$.However, it is recommended that the online ETC at http://irastro.physics.ucdavis.edu/exes/etc/ is checked as well for the latest updates.

High Resolution

SNR = 10 and clock time = 900 seconds
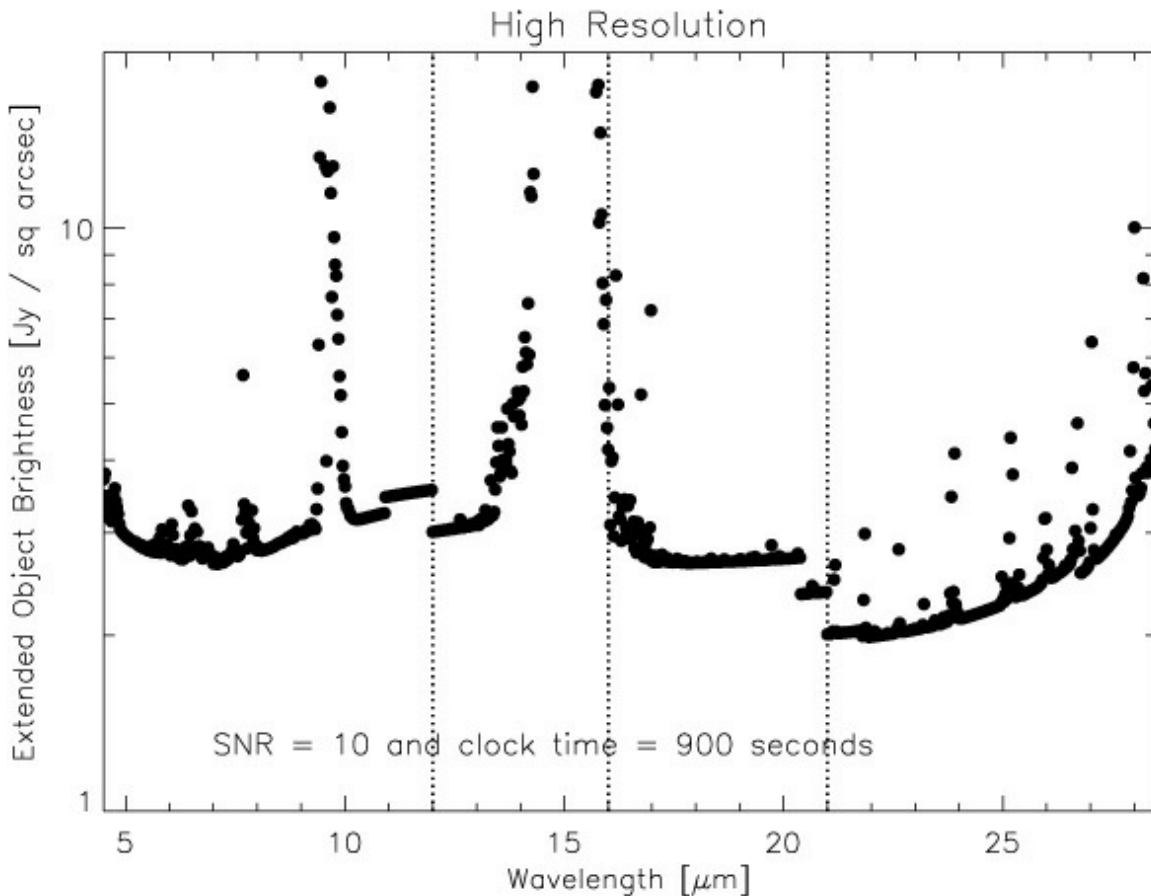
EXES operates in a wavelength region, parts of which are accessible from ground based telescopes. Proposers should carefully check the atmospheric transmission (using ATRAN, for example) and make sure that the observations require, or would greatly benefit from, using SOFIA. The proposer should take into account the Doppler shift of the target(s) due to their motion relative to the Local Standard of Rest, and to the Earth. If proposers find that the atmospheric transmission at the wavelength of interest is lower than the local median (calculated over a range ± 0.0125 μm), then more time will be required to reach the desired S/N. Higher transmission would imply shorter required times. In general the, S/N scales as _transmission_/√((1 - _transmission_) + 0.3). Note that the online ETC includes the impact of the atmosphere at precise wavelength of interest and so may differ from the Figures. The ETC provides the clock-time required to achieve the desired S/N per resolution element on a continuum object at the specific wavelength of interest and then indicates what the expected S/N should be for the entire setting.

Proposers should specify the slit width, which sets the resolving power for each configuration (Table 4). Note that the narrowest slit (1.4") is only effective below 12 μm (above this wavelength no gain in resolving power is achieved, while flux is lost with respect to the wider slits). Similarly, the 1.9" slit can only be used below 16 μm, and the 2.4" slit below 21 μm.

Medium Resolution

SNR = 10 and clock time = 900 seconds

Low Resolution

SNR = 10 and clock time = 900 seconds

In configurations using the medium resolution grating (Medium and High_Medium), the single setting spectral coverage ranges between 0.03 μm at the shortest wavelengths, and 0.3 μm at longer wavelengths (Fig. 4-5). For the low resolution grating (the Low and High_Low configurations) this is 0.2-0.8 μm. Note that while High_Low and High_Medium have the same spectral resolution, the larger wavelength coverage of High_Low comes at the expense of a smaller slit length, which is illustrated in Figure 4-6.
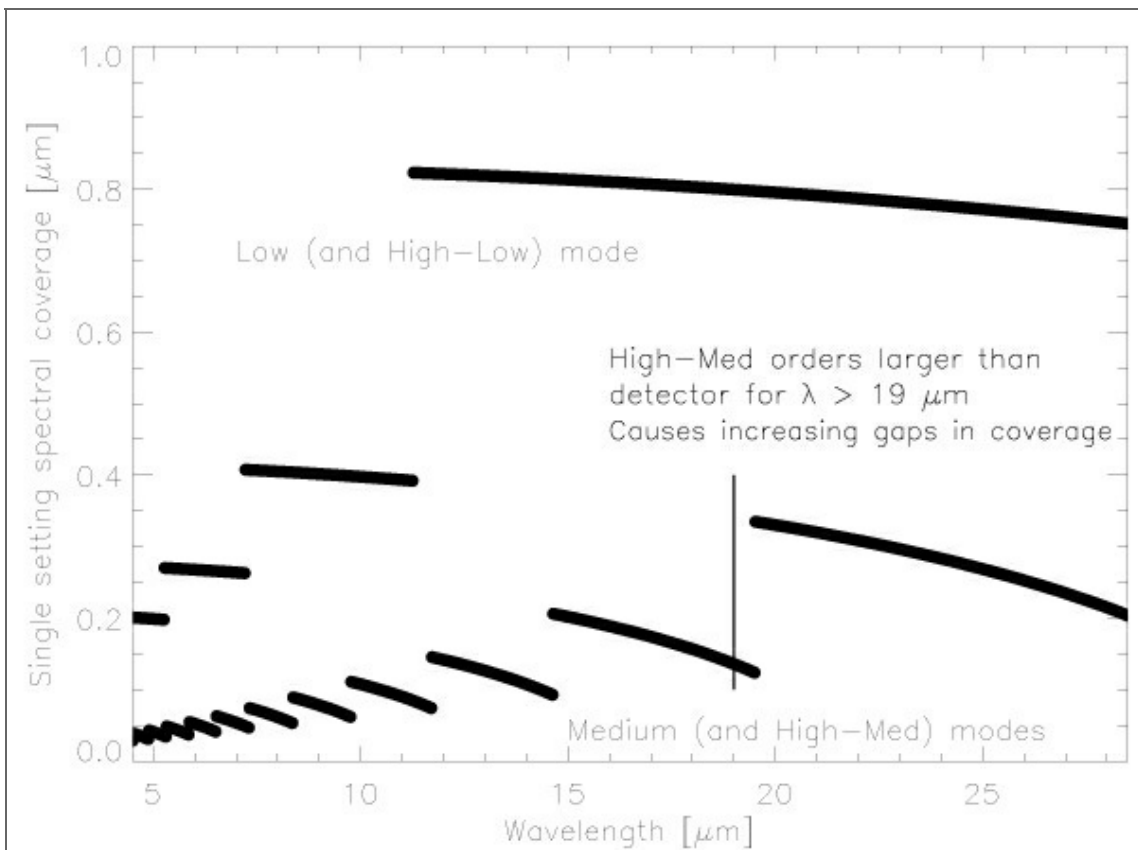
Figure 4-5: The single setting spectral coverage as a function of wavelength. Note that these values are the same for the High_Medium and Medium configurations, and for the High_Low and Low configurations.

Proposers should choose a single line of interest for each observation. Fine tuning of the bandpass to observe lines at the extreme edges of a single setting should be done in consultation with the EXES team to see if existing data indicates such tuning is possible.

The slit orientation on the sky depends upon the time when the target is observed, and therefore the position angle cannot be specified.

HIGH_MED Configuration

13.730 μm
728.33 cm⁻¹

13.629 μm
733.73 cm⁻¹

HIGH_LOW Configuration

14.10 μm
709.22 cm⁻¹

13.76 μm
726.74 cm⁻¹
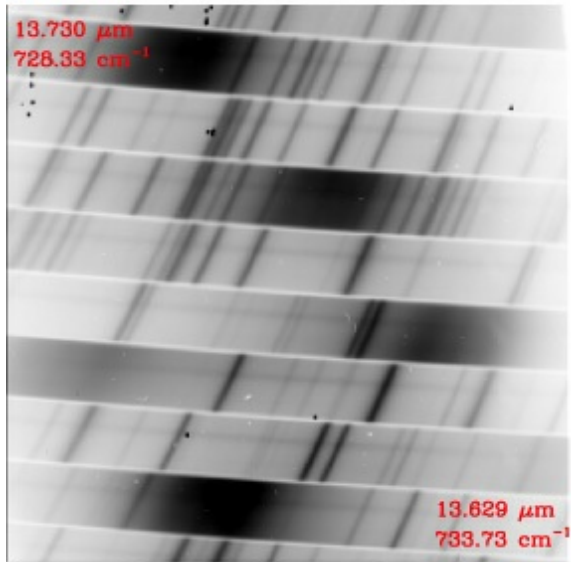
EXES will not use the secondary for chopping in any of its observations. There will be two scientific modes - Nod and Map mode.

Nod mode: In this mode, the telescope is moved to a new position in order to remove the sky background. For point sources observed with a sufficiently long slit, the telescope is moved such that the object remains on the slit. For sources larger than about a quarter of the slit length, the telescope is moved such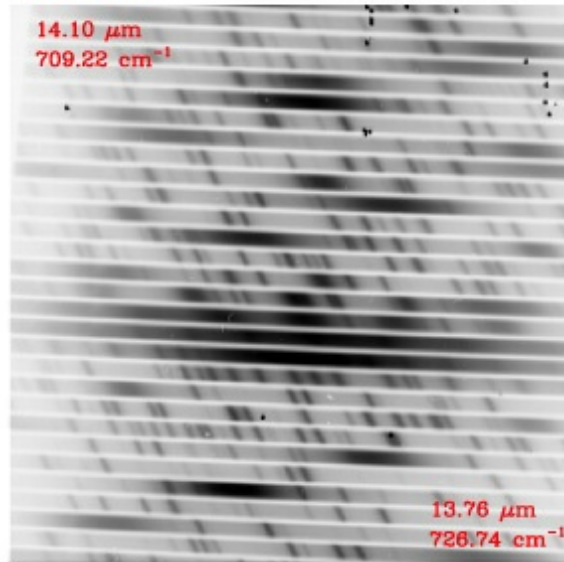 that the object is not on the slit. The time between telescope motions will depend on the sky variation, the telescope settling time, and the integration time. The goal is to maximize the signal-to-noise per clock time. For observations of point sources, the detectable flux plots (Figs. 4-1, 4-2) and the ETC include assumptions regarding whether nodding off the slit is required due to short slit lengths. For nodded observations of extended objects, proposers should contact the EXES team to check if nodding on the slit is possible. If not, the observing time required should be doubled. Unless specific nod parameters are requested for such observations, the instrument team will define the nod amplitude, direction and frequency. The sensitivities for extended source observations shown in Figures 4-3 and 4-4 assume that the source is nodded off-slit and take into account the variation in spatial resolution with wavelength. The atmospheric and overhead factors for nodding are included. If the source is small relative to the slit length, then it may be possible to nod along the slit. In this case, the source brightness given in the figures is for a SNR of 10 in 450 seconds.

Map mode: In this mode, the telescope is moved sequentially such that a series of positions along a straight line on the sky (a "stripe") are observed to create a map. The sky background is taken from the first positions and, depending on the size of the map, from the last positions. In general, we anticipate the telescope motions to be half the slit width to create a well-sampled map.

Proposers should specify the number of steps in a map and the step size. Map steps are generally assumed to be perpendicular to the slit. The first three positions for taking data in a map must be blank sky. These could be the first three positions of the map or at a separate sky offset position specified by the user. It is recommended that additional blank sky positions are observed at the end of the map on the other side of the object. For all maps, the instrument software returns to the sky offset position for three final sky observations at the end of the observation.

Proposers should specify the required clock time based on the flux limit desired, using the values in Figures 4-3 and 4-4, including any assumptions regarding binning of map positions to yield the final required SNR. The SNR for a single map position can be estimated by assuming that the required time is similar to that for nodding an extended object on slit, i.e. 10σ in 450 seconds for a given source brightness. If any spatial binning is required -- at least a 2-step sum is recommended -- then the SNR will improve by the square root of the number of steps in the sum. The online ETC allows the user to specify the number of steps and bins according to the predicted image quality in producing a clock-time estimate.

4.2.1 Wavelength Calibration

Wavelength calibration with EXES will be performed by applying the grating equation to atmospheric lines observed in the source spectra. As long as there is a single telluric feature in the bandpass with depth of at least 5%, the wavelength calibration is expected to be accurate to $\cong 0.5$ km s^{-1}. More concrete values for the calibration accuracy will be available once the commissioning data have been analyzed.

If atmospheric models show no telluric features within the EXES instantaneous band pass for a given observation then obtaining a good wavelength solution will require a few additional steps. Note that the absence of telluric features from SOFIA suggests the observation may be better done from the ground. First, the order sorting filter (OSF) is rotated so that a different order from the echelle is observed that includes a suitable telluric line. The grating equation can then be applied, providing wavelength calibration accuracy down to ≈ 1 km s^{-1}. The process of rotating the OSF, observing blank sky, and rotating the OSF back to the original orientation should take less than 5 minutes of additional time. A demonstration of this procedure can be found in Harper et al. (2009, ApJ, 701, 1464).

4.2.2 Flux Calibration and Atmospheric Line Correction

For every EXES science observation, the EXES temperature-controlled black body source and a nearby blank sky field will be observed. From these, a calibration spectrum will be constructed that, after division over the science observations, will correct for response variations, provide flux calibration, and correct for telluric absorption lines. The flux calibration is expected to be better than 20%, but the true accuracy is currently uncertain. Experiments focused on line profile information and those that can normalize the continuum level, or use past observations for setting the continuum, will likely be more successful. Telluric corrections are expected to be accurate in wavelength regions where the atmospheric transmission is > 0.50. Projects requesting a telluric calibration object, in particular those observing lines near strong telluric features or those observing relatively broad lines, will need to include the observation time required in their proposal. Because of the difficulty of scheduling a given telluric calibrator with the science target in a given flight, the specific calibrator will need to be chosen at the time of flight planning in consultation between the program GI, the instrument PI and the SMO support scientist. For wavelengths below 8-10 μm this will most likely be a hot, bright star (e.g., Vega or Sirius) and at longer wavelengths an asteroid. Galilean moons will also be considered, provided they are well separated from Jupiter.

For the proposal, a separate observation entry should be entered via SPT with name "Cal_target", where "target" is the name of the associate science target (i.e.

"IRC+10216" and "Cal_ICR+10216"), and given the coordinates RA:12:00:00, Dec:+90:00:00. The observing time for such a telluric standard observation will depend on the instrument configuration and wavelength observed, as well as on the signal-to-noise level needed.

Proposers must use the EXES ETC to estimate this, assuming a continuum brightness of 100 Jy below 10 μm and 150 Jy above 10 μm for the High_Medium and High_Low configurations. For the Medium configuration, a brightness of 50 Jy should be assumed, and for Low, 25 Jy at all wavelengths. Proposers are urged to limit the EXES clock times on the telluric standard at a given wavelength and instrument configuration to less than about 30 minutes. Further improvement of the removal of telluric absorption features may be achieved by employing models of the Earth's atmospheric transmission.

4.2.3 Overheads

The treatment of overheads for EXES differs from that of most other SOFIA instruments. Instead of on-source times, users are required to specify "wall clock" times in SPT and SSPOT, which is the on-source time plus all overheads except those related to acquisition and instrument set-up. The overheads include time on "empty" sky in the off-slit nodding and mapping modes, as well as read-out and other telescope and instrument inefficiencies. The ETC and the Figures in this manual give the clock times needed. The figures in this manual only give clock times. SPT and SSPOT will add an additional 15 minutes for peak-up, wavelength optimization, flux calibration, and flat field overheads in the High_Medium, Medium, and Low configurations, and 20 minutes in High_Low. In all configurations, an extra 3 minutes of peak-up time is needed for the narrow (1.4") slit.

If no peak-up is necessary (e.g., after a wavelength change on the same target, if the source is extended, or if the continuum emission is too weak), the overheads can be reduced by using the 'alternative overhead' option in SPT and the "No Peak-Up" option in SSPOT. Overheads can also be reduced if multiple sky positions are observed in the same wavelength setting. In this case, click the "No Wavelength Setup" button in SSPOT. Note however that the time on a given target on a single flight is limited to 90-180 minutes, so full overheads may be needed again once the sum of AOR times exceeds 90 minutes. Conversely, if a single observation takes more than 90 minutes, it may need to be split into multiple AORs, each with full overheads. Please consult the EXES and SOFIA staff in these cases.

4.3 EXES as a Principal Investigator Instrument

EXES is a Principal Investigator (PI) class instrument. The proposer is encouraged (but not required) to contact the Instrument PI, Dr. Matt Richter, before preparing or submitting the proposal, since the PI has the most up to date information about the instrument capabilities. However, it is recommended that they do so, in order to get the most up to date information about instrument capabilities. The data collection and reduction will be done by the instrument team, and it is expected that data analysis and preparation of the results for publication will be done by the General Investigator(s) in collaboration with the Instrument Team.

5. Instruments II: FIFI-LS

5.1 FIFI-LS Instrument Overview

The Far Infrared Field-Imaging Line Spectrometer (FIFI-LS) is an integral field, far infrared

spectrometer. The instrument includes two independent grating spectrometers sharing one common field-of-view (FOV). Each spectrometer has a detector consisting of 400 pixels of Germanium Gallium-doped photoconductors. The short wavelength spectrometer (blue channel) operates at wavelengths between 50μm and 125 μm, while the long wavelength spectrometer (red channel) covers the range from 105 μm up to 200 μm. One of two dichroics has to be selected for an observation affecting the wavelength range of both channels in the overlap region.

The projection onto the sky of the 5 x 5-pixel FOVs of both channels is concentric (10'' offset), but the angular size of the FOVs differs. The red channel has a pixel size of 12" x 12" yielding a square 1' FOV , and the blue channel has a pixel size of 6" x 6", which yields a square 30" FOV.

The resolving power of both channels varies between 1000 and 2000 dependent on the observed wavelength. The higher values are reached towards the long wavelength ends of each spectrometer.

The detectors are cooled down to about 1.7K with super fluid helium. The spectrometers and all mirrors are cooled down to 4K with liquid helium. The exception is the entrance optics featuring a K-mirror (see Sect. 5.1.3) and an internal calibration source. These optical components are cooled to about 80K with liquid nitrogen.

5.1.1 Integral Field Concept

The integral field unit (IFU) allows FIFI-LS to obtain spectra at each point in its FOV in contrast to a spectrometer with a slit which only provides spectra along the slit. Each channel in FIFI-LS has an IFU, which consists of 15 specialized mirrors to "slice" the two dimensional 5x5 pixel FOV into five slices (of five pixels length each) which are then reorganized along a (one dimensional) line (25x1 pixel). This line forms the entrance slit of the actual spectrometer. The diffraction grating disperses the incoming light in the spectral dimension. Finally the dispersed light reaches the 16x25 pixel detector array. The result is a "data cube" with 5x5 spatial pixels (spaxels) and 16 pixels in the spectral "dimension". Figure 5-1 shows the concept.
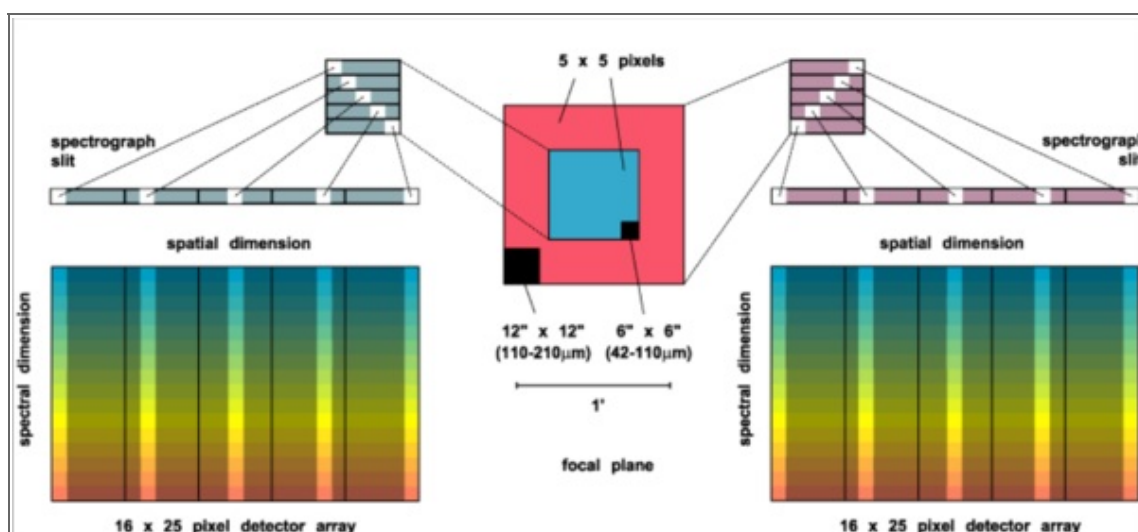

Figure 5-1: Illustration of the field imaging concept in FIFI-LS. The optics slice the rows of the 5x5 pixel field of view into a 25x1 pixel pseudo slit.

5.1.2 Selection of the Dichroic

The two channels have an overlap in their wavelength range. That is necessary because a dichroic splits the light between the two channels allowing the common FOV for both channels. The drawback is that a dichroic has a transition region where neither the transmission nor the reflection is good. Thus, FIFI-LS has two dichroics with transitions at different wavelengths. The The D105 cuts off the blue channel at about 100 μm and opens the red at about 115 μm. he D130 cuts off the blue channel at 120 μm and opens the red at 130 μm. One should look at Figure 5-2 to choose the best dichroic and line combinations. The user needs to pair up wavelengths so that each pair can be observed efficiently with one of the dichroics. Typically, the D105 is used unless a wavelength between 100 and 115 μm is observed.

5.1.3 Beam Rotator

The SOFIA telescope is essentially an Alt-Az-mounted telescope.Thus, the sky rotates while tracking an object. However, the telescope can rotate around all three axes. The amount it can rotate in cross-elevation and line-of-sight is limited though. Thus, the normally continuous sky rotation is frozen-in for some time while the telescope is inertially stabilized. When the telescope reaches its limit in line-of-sight rotation, it needs to "re-wind" resulting in a rotated FOV of the telescope.

FIFI-LS has a beam rotator (K-mirror) that rotates the instrument's FOV, counteracting the sky rotation experienced by the SOFIA telescope. When a "re-wind" happens, the FIFI-LS beam rotator will automatically rotate the FOV of the instrument, so that the position angle of the instrument's FOV on the sky is maintained. An additional benefit is that the beam rotator enables the observer to line up the FOV with e.g. the axes of a galaxy and keep the alignment. The desired position angle of the FOV can be specified in Phase II of the proposal process.

5.1.4 Comparison with the PACS-Spectrometer

The FIFI-LS design is very similar to the Herschel/PACS-spectrometer sharing much of the design. The detectors are basically the same and the optical design is very similar (same sized gratings in Littrow configuration, same IFU). The difference is that FIFI-LS features two grating spectrometers whereas the PACS-spectrometer had only one. The two gratings make it possible to observe two different wavelengths simultaneously and independent of each other (one in each channel). This design also allows different pixel sizes (6'' vs 12'') in each spectrometer, which means a better match to the beam size. The spectral range of FIFI-LS also goes down to 51 μm whereas PACS did not routinely observe the [OIII] 52 μm line.

5.2 Performance
5.2.1 Spectral Resolution

The blue spectrometer operates in 1st and 2nd order. An order-sorting filter blocks the unwanted order. The red spectrometer only operates in 1st order. The spectral resolution of FIFI-LS depends on the observed wavelength. It ranges from $R = \lambda/\Delta\lambda$ ~500 to 2000. That corresponds to a velocity resolution of 150 to 600 km/s. The top panel of Figure 5-3 shows the spectral resolution in velocity resolution and in R vs. wavelength as measured in the lab.

FIFI-LS has 16 pixels in the spectral direction. The wavelength range covered by these 16 pixels also depends on the observing wavelength. The bottom panel of Figure 5-3 shows the instantaneous spectral coverage or bandwidth (BW) in micron.
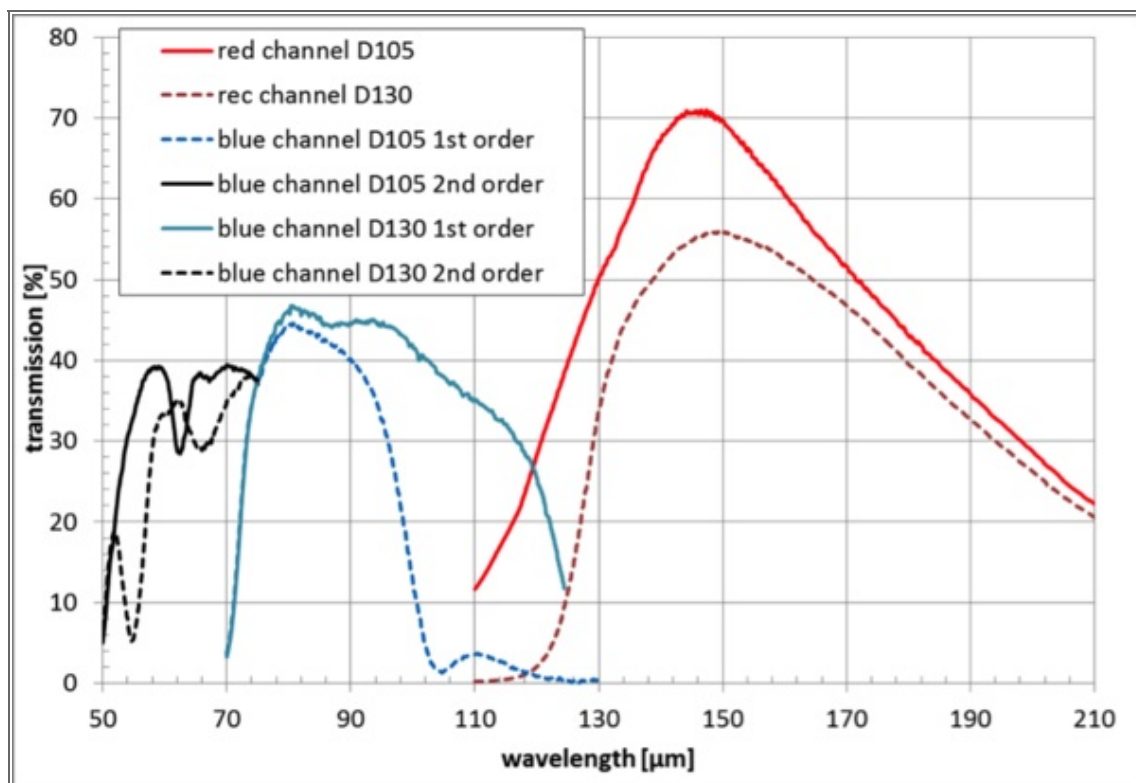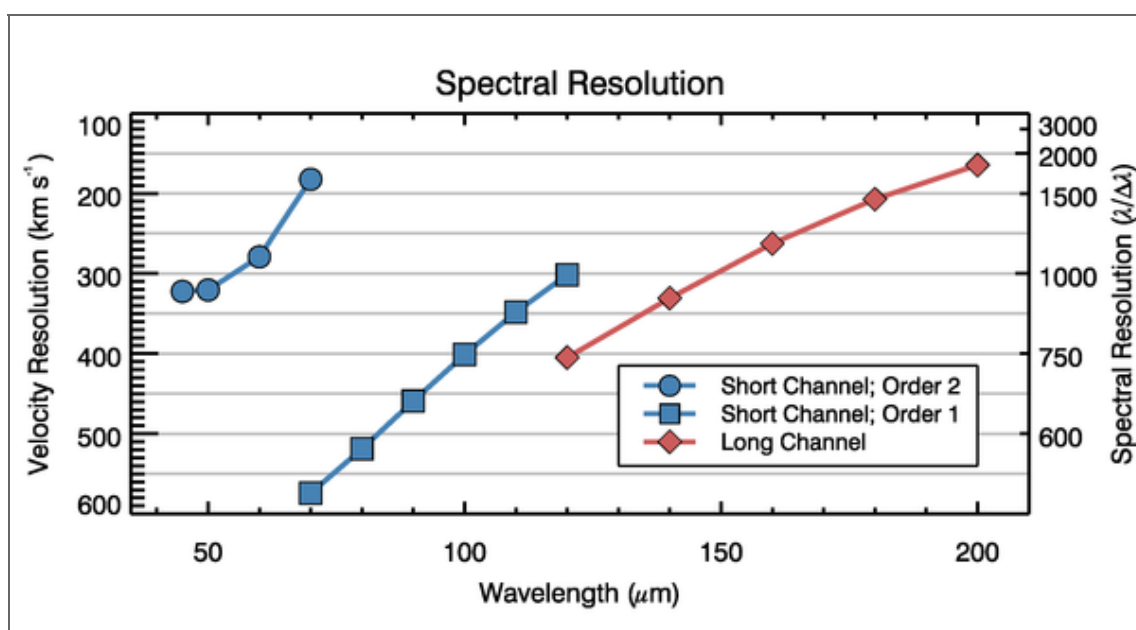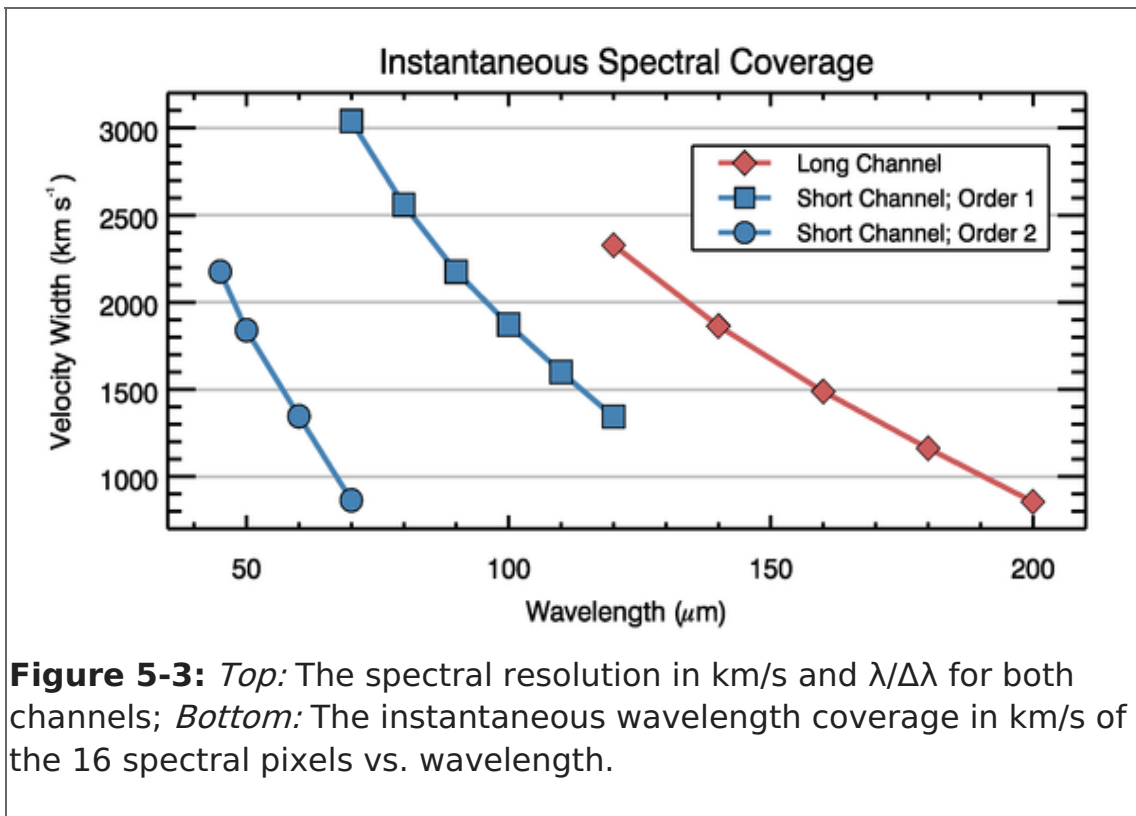

Figure 5-2. Throughput of optical system -- here the transmission of the overall optical system is shown for the six possible optical configurations using two dichroic beam splitters (D105 and D130) and both grating orders (blue channel only).

Figure 5-3: *Top:* The spectral resolution in km/s and λ/Δλ for both channels; *Bottom:* The instantaneous wavelength coverage in km/s of the 16 spectral pixels vs. wavelength.

5.2.2 Integration Time Estimates

FIFI-LS will operate such that the detectors are always background-limited, infrared photodetectors. Under this assumption, the overall performance of FIFI-LS as a function of wavelength has been estimated. Further assumptions about the emissivity of the telescope, optics, and baffling, the efficiency of the detectors had to be made. Figure 5-3 shows the resulting sensitivities for continuum and unresolved lines as minimum detectable fluxes per pixel, i.e. detected with a signal to noise ratio (SNR) of 4 and an on-source integration time of 900 s or 15 min.

The FIFI-LS on-line exposure time estimator should be used to estimate the on-source exposure times used in proposals and observing preparation. The time estimator requires the following input:

- Observatory Altitude (in feet; < 60,000 ft): default 38,000 ft
  This value is used in ATRAN to derive the atmospheric absorption. For more details about ATRAN (see Sect. 3.6).
  On a typical SOFIA flight, observations start at 38,000 ft or 39,000 ft and 43,000 ft are reached 3.5 h before the observations end. The default value of 38,000 ft ensures that time estimate does not underestimates the water vapor overburden. If an observations is rather sensitive to the water vapor, a higher altitude can be entered and justified in the proposal. In Phase II, select "Low" or "VeryLow" for "Requested WV Overburden" in the "Observing Condition"-panel in SSPOT, if the altitude used in the time estimation is 41,000 ft or 43,000 ft, respectively. Note, that this limits the schedulability of the observation to the last 5.5 h or 3.5 h of observations.
- Water Vapor Overburden (in microns; 0 if unknown): default 0 If a value of 0 is given, ATRAN assumes a typical amount of water vapor to derive the atmospheric absorption.
- Telescope elevation (between 20 and 60 deg): default 40 For northern sources an elevation of 40° is okay, but sources south of a declination of -15° will most likely be

observed at a respectively lower elevations unless an observation from the southern hemisphere is required.

- Signal to Noise Ratio or Integration Time (s): default SNR of 5 Specify either a requested SNR and the required on-source exposure time is returned, or specify an on-source exposure time and the resulting SNR is returned.
- Wavelength (in microns, between 51 and 203): default 157.741 μm (rest wavelength of [CII] line) Specify the rest wavelength of the requested transition.
- Source: default 2.087e-17 W m^{-2} line flux (MDLF per pixel for [CII]) Specify the expected source flux *per FIFI-LS pixel* either as integrated line flux in W/m^2 or as continuum flux density in Jansky. Make it obvious in the technical feasibility section of the proposal that the referenced flux estimates have been converted to FIFI-LS pixels sizes.
- Velocity correction (source VLSR, in km/s): default 0 km/s Enter the source velocity relative to the local standard of rest. The resulting Doppler-shift is important to estimate the atmospheric extinction.
- Bandwidth: default 0 km/s Enter the desired width of the spectrum. The width should allow for sufficient baseline on both sides of the expected line/spectral feature to allow a good estimate of the underlying continuum telluric or astronomical. This value enters the time estimate only, if the requested bandwidth is larger than the instantaneous bandwidth. The time estimator calculates the on-source integration time per map position for a source flux, *F* and a desired SNR using,

$$t_{on} = l \left(\frac{SNR/4}{\alpha F/MDF(\lambda)} \right)^2 900 \, s,$$

where MDF(λ) is either the Minimum Detectable Continuum Flux (MDCF) in Jy per pixel or the Minimum Detectable Line Flux (MDLF) in W m^{-2} per pixel at the entered wavelength (see Figure 5-4). The factor α is the transmission of the atmosphere for the observing wavelength derived by ATRAN. The on-line time estimator includes a plot of the transmission smoothed to the spectral resolution of FIFI-LS at the observing wavelength over the bandwidth from ATRAN. If the desired spectrum is wider than the instantaneous bandwidth, *l* is the ratio of the requested width of the spectrum and the bandwidth (Figure 5-3). Otherwise *l* is equal to 1.

The exposure time estimator returns the *on-source* exposure time *per map position* t_{on}. If mapping is planned, this values has to be multiplied with *N*, the number of map positions, to derive the total on-source observing time. More on mapping can be found in Sect. 5.3.5. The total on-source observing time *N* x t_{on} has to be entered into SPT during phase I of the prosal process. The overhead depends on the observing mode (Sect. 5.3.5) and gets automatically added by SPT.

Be conservative with the time estimates! Unforeseen issues like thunderstorms or computer crashes may cut the observing time short. Better to aim for 5σ and get a 4σ result, than aim for a 3σ and then wonder, if there is a 2.4σ signal.

Minimum Detectable Continuum Flux

Minimum Detectable Line Flux
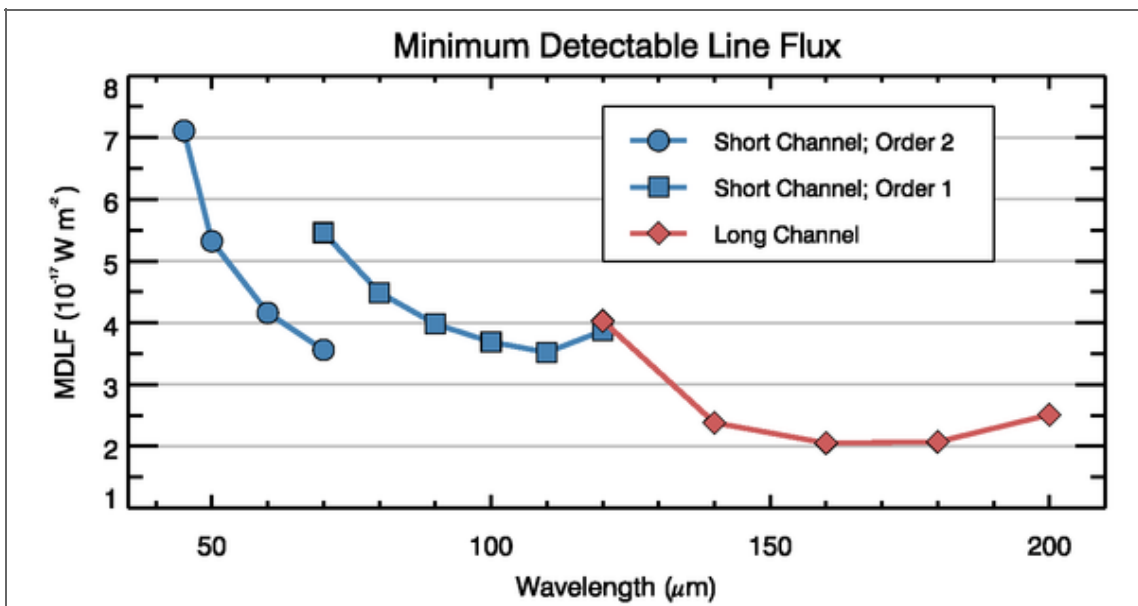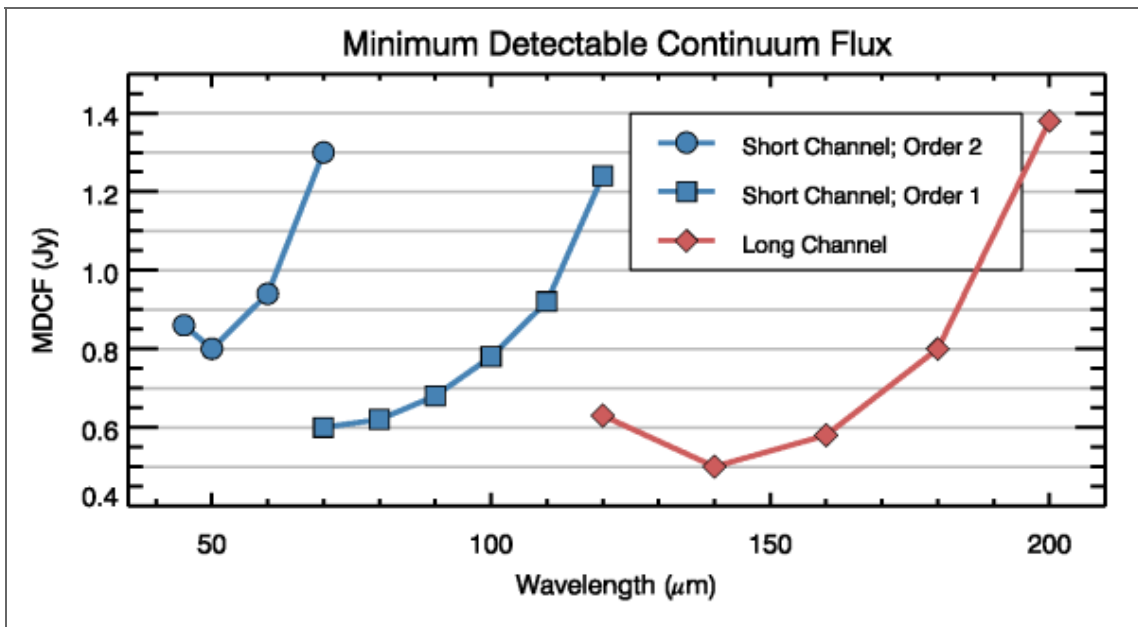
Figure 5-4: Continuum and emission line sensitivities for a monochromatic point source: The values are calculated for a *SNR* of 4 in 900 s. The MDCF is in Jy per pixel and the MDLF is in Wm^{-2} per pixel. Both sensitivity values scale as SNR / $\sqrt{t}$, where t is the on-source integration time.

5.3 Observing Modes

The high sky background in the far infrared requires careful subtraction. That is achieved by chopping with SOFIA's secondary mirror and by nodding the telescope. The secondary will chop at 2Hz to efficiently remove the sky emission. To remove residual background not canceled by chopping, the telescope is nodded typically every 30s either to move the source to the other chop-beam or to an off-position. Since the instrument telescope communications and the telescope move take 10 s, a whole nod-cycle takes typically 80 s."

The following sections describe the possible observing modes. In the discussion of the overheads, N is the number of map positions and t_{on} is the on-source exposure time per map position. The main driver to choose the observing mode is to figure out possible

chop configuration. However, the details like the exact chop throw and angle and other observing details do not need to be fixed until phase II of the proposal process. Information on how all the parameters for each mode has to be entered into SSPOT during phase II of the proposal process can be found on the Cycle 4, Phase II web page.

5.3.1 Observing Mode: Symmetric Chop

If possible this observing mode should be used, because the most efficient mode. This mode combines chopping symmetrically to the telescope's optical axis with a matched telescope nod to remove the residual telescope background. This mode is also known as nod-match-chop (NMC) mode (cf. FORCAST Sect. 7.3.1) or beam switching (BSW, cf. GREAT Sect. 9.1.1).

When observing using a symmetric chop, large chop amplitudes degrade the image quality due to the introduction of coma. This effect causes asymmetric smearing of the PSF in the direction of the chop. However, the effect is small (effect on SNR less than 10%) in the red channel for all chop throws and in the blue channel for total chop throws less then 5' and wavelengths longer than 63 µm.> For wavelengths shorter than 63 µm, we recommend total chop throws of less than 4'. Generally, it is recommended to use a chop as small as possible, but keep the FOV in the off-positions outside of any detectable emission.

The position angle of the chop can be specified relative to equatorial coordinates or telescope coordinates (e.g. horizontal). Keep in mind that the telescope nod matched to the chop creates two off-positions symmetric to the on-position (Figure 5-5, Left).

The total overhead in this mode is about 1.7 N t_{on} + 300 s, since the source is only observed during 50% of the observation and additional time is required for telescope moves, plus 300 s for the setup. This overhead estimate assumes that the on-source exposure time per map position t_{on} is at least 30 s. If the on-source exposure time per map position t_{on} is less than 10 s, the Bright Object Mode should be used. For values of t_{on} in between, one needs to enter an alternate overhead in SPT. The total alternate overhead is $N(t_{on}$ + 20 s) + 300 s.
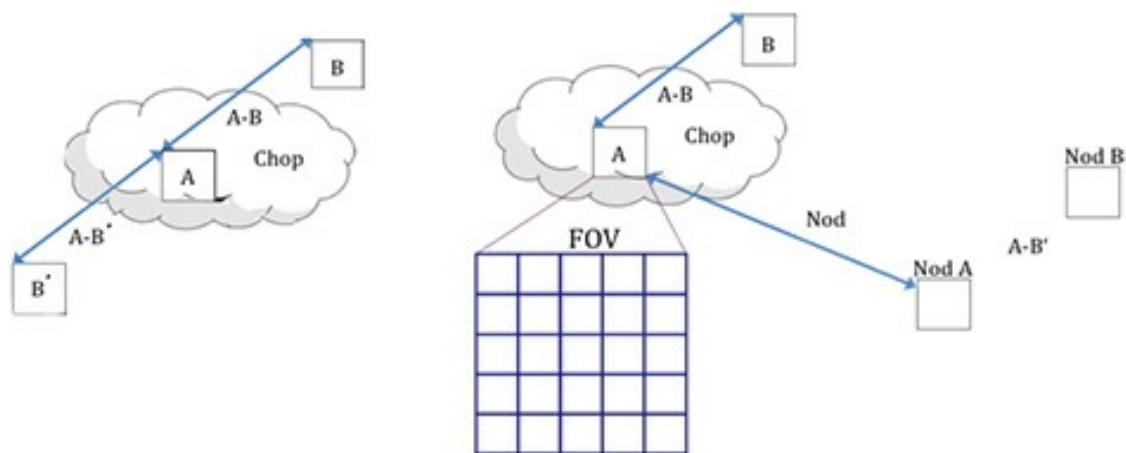
5.3.2 Observing Mode: Asymmetric Chop and Fast Asymmetric Chop

If the target's size or environment does not allow to use the Symmetric Chop Mode, one has to use the Asymmetric Chop Mode allowing larger chop throws at shorter

wavelengths and is not creating symmetric off-positions around the source. The asymmetric chop keeps the on-beam on the optical axis. This results in an image unaffected by coma. Consequently, the off-beam is off-center by twice the amount compared to the symmetric chop with the same chop throw resulting in twice as much coma. But that is of no consequence as the off-beam should only see empty sky. The telescope is nodded to an off-position where the same chopped observation is executed to provide the residual background subtraction. Figure 5-4 illustrates this geometry. Note that this mode is similar to FORCAST's asymmetric chop-offset-nod (C2NC2) mode (see 5.3.1).

The total overhead in this mode is about $4.3N\, t_{on} + 300$ s, since the source is observed during 25% of the observation plus additional time for telescope moves and 300 s for the setup. This overhead estimate assumes that the on-source exposure time per map position t_{on} is at least 15 s. For shorter values of t_{on}, the Bright Object Mode should be used.

5.3.3 Observing Mode: Bright Object

For very bright objects, where the estimated on-source exposure time per map position is 10 s or less, the total observing time is dominated by telescope moves. The efficiency of mapping such bright objects can be improved by observing two map positions and one off-position per nod-cycle using an asymmetric chop. In this mode, the total overhead is $5\, N\, t_{on} + 300$ s assuming an on-source exposure times per map position of about 5 s.

5.3.4 Observing Mode: Spectral Scan

This mode is offered on a shared risk basis. In contrast to the other observing modes, this experimental mode targets spectral features much wider than the bandwidth (see Sect. 5.2.1) like solid state features. The problem is a good atmospheric calibration over the whole observed wavelength range. The spectrum has to pieced together from many different exposures. In Cycle 3, such an observation is being conducted. The best way to take such data and how to reduce it is still being investigated. If this observing mode is considered, please contact the instrument scientist via the SOFIA Help Desk.

5.3.5 Spectral Dithering

Spectral dithering is always employed for self flat-fielding and increased redundancy. Spectral dithering implemented via a grating scan. The grating is moved in small steps, so that the spectrum moves over different pixels in the spectral dimension of the detector array.

The default pattern to cover the instantaneous bandwidth (BW, Sect. 5.2.1) is to move the grating 12 steps, each corresponding to half a spectral pixel width. This pattern results in a spectrum about 30% wider than the BW. The central 70% of the BW are observed during the whole observing time reaching the full SNR, while the remaining 15% on each side of the BW should reach on average 86% of the SNR. The SNR reached on the extra 30% should still be 46% on average based on the observing time for each part of the spectrum. For wider spectral coverage, the step size and number of steps of the grating scan will be adjusted by the instrument operators to achieve the desired spectral coverage. The steps will be evenly distributed over the nod-cycles.

5.3.6 Mapping

Mapping is supported by all of the three regular observing modes. It can be done on a rectangular grid with a user-defined spacing and extent. It is also possible to supply a list of mapping positions to achieve a map with a custom shape optimized to the source geometry. For both map types, a spacing of half a red array or 30'' might be a good choice, providing half pixel steps to achieve super-resolution with a good overlap for the red array and full coverage (but no overlap) for the blue array. Similarly, a spacing of 15'' yields super-resolution with a good overlap for the blue array and a very strong overlap for the red array. These details need to be specified only in Phase II of the proposal process (see the FIFI-LS Cycle 4, Phase II web page). In Phase I, the effective map area needs to be entered in SPT and the proposal should explain the suggested mapping strategy. The on-source integration time to be entered in SPT has to be the on-source integration time per raster point multiplied by the number of raster map points $N\, t_{on}$.

If the source geometry allows the off-beam to be positioned symmetrically on both sides of the source, then one should use the much more efficient Symmetric Chop Mode for mapping. If that is not possible the Asymmetric Chop Mode has to be used. An asymmetric chop is also used in the bright object mode. Figure 5-6 illustrates mapping with an asymmetric chop. The off-beam (positions B1 to B3) covers an area while chopping that is the same size as the map itself. If this is undesirable, the map needs to be broken up into sub-maps with varying chop parameters to be specified in Phase II. The availability of guide stars might be another reason to break up a large map into sub-maps. In this case the sub-maps will be identified between Phase II and the actual observation by the support scientist in close collaboration with the guest investigator and the telescope operator.

When estimating the on-source integration time (Sect. 5.2.2), take into account the differing overlap of the red and blue FOV at the desired raster map spacing. The SNR entered into the calculation of t_{on} is the SNR for a single raster map point. The final SNR for a point in the map should reach &radic(n) x SNR with n being the number of raster points from which a point is covered by the respective FOV. For example in Fig. 5-6, the area of the pixel in the middle is covered by 3 FOVs while 16 pixels are covered by 2 FOVs and the outer parts of the map are covered by 1 FOV.
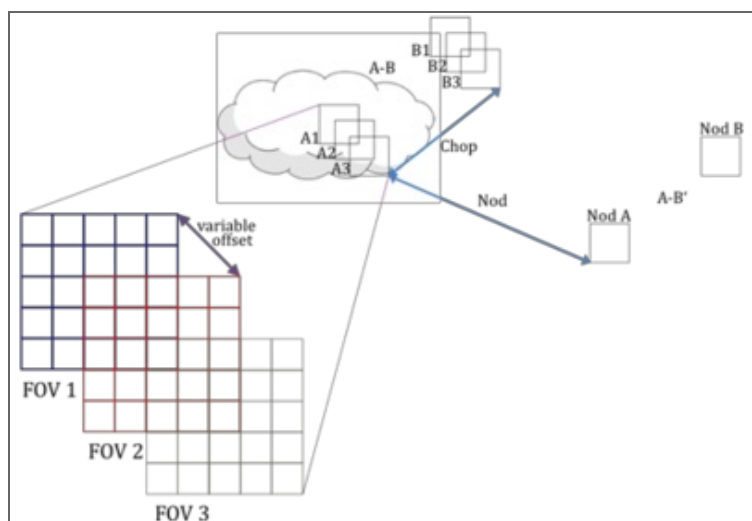

Figure 5-6: The geometry of chopping and nodding while mapping using the asymmetric chop mode.

6. Instruments III: FLITECAM

6.1 FLITECAM Instrument Overview

The **F**irst **L**ight **I**nfrared **TE**st **CAM**era (FLITECAM) is an infrared camera operating between 1.0 - 5.5 microns. It consists of a 1024x1024 InSb detector with 0.475''x0.475'' pixels and uses refractive optics to provide a ~8' diameter field of view. The instrument has a set of broadband filters for imaging, as well as grisms for moderate resolution spectroscopy.

Additionally, FLITECAM was designed to be co-mounted on the telescope with the **H**igh-speed **I**maging **P**hotometer for **O**ccultations (HIPO), providing simultaneous optical through near-IR (NIR) imaging capabilities. This mode, called FLIPO, is described in detail under Section 7, below.

6.1.1 Design

FLITECAM consists of a cryogenically cooled near-IR (NIR) camera that can be used for both imaging and grism spectroscopy. A schematic of the optical bench is shown in Figure 6-1 with a full ray trace diagram in Figure 6-2. The incoming beam first passes through the entrance aperture and into the collimator assembly, a stack of custom designed lenses that allow imaging of nearly the entire 8'x8' SOFIA field of view (FOV). The beam is then repositioned using three flat fold-mirrors so that it passes through the image pupil and through a pair of 12-position filter wheels. A fourth flat fold-mirror redirects the beam through the f/4.7 refractive imaging assembly, which then focusses the beam on the array.

When observing in spectroscopy mode, only minimal changes to the optical path are required. First, the slit mask is inserted into the beam immediately behind the aperture window at the telescope focus. The slit is a single 16.5 mm long slit (2' on the detector) divided in half with two different widths, one approximately 2'' and the other 1''. Second, the chosen grism and order sorting filter, located in filter wheel #2 and #1, respectively, are set in place. Details are presented in Section 6.1.5 below.
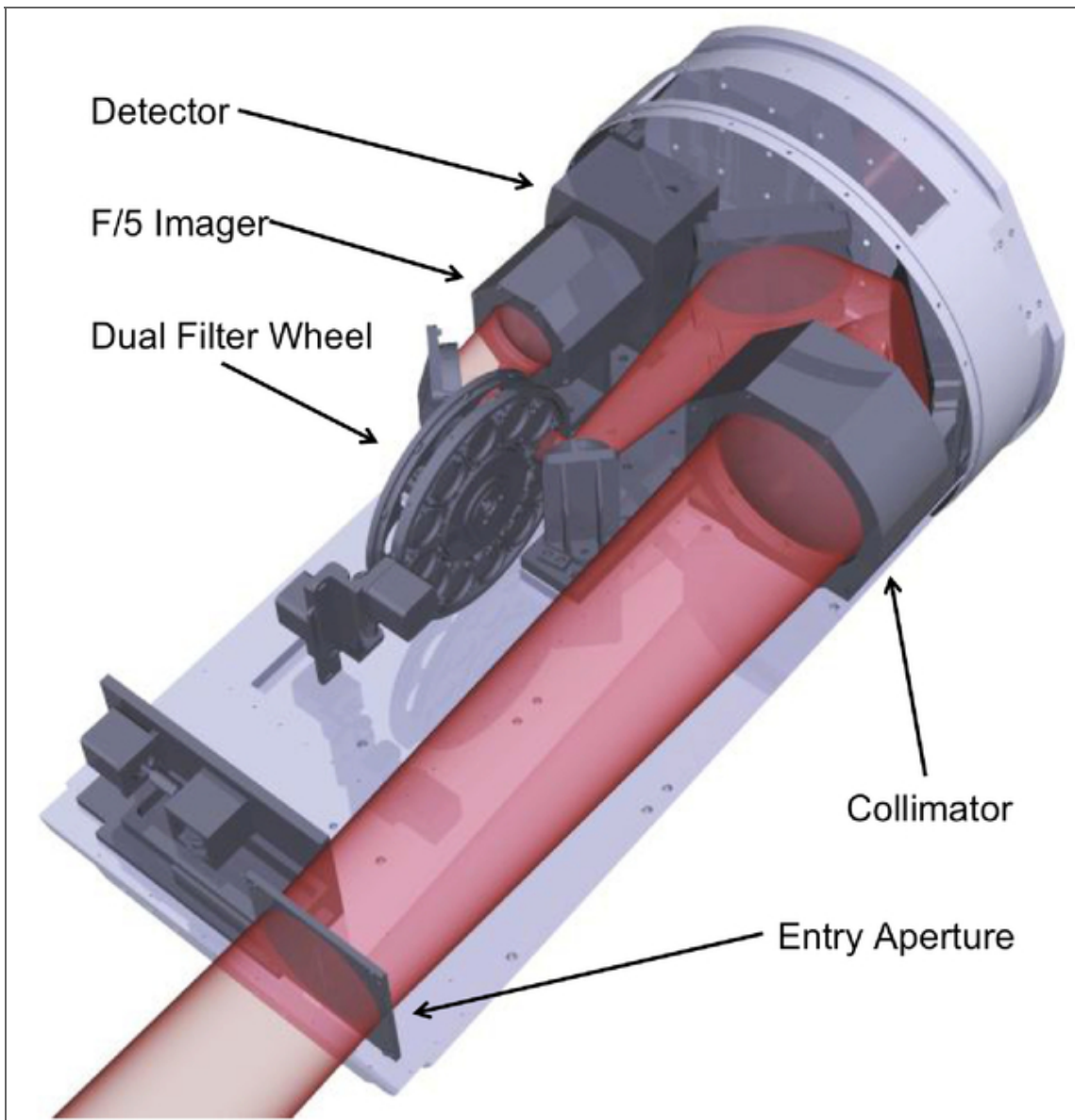
Figure 6-1: This is a block diagram of the front end of the FLITECAM instrument with labels of important components.
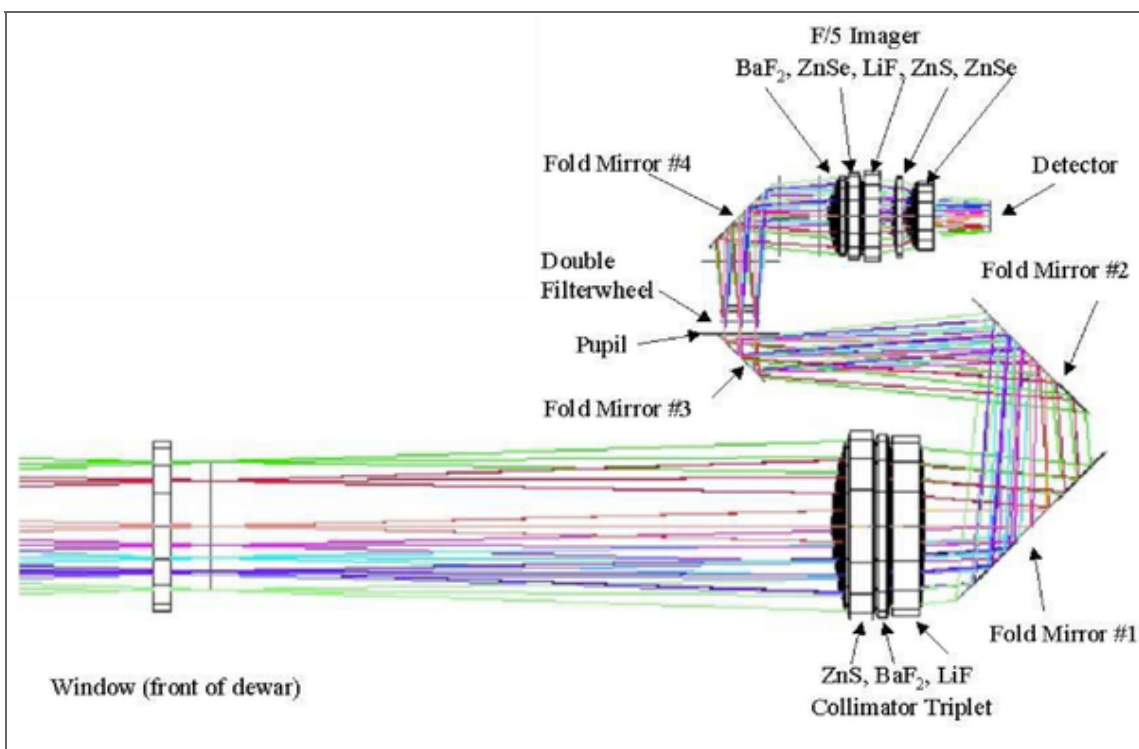
Figure 6-2: This is the ray diagram for the FLITECAM instrument. The inset at the upper left displays the additional lenses inserted into the light path for the pupil-viewing mode.

6.1.2 Camera Performance

The FLITECAM detector is a 1024x1024 pixel indium antimonide (InSb) Raytheon ALADDIN III array cryogenically cooled to 30 K. The detector has 27 μ pixels which translate to a plate scale of 0.475 per pixel, resulting in a nearly 8' square FOV. The detector is optimized for use between 1 - 5.5 microns, and has a read noise of ~40 e$^-$ and dark current of ≤1 e$^-$ sec^{-1}.

The on-axis image quality (IQ) of the camera is excellent and images obtained with FLITECAM are expected to be diffraction limited from 3 - 5.5 μm. From 1 - 3 μm, the IQ will be limited by contributions from the telescope optics, telescope jitter, shear layer seeing, and the diffraction limit. Ground based tests under the best conditions at the Lick Observatory indicated that the IQ is stable within 1.5' of the optical axis, but that beyond this distance, coma begins to appear. The extent of the coma has not yet been parameterized.

The detector well depth is relatively shallow, ~80,000 e$^-$, which, when combined with the detector QE, may necessitate relatively short exposure times, particularly on bright sources or in regions of high sky background. The shortest exposure time available for a full 1024x1024 detector readout is 0.2 seconds. However, faster readout times can be achieved using sub-arrays -- 0.08 seconds for a 512x512 sub-frame and 0.015 sec (~67 Hz) for a 64x64 pixel sub-frame. These subarrays are required to be symmetric and relative to the center of the detector. An additional movie'' mode is avaiable to sample a single 512x512 quadrant at ~0.08 seconds without any deadtime between images, or down to the 32x32 sub-frame (closest to the detector center) at < 0.015 seconds. Users interested in these modes should consult the FLITECAM Instrument Scientist via the SOFIA Help desk (sofia_help@sofia.usra.edu).

Care must be taken not to over-expose the detector since charge persistence can be a significant problem for InSb arrays. If the detector is over-exposed, it is necessary to take several long exposures (~5 minutes each) of blanks mounted in the filter wheel to allow the detector to recover. To help mitigate the problem of accidental saturation of the detector, filter changes are carefully orchestrated to ensure that the sky is never viewed through the two open filter wheel positions.

6.1.3 Filter Suite

The core of the FLITECAM filter suite is a set of standard Barr bandpass filters used for imaging at J, H, K, L, & M, which are all located in filter wheel #1. In addition, filter wheel #2 holds a selection of specialty, narrow-band imaging filters, including Paschen α and Paschen α continuum filters, an ice filter centered on the 3.07 μm H_2O ice feature, a polycyclic aromatic hydrocarbon (PAH) filter centered on the prominent 3.3 μ feature, and L_{narrow} and M_{narrow} filters. Finally, there are a number of order sorting filters (OSFs) for use with the grisms, including J and H (both dual purpose), K_{wide}, K_{long}, and ''L+M''. Additional details of the OSFs are given in Section 6.1.5.

As the bulk of the instrument commissioning was performed in the combined

FLITECAM/HIPO (FLIPO) mode, some of the FLITECAM observation modes lack detailed performance characterics. This is due to the lack of circulation of stratospheric air down the Naysmyth tube which keeps the FLIPO foreoptics at cabin temperature, greatly increasing the observed background. Some experience in these modes (generally longward of 3.5 microns) was obtained during the first FLITECAM-only flight series in September/October 2015 and are undergoing analysis at the time of writing.

In the combined FLITECAM/HIPO configuration, imaging observations past 3 microns are required to use increasingly small subarrays; spectroscopic observations past 4 microns are not possible at all. In the FLITECAM-solo configuration, however, full-frame imaging observations are possible out to 4 microns, and the full suite of FLITECAM grisms are available.

The central wavelengths and band widths of the available imaging filters are provided in Table 6-1. This table also includes the sensitivity values (Minimum Detectable Continuum Flux; MDCF) discussed in Section 6.1.4. Filters that will only be available on a *shared risk* basis during Cycle 4 are indicated. Figure 6-3 displays the transmission profiles (normalized to their peak transmission) for the imaging filters over-plotted on an ATRAN model of the atmospheric transmission. The filter transmission curves are available on the SOFIA 'Science Instrument Suite'' website in the section for FLITECAM.

Table 6-1: FLITECAM Filter Characteristics

FLITECAM Filter Characteristics

Desig-nation	Pass-band	λ_{eff} (µm)	Peak Trans. (%)	5% Band-width[a] (µm)	R ($\Delta\lambda/\lambda$)	MDCF[b] (µJy)	MDCF[c] (µJy)	Profile
Standard Filters								
FLT_J	J	1.239	93.7	0.293	22.3	25.7	27.4	PNG DAT
FLT_H	H	1.631	95.3	0.305	17	33.5	35.7	PNG DAT
FLT_K	K	2.104	95.4	0.395	16.8	38.7	57.5	PNG DAT
FLT_Lprime	L′	3.855	93.5	0.7	15.7	-	-	PNG DAT
FLT_L	L[d]	3.53	94.1	0.65	15.7	440	-	PNG DAT
FLT_M	M[d]	4.838	91.8	0.645	10.8	2720	-	PNG DAT

Desig-nation	Pass-band	λ (µm)	Peak Trans. (%)	5% Band-width (µm)	R (Δλ/λ)	MDCF (µJy)	MDCF (µJy)	Profile
Specialty Filters								
FLT_Pa	Pa α	1.874	84.2	0.033	1.2	179	195	PNG DAT
FLT_Pa_cont	Pa α Cont.	1.9	88.3	0.033	1.2	178	195	PNG DAT
FLT_ICE_308	Ice[d]	3.049	88.1	0.191	5.2	504	1130	PNG DAT
FLT_PAH_329	PAH[d]	3.302	91.4	0.115	2.7	1070	2260	PNG DAT
FLT_NbL	L_{narrow}[d]	3.602	90.5	0.231	5.1	1010	2110	PNG DAT
FLT_NbM	M_{narrow}[d]	4.804	89.5	0.19	3.1	5430	-	PNG DAT
Order Sorting Filters[e]								
Hwide	H_{wide}	1.794	97.1	0.587	29.1	-	-	PNG DAT
Kwide	K_{wide}	2.299	96	0.882	35.3	-	-	PNG DAT
Klong	K_{long}	2.45	95.5	0.55	19.3	-	-	PNG DAT
L+M	L+M	4.11	92.5	2.715	64.2	-	-	PNG DAT

[a] Bandwidth for transmission level is >5%

[b] See Section 6.1.4

[c] Empirically measured MDCF values when FLITECAM is co-mounted with HIPO in the FLIPO configuration.

[d] Will be offered as *Shared Risk* during Cycle 4

[e] Will not be available for imaging
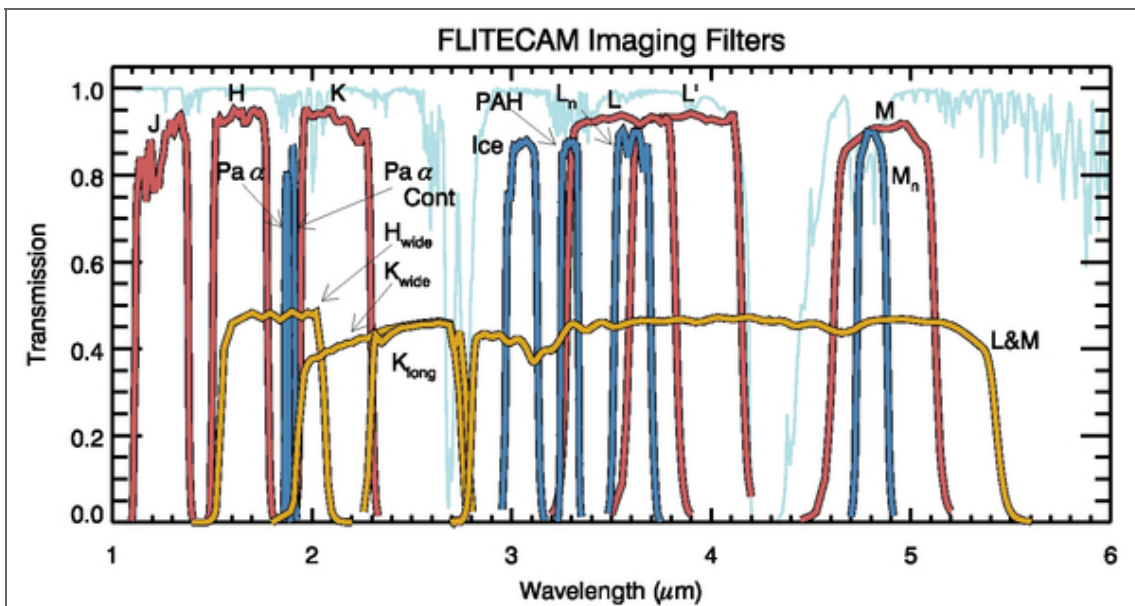
Figure 6-3: Plotted here are the FLITECAM filter transmission curves overlayed on an ATRAN model of the atmospheric transmission across the FLITECAM bandpass assuming a zenith angle of 45 degrees and 7 μm of precipitable water vapor. The transmission profiles of the standard filters are shown in red, specialty filters are shown in blue, and OSFs in gold. The OSF transmission profiles have been scaled by 50% for clarity.

6.1.4 Imaging Sensitivities

At the time of writing, the commissioning of FLITECAM has yet to be completed, and therefore the results of the analysis of in-flight data are not available. Instead, the Minimum Detectable Continuum Flux (MDCF; 80% enclosed energy) in μJy needed to get S/N = 4 in 900 seconds has been estimated for each filter for an altitude of 41,000 feet (7.3 μm of precipitable water vapor) from a model of the instrument and the atmosphere. The values are presented in Table 6-1 above and are plotted in Figure 6-4. The horizontal bars on the data in the figure indicate the effective bandpass at each wavelength. At the shorter wavelengths the bandpass is sometimes narrower than the symbol size.

Atmospheric transmission will affect sensitivity, particularly at wavelengths >4 μm, depending on water vapor overburden. In addition to the theoretical sensitivity values for FLITECAM we have included the as-measured imaging sensitivities in the FLIPO (combined HIPO+FLITECAM) mode. Until the instrument has been more accurately characterized at these longer wavelengths, the L and M band filters will be offered on a *shared risk* basis.

Figure 6-4: Theoretical FLITECAM imaging sensitivities for a continuum point source at the effective wavelengths of the FLITECAM filters listed above (red boxes). Yellow boxes indicate the imaging sensitivities for the FLIPO configuration (i.e. FLITECAM co-mounted with HIPO). The values reported are for a S/N of 4 in 900 seconds at water vapor overburdens of 7 μm. The horizontal bars correspond to the photometric band pass.

6.1.5 Grisms

A selection of three grisms is available in FLITECAM to provide medium resolution spectroscopic capabilities across the entire 1 - 5.5 μm range. The grisms are mounted in filter wheel #2 and are used along with Order Sorting Filters (OSFs) mounted in filter wheel #1 (see Table 6-1) to prevent order contamination. A summary of the grism properties is provided in Table 6-2.

Grisms were chosen for use in FLITECAM since they minimize the changes necessary to the optical path while still allowing moderate spectral resolution. The grisms are made of direct-ruled (i.e. etched) KRS-5 (thallium bromoiodide) material that provides a relatively high index of refraction (n ~ 2.4) without the significant absorption features that plague grisms with adhered transmission gratings. The three grisms were fabricated by Carl-Zeiss (Jena, Germany) each with an apex angle of 34.4°, but with different groove spacings to allow coverage of the entire 1 - 5.5 μm band (see Table 6-2).

Table 6-2: FLITECAM Grism Characteristics

FLITECAM Grism Characteristics

Groove					Coverage (μm)	High-Res (R=λ/Δλ)	Low-Res (R=λ/Δλ)
Designation[a]	Grism	Sep. (l/mm)	Order	OSF[b]			

Groove					Coverage (μm)	High-Res (R=λ/Δλ)	Low-Res (R=λ/Δλ)
FLT_A1_LM	A	162.75	1	L+M[c]	4.395-5.533	N/A	N/A
FLT_A2_KL			2	K_{long}	2.270-2.722	1690	1140
FLT_A3_Hw			3	H_{wide}	1.550-1.828	1710	1290
FLT_B1_LM	B	217	1	L+M[c]	3.303-4.074	1780	1200
FLT_B2_Hw			2	H_{wide}	1.675-2.053	1750	1320
FLT_B3_J			3	J	1.140-1.385	1720	1425
FLT_C2_LM	C[d]	130.2	2	L+M	2.779-3.399	1670	1300
FLT_C3_Kw			3	K_{wide}	1.910-2.276	1650	1390
FLT_C4_H			4	H	1.500-1.718	1640	1400

[a] Order Sorting Filter

[b] Identifier used in the SOFIA Proposal Tool (SPT)

[c] This combination of Grism and OSF will be available on a *Shared Risk* basis during Cycle 4

[d] The C Grism suffers from excess light at the blue end of each order. This issue is under investigation at the time of this writing.

The FLITECAM slit mask is mounted in a fixed slide mechanism at the telescope focus, immediately inside the entrance window to the dewar.

No calibration lamps are installed in FLITECAM. Consequently, wavelength calibration will be performed using atmospheric absorption lines.
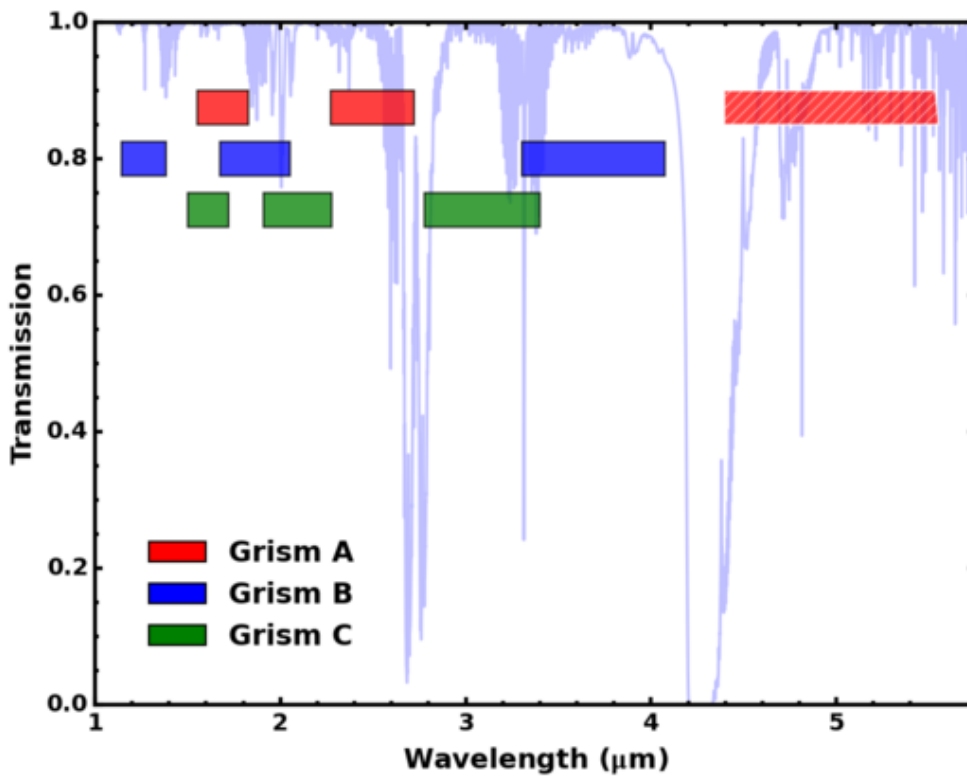
Figure 6-5: Plotted here are band passes for each of the grism + order sorting filter (OSF) combinations available for FLITECAM grism spectroscopy. The grism used for each OSF set is labeled on the right. In light blue is a plot of the ATRAN model of the atmospheric transmission across the FLITECAM bandpass (assuming a zenith angle of 45 degrees and 7 µm of precipitable water vapor).

6.1.6 Spectroscopic Sensitivities

Figure 6-6 presents the *expected* continuum point source sensitivities for the FLITECAM grisms combined with an ATRAN model of the atmospheric transmission. The Minimum Detectable Continuum Flux (MDCF; 80% enclosed energy) in Jy needed for a S/N of 4 in 900 seconds at a water vapor overburden of 7.3 µum, an altitude of 41K feet, and an elevation angle of 45°: (an airmass of 1.4) is shown.
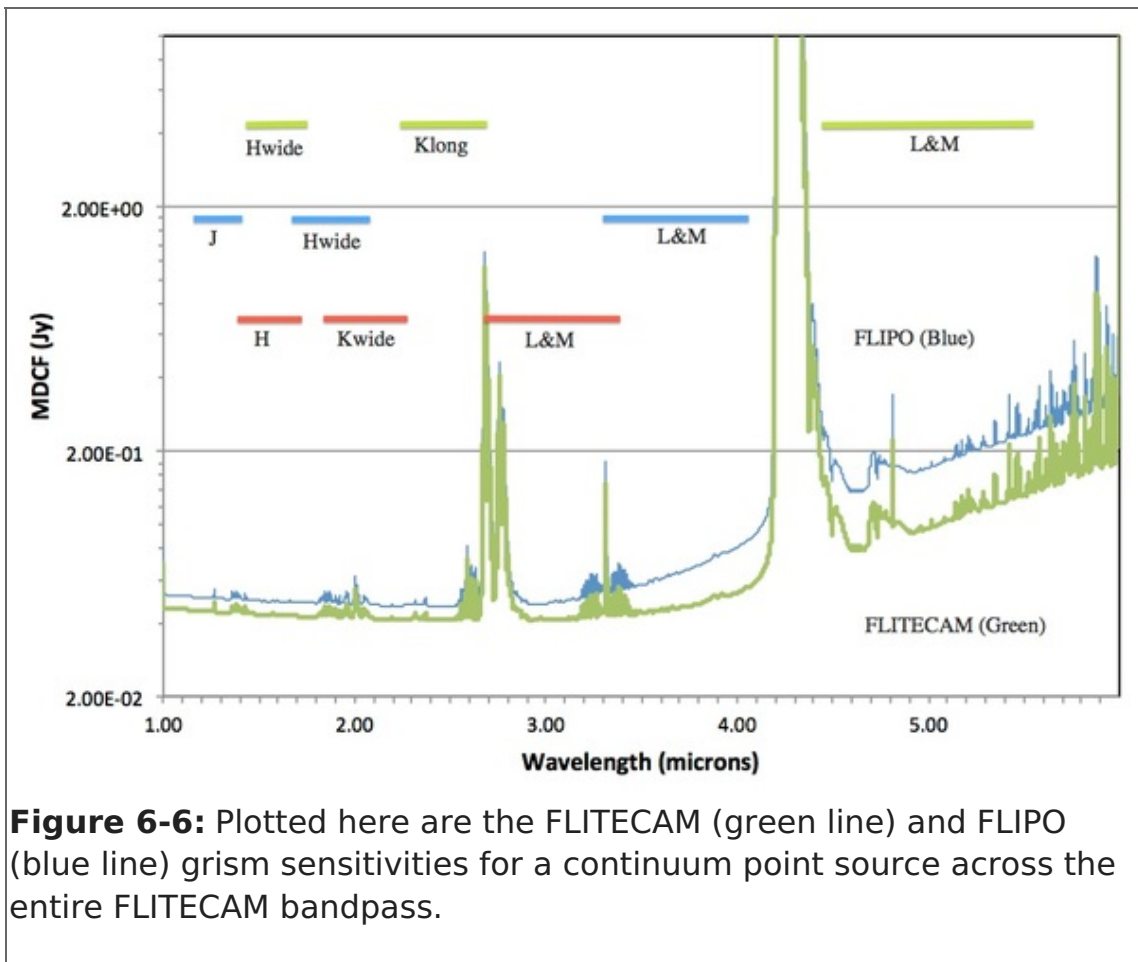
Figure 6-6: Plotted here are the FLITECAM (green line) and FLIPO (blue line) grism sensitivities for a continuum point source across the entire FLITECAM bandpass.

6.2 Planning FLITECAM Observations

Two basic observing modes are available during Cycle 4, imaging and grism spectroscopy. However, commissioning of FLITECAM's longest wavelength modes are still ongoing. For this reason, it is important for GIs to verify that they are using the most recent version of this document as it will be updated regularly as new information becomes available.

6.2.1 Planning Imaging Observations

FLITECAM Imaging observations can be obtained in two different modes, Stare (we recommend using dithers ≥ 9 points) or Nod mode, depending on the target and astronomical background. Chopping is not used.

Stare mode observations involve a single telescope pointing centered on the source with many taken in a pattern relative to it to facilitate background subtraction and image calibration. Dithering can be performed by selecting from pre-programmed dither patterns, or by defining a custom pattern.

If the science target is extended or if it is located in a crowded region or region of extended emission, dithering alone may not be able to produce a suitable sky background frame. In this case the GI may elect to observe using Nod mode which will complete a dither on-source and then nod the telescope to a defined "sky" position and complete a dither there as well. Selection of the nod direction and amplitude depends on the field of view around the target and will need to be chosen carefully to access a clean "sky" position and allow proper background subtraction.

The observing efficiency for FLITECAM Stare mode observations with dithering is

expected to be on the order of 70%. Observations in Nod mode are expected to result in a decrease in observing efficiency to around 35%. However, these efficiencies are built-in to the SOFIA Proposal Tool (SPT; further details in Section 11.1) and do not need to be specified by the GI.

6.2.2 Planning Spectroscopic Observations

Spectroscopic observations with the FLITECAM grisms may be obtained with either an "ABBA" or an "AB" nod pattern that is either on-slit or off-slit.

Guiding during spectroscopic observations will be conducted with either the telescope guide cameras or with HIPO, if FLITECAM and HIPO are co-mounted in the FLIPO configuration (see Section 7).

It is important to note that due to the fixed position of the grisms/slits in the filter/aperture wheels, the orientation of the slit on the sky will be dependent on the flight plan and will not be able to be predetermined. Further, the slit orientation rotates on the sky with each telescope Line-of-Sight (LOS) rewind. These limitations may be especially important to consider when proposing observations of extended objects.

6.2.3 Estimation of Exposure Times

The exposure times for FLITECAM imaging observations should be estimated using the on-line exposure time calculator, SITE. SITE can be used to calculate the signal-to-noise ratio (S/N) for a given "total integration time", or to calculate the total integration time required to achieve a specified S/N. The format of the S/N values output by SITE depends on the source type. For Point Sources, the reported S/N is per resolution element, but for Extended Sources, it is the S/N per pixel. The total integration time used by SITE corresponds to the time for a single chop/nod pair, without overheads.

The exposure times for FLITECAM grism mode spectroscopic observations should be estimated using the on-line exposure time calculator. This calculator can be used to calculate the signal-to-noise ratio (S/N) for a given "total integration time", to calculate the total integration time required to achieve a specified S/N, or to estimate the limiting flux for a desired S/N. For both imaging and spectroscopy modes, the estimated total integration time from the respective calculators should be used as the time for an observation in the SOFIA Proposal Tool (SPT; further details in Section 11.1). **Overheads should not be included**, as SPT calculates them independently.

7. Instruments IV: FORCAST

7.1 FORCAST Instrument Overview

The **F**aint **O**bject infra**R**ed **CA**mera for the **S**OFIA **T**elescope (FORCAST) is a dual-channel mid-infrared camera and spectrograph sensitive from 5 - 40 μm. Each channel consists of a 256x256 pixel array that yields a 3.4'x3.2' instantaneous field-of-view with 0.768'' pixels, after distortion correction. The Short Wave Camera (SWC) uses a Si:As blocked-impurity band (BIB) array optimized for $\lambda < 25$ μm, while the Long Wave Camera's (LWC) Si:Sb BIB array is optmized for $\lambda > 25$ μm. Observations can be made through either of the two channels individually or, by use of a dichroic mirror, with both channels simultaneously across most of the range. Spectroscopy is also possible using a suite of six grisms, which provide coverage from 5 - 40 μm with a low spectral resolution of R =

λ/Δλ ~ 200. The instrument has space for cross dispersing grisms allowing for high resolution cross-dispersed (XD) spectroscopy at R ~ 800 - 1200 in the 5 - 14 μm range.The availability of the XD modes during a given Cycle is published in the Call-for-Proposals.

7.1.1 Design

The FORCAST instrument is composed of two cryogenically cooled cameras of functionally identical design. A schematic of the instrument layout is provided in Figure below. Light enters the dewar through a 7.6 cm (3.0 in) CsI window and cold stop and is focused at the field stop, where a six position aperture wheel is located. The wheel holds the imaging aperture, the slits used for spectroscopy, and a collection of field masks for instrument characterization. The light then passes to the collimator mirror (an off-axis hyperboloid) before striking the first fold mirror, which redirects the light into the LHe-cooled portion of the cryostat.

Figure 7-1.
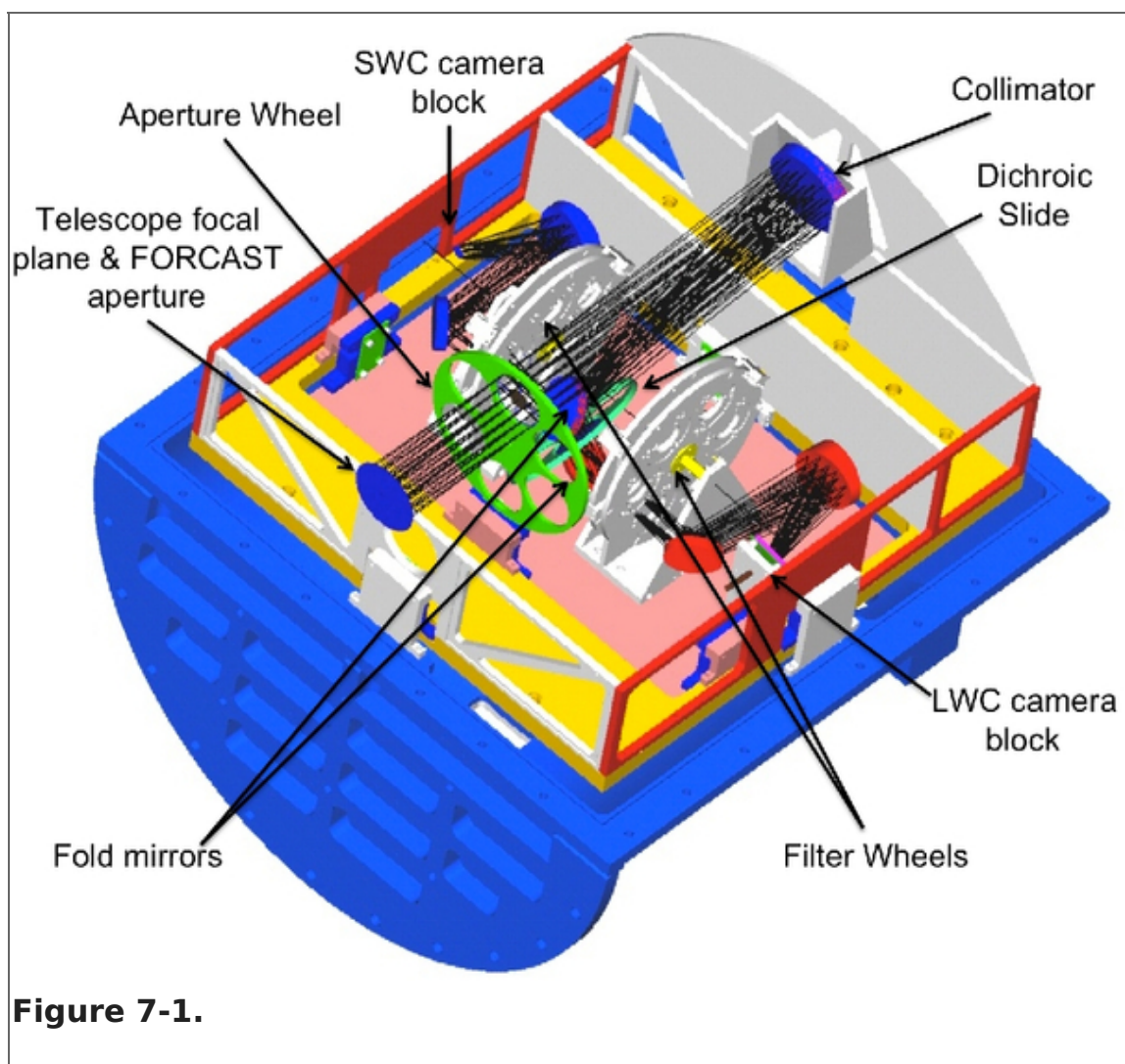
The incoming beam then reaches a four-position slide, which includes an open position, a mirror, and two dichroics, one for normal use and the other as a spare. The open position passes the beam to a second fold mirror, which sends the beam to the LWC, while the mirror redirects the light to the SWC. The magnesium oxide (MgO) dichroic reflects light below 26 μm to the SWC and passes light from 26 - 40 μm to the LWC. The light then passes through a Lyot stop at which are located two filter wheels of six positions each, allowing combinations of up to 10 separate filters and grisms per channel. Well characterized, off-the-shelf filters can be used, since the filter wheel apertures have a

standard 25 mm diameter (see Section 7.1.3).

Finally, the incoming beam enters the camera block and passes through the camera optics. These two-element catoptric systems are composed of an off-axis hyperboloid mirror and an off-axis ellipsoid mirror that focuses the light on the focal plane array. Also included is an insertable pupil viewer that images the Lyot stop on the arrays to facilitate alignment of the collimator mirror with the telescope optical axis and to allow characterization of the emissivity of both the sky and telescope.

7.1.2 Camera Performance

The SWC and LWC arrays were selected to optimize performance across the 5 - 40 µm bandpass. Both arrays have a quantum efficiency (QE) greater than 25% over most of their spectral range. The cameras can be operated with variable frame rates and in either high or low capacitance modes (with well depths of 1.8×10^7 and 1.9×10^6 e⁻ respectively) depending upon the sky background and source brightness.

The best measured image quality (IQ) obtained by FORCAST on SOFIA is in the 7 - 11 µm range with a FWHM PSF of ~2.7''. This measured image quality in-flight is limited by telescope jitter arising from vibrations of the telescope itself (e.g., due to wind loading in the cavity), turbulence, and tracking accuracy. The figure below shows a sample of FWHM IQ measurements made during a single observatory characterization flight during the winter of 2010 in comparison to the theoretical diffraction limit calculated for a 2.5-m primary with a 14% central obstruction combined with the FWHM telescope jitter, here assumed to be 2.08'' (1.25'' rms).
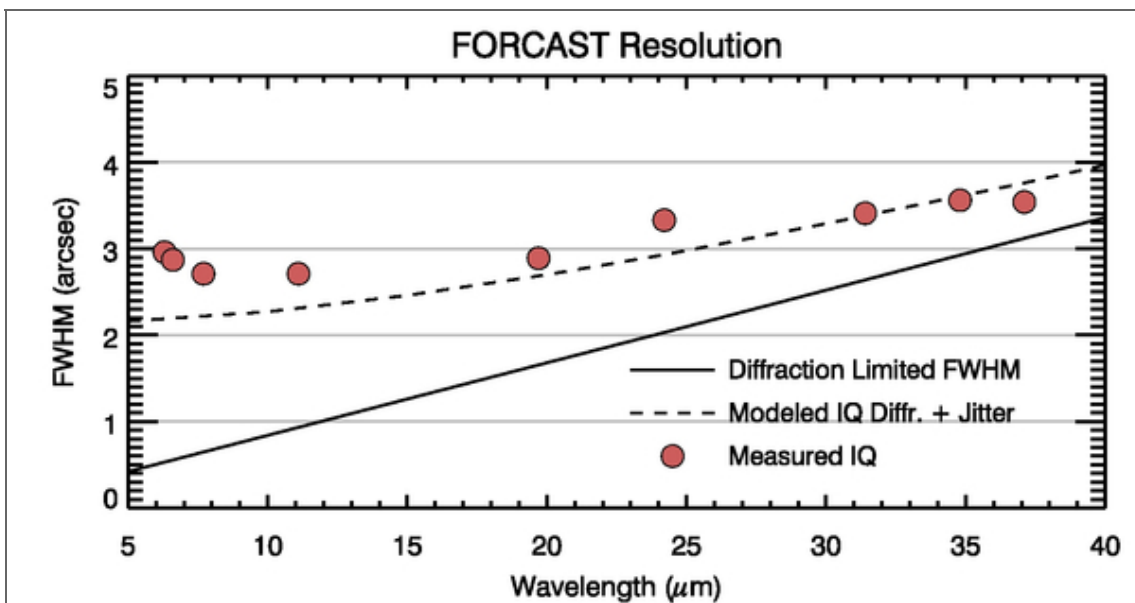
Figure 7-2: Measured FWHM Image Quality of the FORCAST camera in select filters relative to the diffraction limited FWHM (solid line; calculated for a 2.5-m primary with a 14% central obstruction) and the modeled IQ (dashed line), which includes shear layer seeing and 1.25'' rms telescope jitter.

7.1.3 Filter Suite

Imaging with FORCAST can be performed in either a single channel or in both the SWC and LWC channels simultaneously (dual channel mode). In single channel mode any one

of the available filters may be used. In dual channel mode, a dichroic is used to split the incoming beam, directing it to both the SWC and LWC.

The dichroic reduces the overall throughput. Table 7-1 shows the throughput with the dichroic in (Dual Channel mode) relative to that for the Single Channel mode. The degradation of the system throughput by the dichroic can have a significant effect on the instrument sensitivities as discussed in more detail in Section 7.1.4. In addition, since there are more short wavelength filters available than slots in the SWC filter wheels, some short wave filters will be housed in the LWC. The final filter wheel configuration for each observing cycle will be driven by proposal pressure. Depending on the final filter configuration, it is possible that not all LWC filters will be able to be used in dual channel mode due to the cutoff in the dichroic transmission at short wavelengths. Additional details are provided below and will be updated once the results of each cycle's Call-for-Proposals are known.

Table 7-1: FORCAST Dichroic Throughput

FORCAST Dichroic Throughput

Bandpass	Throughput
5-10 μm	60%
11-25μm	85%
25-40 μm	40%

The filters in the SWC are standard Optical Coating Laboratory, Inc. (OCLI) thin-film interference filters. These filters are stacked with blocking filters to prevent light leaks. The only exception is the 25.4 μm (FOR_F253) University of Reading filter, which is a custom double half-wave (three mesh) scattering filter stacked with a diamond scattering blocking filter to provide blue-light rejection. The 33.6 (FOR_F336), 34.7 (FOR_F347), and 37.1 μm (FOR_F371) filters in the LWC are LakeShore custom double half-wave (three mesh) scattering filters. The 31.5 μm filter is a Fabry-Perot Interferometer filter.

The central wavelengths, bandwidths, and the expected FWHM IQ in each of the filters are given in Table 7-2 below. The first column under "Imaging FWHM" presents the best measured FWHM IQ with a telescope jitter of ~1.25'' rms. These values are representative of the IQ observed in Cycle 2. The second column is the average measured FWHM IQ from Basic Science with a ~2.1'' rms jitter and indicates the "worst case" IQ. Not all of the filters have measured IQ values, but we expect that they will be comparable to those with measured values that are of similar λ_{eff}. Figure 7-3 shows the filter transmission profiles (normalized to their peak transmission) over-plotted on an ATRAN model of the atmospheric transmission. The filter transmission curves (text tables) are available as a zip file or individually from Table 7-2.

Due to the limited number of slots available in the filter wheels, not all of the filters listed in Table 7-2 are available at any one time. For Cycle 4, there will be a "default" filter set (indicated by bold type in Table 7-2). GIs may request that other filters be used for their observations, but they must make a convincing scientific argument to justify swapping

out the existing filters for those they desire. We anticipate that a single filter swap may be permitted during Cycle 4 provided there is adequate scientific justification. More details are available in the Cycle 4 Call for Proposals.

Table 7-2: FORCAST Filter Characteristics

FORCAST Filter Characteristics

Channel	Filter	λ_{eff} (μm)	Δλ (μm)	Imaging FWHM ('')		Profiles
SWC	FOR_F054	5.4	0.16	–[b]	–	txt file
	FOR_F056	5.6	0.08	–	–	
	FOR_F064	**6.4**[a]	**0.14**	**3.0**	**3.5**	txt file
	FOR_F066	**6.6**	**0.24**	**2.9**	**3.5**	txt file
	FOR_F077	**7.7**	**0.47**	**2.7**	**3.5**	txt file
	FOR_F111	**11.1**	**0.95**	**2.7**	**3.6**	txt file
	FOR_F197	**19.7**	**5.5**	**2.9**	**3.8**	txt file
	FOR_F253	**25.3**	**1.86**	**–**	**–**	
LWC	FOR_F086	8.6	0.21	–	–	txt file
	FOR_F113	11.3	0.24	–	–	txt file
	FOR_F118	11.8	0.74	–	–	
	FOR_F242	24.2	2.9	3.3	4.0	txt file
	FOR_F315	**31.5**	**5.7**	**3.4**	**4.3**	txt file
	FOR_F336	**33.6**	**1.9**	**–**	**4.5**	txt file
	FOR_F348	**34.8**	**3.8**	**3.6**	**4.5**	txt file
	FOR_F371	**37.1**	**3.3**	**3.5**	**4.7**	txt file

[a] Entires in **bold** font are expected to be part of the "default" filter set for Cycle 4.

[b] IQ values for some filters have not been measured at this time, but it is expected that they will be similar to those of similar λ_{eff} with measured values.
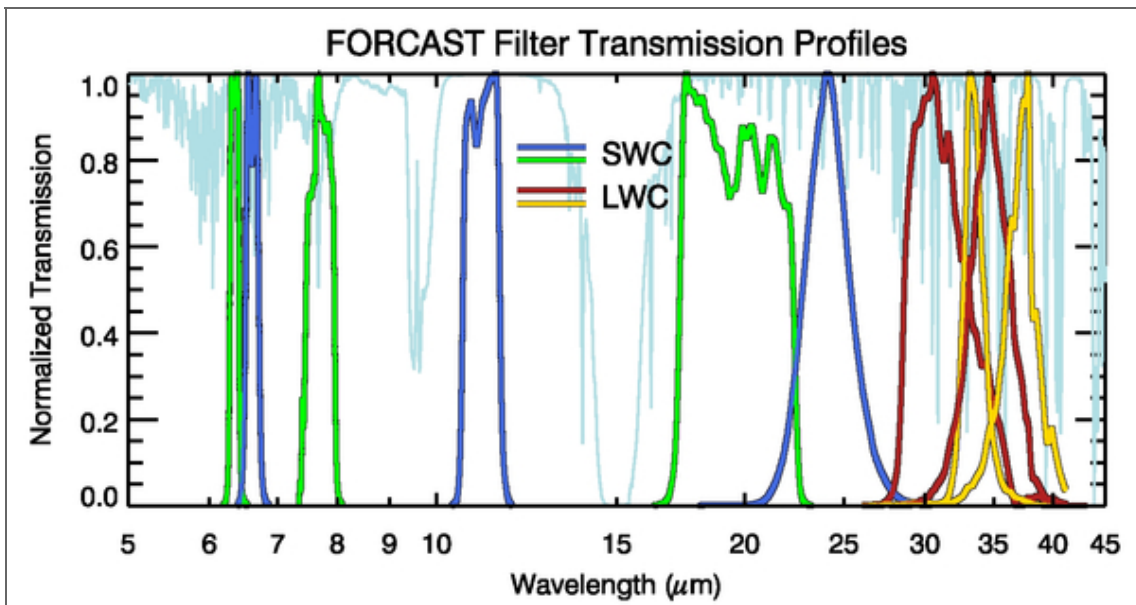
Figure 7-3: FORCAST filter transmission profiles along with an ATRAN model of the atmospheric transmission across the FORCAST band (assuming a zenith angle of 45 degrees and 7 μm of precipitable water vapor). For clarity the filter profiles have been normalized to their peak transmission. SWC filters alternate between green and blue, while LWC filters alternate between red and yellow.

7.1.4 Imaging Sensitivities

The FORCAST imaging sensitivities for a continuum point source for each filter are presented in Table 7-3 and Figure 7-4. The Minimum Detectable Continuum Flux (MDCF; 80% enclosed energy) in mJy needed to obtain a S/N = 4 in 900 seconds of on-source integration time is plotted versus wavelength. The MDCF scales roughly as (S/N) / √(t) where t = net integration time. The horizontal bars indicate the effective bandpass at each wavelength. At the shorter wavelengths the bandpass is sometimes narrower than the symbol size.

Atmospheric transmission will affect sensitivity, depending on water vapor overburden. The sensitivity is also affected by telescope emissivity, estimated to be 15% for Figure 7-4.

Observations with FORCAST will be performed using standard IR chop-nod techniques. The GIs can choose chop/nod amplitudes small enough to leave the source on the array in each position or large enough that the source is positioned off the chip for one of the chop positions. For background-limited observations, as will be the case with FORCAST on SOFIA, chopping and nodding off-chip in nod-match-chop (NMC; see Section 7.2.1) will generally result in the same signal to noise (S/N) as chopping and nodding on-chip in nod-perp-chop (NPC; see Section 7.2.1) Calculations of S/N for various chop-nod scenarios are provided here.
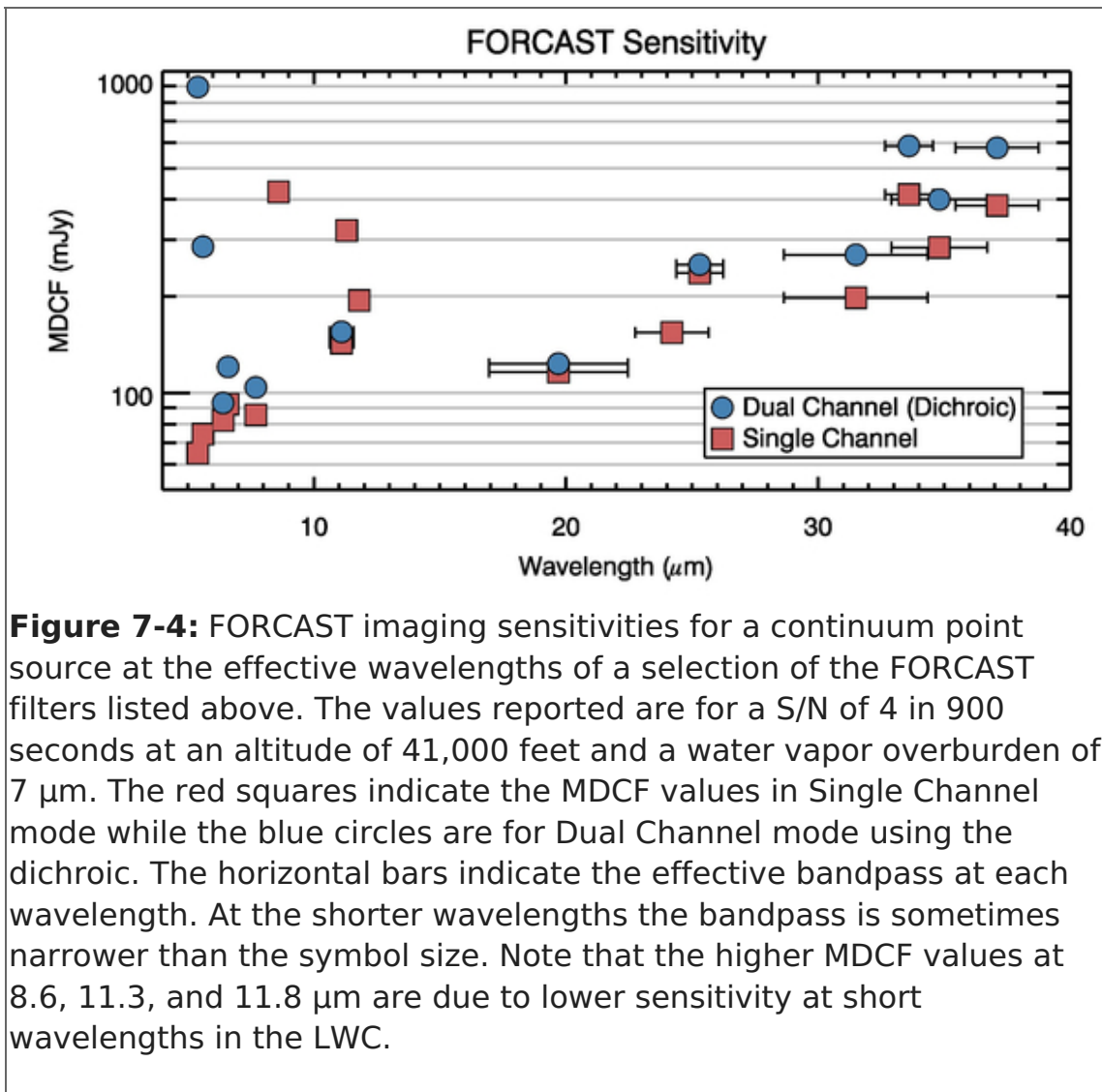
Table 7-3: FORCAST Filter Sensitivities

FORCAST Filter Sensitivities

Filter	Channel	Single Chan. MDCF (mJy)	Dual Chan. MDCF (mJy)

Filter	Channel	Single Chan. MDCF (mJy)	Dual Chan. MDCF (mJy)
FOR_F054[a]	SWC	65	895
FOR_F056[b]	SWC	74.5	285.2
FOR_F064	SWC	82.1	92.1
FOR_F066	SWC	92.4	120.6
FOR_F077	SWC	85.5	104.1
FOR_F086[a]	LWC	422	-
FOR_F111[a]	SWC	143	155
FOR_F113[a]	LWC	320	-
FOR_F118[a]	LWC	194	-
FOR_F197	SWC	116.2	123.4
FOR_F242	LWC	154.3	-
FOR_F253	SWC	236.2	250.9
FOR_F315	LWC	197.9	269.1
FOR_F336	LWC	414.1	586.9
FOR_F348	LWC	283.6	399.9
FOR_F371	LWC	383	579.3

[a] MDCF values shown are those measured from Cycle 2 and Cycle 3 data.

[b] No observations were available to test the theoretical MDCF values.

Figure 7-4: FORCAST imaging sensitivities for a continuum point source at the effective wavelengths of a selection of the FORCAST filters listed above. The values reported are for a S/N of 4 in 900 seconds at an altitude of 41,000 feet and a water vapor overburden of 7 μm. The red squares indicate the MDCF values in Single Channel mode while the blue circles are for Dual Channel mode using the dichroic. The horizontal bars indicate the effective bandpass at each wavelength. At the shorter wavelengths the bandpass is sometimes narrower than the symbol size. Note that the higher MDCF values at 8.6, 11.3, and 11.8 μm are due to lower sensitivity at short wavelengths in the LWC.

7.1.5 Grisms

The suite of 6 grisms available for FORCAST provide low to medium resolution coverage throughout most of the range from 5 - 40 μm. The grisms are situated in the four filter wheels, two in each SWC wheel and one in each LWC wheel. The arrangement is chosen to minimize the impact on the imaging capabilities of the instrument. The grisms are blazed, diffraction gratings used in transmission and stacked with blocking filters to prevent order contamination. A summary of the grism properties is provided in Table 7-4. **Note that during Cycle 4, the cross-dispersed XD configuration will not be available. The information on XD modes below is for informational purposes.**

Grisms FOR_G063, FOR_G227, FOR_G329, and the FOR_XG063 dispersing grism provided by the University of Texas at Austin, are made of silicon to take advantage of its high index of refraction, which allows optimum spectral resolution. However, these grisms suffer from various absorption artifacts precluding their use in the 8 - 17 μm window. Coverage in this region is provided by the FOR_G111 grism, constructed of KRS-5 (thallium bromoiodide) by Carl-Zeiss (Jena, Germany). These latter two grisms have a lower spectral resolution due to the lower index of refraction of the KRS-5 material.

Three slits are available, two long slits (2.4'' x 191'', 4.7'' x 191'') and a short slit (2.4'' x 11.2''). The narrow slits yield higher resolution data. All of the slits are located in the aperture wheel of the instrument. The cross-dispersed spectra are obtained by using the short slit and passing the beam first through the low-resolution grism (either FOR_G063

or FOR_G111), followed by a disperser. Although grisms are available in both cameras, during Cycle 4 grism spectroscopy will be available only in single channel mode.

It is important to note that due to the fixed position of the slits in the aperture wheels, the lack of a field de-rotator, and the fact that SOFIA behaves in many respects as an Alt-Az telescope, the orientation of the slit on the sky will be dependent on the flight plan and will not be able to be predetermined. Furthermore, the slit orientation rotates on the sky with each telescope Line-of-Sight (LOS) rewind. These limitations may be especially important to consider when proposing observations of extended objects.

Table 7-4: FORCAST Grism Characteristics

FORCAST Grism Characteristics

Channel	Grism	Material	Groove Sep. (µm)	Prism Angle (°)	Order	Coverage (µm)	R (λ/Δλ
SWC	FOR_G063	Si	25	6.16	1	4.9 - 8.0	90/180[a]
	FOR_XG063[b]	Si	87	32.6	15 - 23	4.9 - 8.0	1200[c]
	FOR_G111	KRS-5	32	15.2	1	8.4 - 13.7	150/300
LWC	FOR_G227	Si	87	6.16	1	17.6 - 27.7	70/140[a]
	FOR_G329	Si	142	11.07	2	28.7 - 37.1	110/220

[a] For the 4.7'' x 191'' and the 2.4'' x 191'' slits, respectively

[b] Not available during Cycle 4

[c] Only available with the 2.4'' x 11.2'' slit

7.1.6 Spectroscopic Sensitivity

Tables 7-5 and 7-6 provide samples of the MDCF and Minimum Detectable Line Flux (MDLF) calculated at three different wavelengths across each grism bandpass for each of the available spectroscopic modes – long slit and cross-dispersed. The data are provided for point sources only. The MDCF and MDLF estimates are for the raw integration time of 900 seconds and do not include observing overheads, but do account for a a two-position chop (perpendicular to the slit).

Figures 7-5 and 7-6 below present the continuum point source sensitivities for the FORCAST grisms. The plots are the MDCF in Jy needed for a S/N of 4 in 900 seconds at a water vapor overburden of 7 µm, an altitude of 41K feet, and a zenith angle of 60°. The rapid variations with λ are due to discrete atmospheric absorption features (as computed by ATRAN).

To determine the required integration time necessary to achieve a desired S/N ratio for a given source flux, GIs should use the FORCAST on-line grism exposure time calculator. The on-line calculator also allows for calculation of the limiting flux for a given integration time and required S/N. Since FORCAST observations are background limited, the values given in Tables 7-5 and 7-6 and Figures 7-5 and 7-6 can be used to make an estimate of the required integration time using the following relation,

$$\frac{[S/N]_{req}}{4} = \frac{F_{src} \cdot \sqrt{t_{exp}}}{MDCF \cdot \sqrt{900}},$$

where $[S/N]_{req}$ is the desired signal-to-noise ratio, F_{src} is the continuum flux of the target, t_{exp} is the exposure time on source (without taking into consideration observational overheads), and the MDCF is taken from the tables for the point-source sensitivities or estimated from the figures. For emission lines, simply use the line flux for F_{src} and use the MDLF value instead of the MDCF. However, these tables may not contain the most recent or best determined sensitivity values and therefore the on-line calculator results should be used in the actual proposal.

Table 7-5: FORCAST Long Slit Point Source Sensitivities

FORCAST Long Slit Point Source Sensitivities

Grism	λ (μm)	R = (λ/Δλ)	MDCF (mJy)	MDLF (W m⁻²)	R= (λ/Δλ)	MDCF (mJy)	MDLF (W m⁻²)
			4.7'' Slit			**2.4'' Slit**	
FOR_G063	5.1	90	79	2.3E-16	180	98	2.9E-16
FOR_G063	6.4	90	219	5.2E-16	180	268	6.3E-16
FOR_G063	7.7	90	496	5.2E-16	180	724	6.3E-16
FOR_G111	8.6	150	419	4.9E-16	300	532	6.2E-16
FOR_G111	11.0	150	449	4.1E-16	300	575	5.2E-16
FOR_G111	13.2	150	593	4.5E-16	300	764	5.8E-16
FOR_G227	17.8	70	715	8.6E-16	140	936	1.1E-15
FOR_G227	22.8	70	834	7.9E-16	140	989	9.3E-16
FOR_G227	27.2	70	1979	1.6E-15	140	2586	2.0E-15
FOR_G329	28.9	110	1365	6.5E-16	220	1899	9.0E-16
FOR_G329	34.1	110	1408	5.6E-16	220	1994	8.0E-16

Grism	λ (µm)	R = (λ/Δλ)	MDCF (mJy)	MDLF (W m⁻²)	R= (λ/Δλ)	MDCF (mJy)	MDLF (W m⁻²)
FOR_G329	37.0	110	1763	5.6E-16	220	2439	8.0E-16

Table 7-6: FORCAST Cross-Dispersed Point Source Sensitivities[a]

FORCAST Cross-Dispersed Point Source Sensitivities[a]

Grism	λ (µm)	R = (λ/Δλ)	MDCF (mJy)	MDLF (W m⁻²)
		2.4'' x 11.2'' Slit		
FOR_XG063	5.1	1200	238	1.2E-16
FOR_XG063	6.4	1200	703	2.8E-16
FOR_XG063	7.7	1200	918	3.0E-16

[a] XD modes are not available during Cycle 4
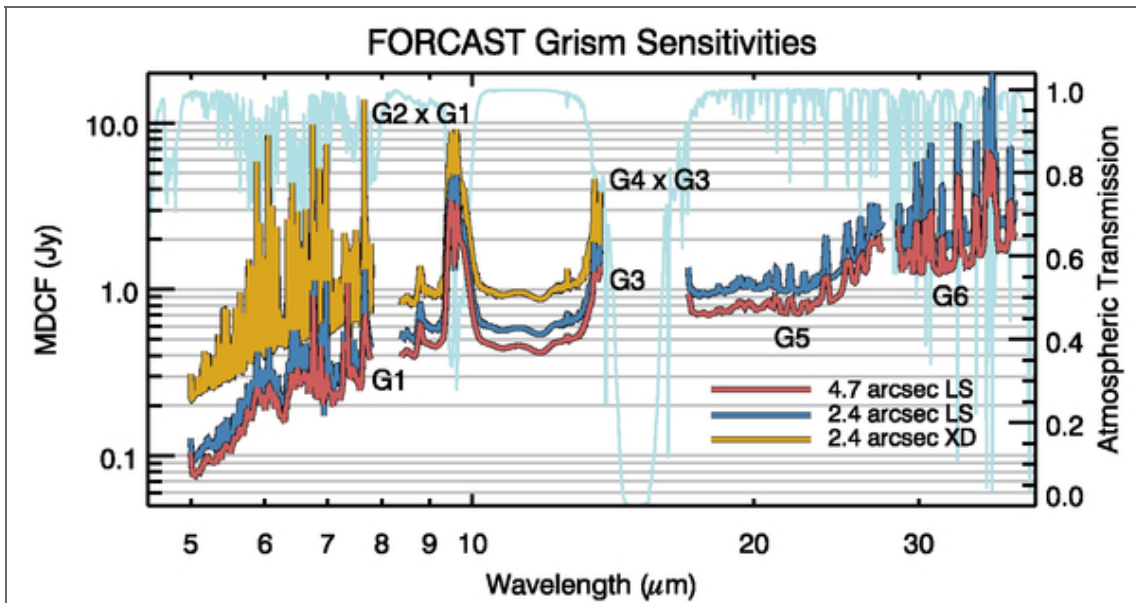
Figure 7-5: FORCAST grism sensitivities for a continuum point source in each of the grisms listed above in Table 7-3 overlaid on an ATRAN model in light blue. The values reported are for a S/N of 4 in 900 seconds at a water vapor overburdens of 7 µm at an altitude of 41K feet and a 60° zenith angle. Sensitivities are plotted for each of the three available slits.

Figure 7-6: FORCAST grism sensitivities for a continuum point source using the grisms 1 and 2 listed above in Table 7-3. Otherwise as above.
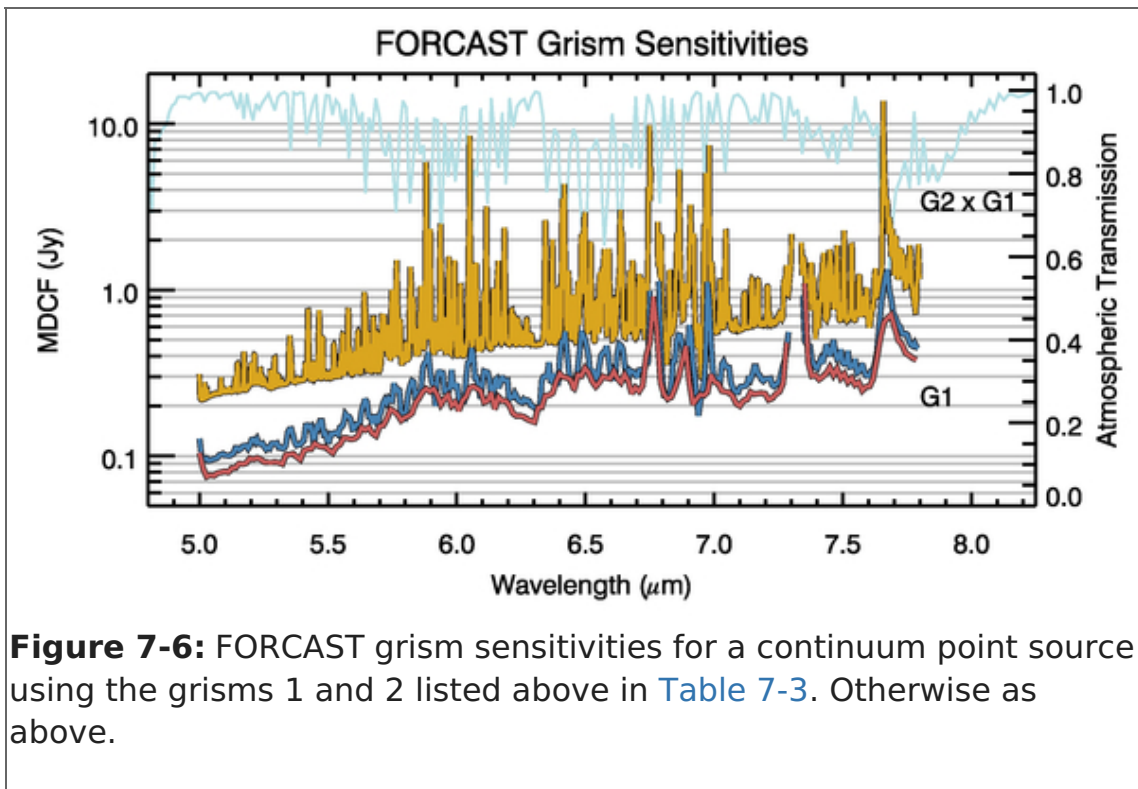
7.2 Planning FORCAST Imaging Observations

As is the case with ground based observations at mid-IR wavelengths, individual FORCAST exposures will be dominated by the sky and telescope background. Therefore chopping and nodding are essential for each observation. Selection of the observing mode, including the distance and direction of chop and nod throws, depends on the details of the field of view around the target. The source(s) of interest may be surrounded by other IR-bright sources or may lie in a region of extended emission, which needs to be avoided to ensure proper background subtraction.

7.2.1 Chopping and Nodding in Imaging Mode

FORCAST can use three different imaging observation modes including: (1) symmetric nod-match-chop (NMC), (2) symmetric nod-perp-chop (NPC), and (3) asymmetric chop-offset-nod (C2NC2). NMC and NPC are both variations of the standard two-position chop with nod (C2N) IR observing mode. NMC is the default C2N observing mode. A brief description of each observing mode is provided below, but users are strongly encouraged to read the more complete description provided in the FORCAST Observing Modes document.

- **NMC:** In NMC mode, the chop is symmetric about the optical axis of the telescope with one of the two chop positions centered on the target. The nod throw is oriented 180° from the chop, i.e. anti-parallel, such that when the telescope nods, the source is located in the opposite chop position. The chop/nod subtraction results in two negative beams on either side of the positive beam, which is the sum of the source intensity in both nod positions and therefore has twice the intensity of either negative beam. This mode uses the standard ABBA nod cadence. An example of an observation taken in this mode is presented in the left panel of Figure 7-7.

- **NPC:** NPC mode also uses a chop that is symmetric about the optical axis, but in this case the nod is perpendicular to the chop. The final images produced using NPC show four sources arranged in a parallelogram with alternating positive and negative beams. Unlike NMC, each beam in NPC has the same relative intensity. This mode also uses the standard ABBA nod cadence. The right side of Figure 7-7 shows data obtained using NPC.
- **C2NC2:** The third supported observing mode is asymmetric chop with offset nod (C2NC2). This mode is particularly useful for large extended objects, smaller objects that are situated within crowded fields, or regions of diffuse emission with only limited sky positions suitable for background removal. In this mode, the chop throw is asymmetric, such that one chop position is centered on the optical axis (and the target) while the second (sky) position is off-axis. Rather than nodding, the telescope then slews to an offset position free of sources or significant background and the same chop pattern is repeated. Observations in C2NC2 mode follow a nod cadence of ABA and, by default, are dithered to remove correlated noise.

Figure 7-8 is a cartoon demonstrating how a C2NC2 observation might be designed for a large, extended object. Each source position (solid line) with its associated asymmetric chop position (dashed line) have matching colors. After a full chop cycle at each position, the telescope is slewed to a location off of the source, shown in black and labeled with the coordinates (600, 600). The chop throw and angle at that position is the same as it is for the source position to which it is referenced (not shown in the figure). It is immediately apparent from the figure, that C2NC2 has an efficiency of only ~20%. This is a much lower efficiency than either NMC or NPC since only a single chop position out of a full chop/nod cycle is on source. This should be taken into consideration when designing science proposals.
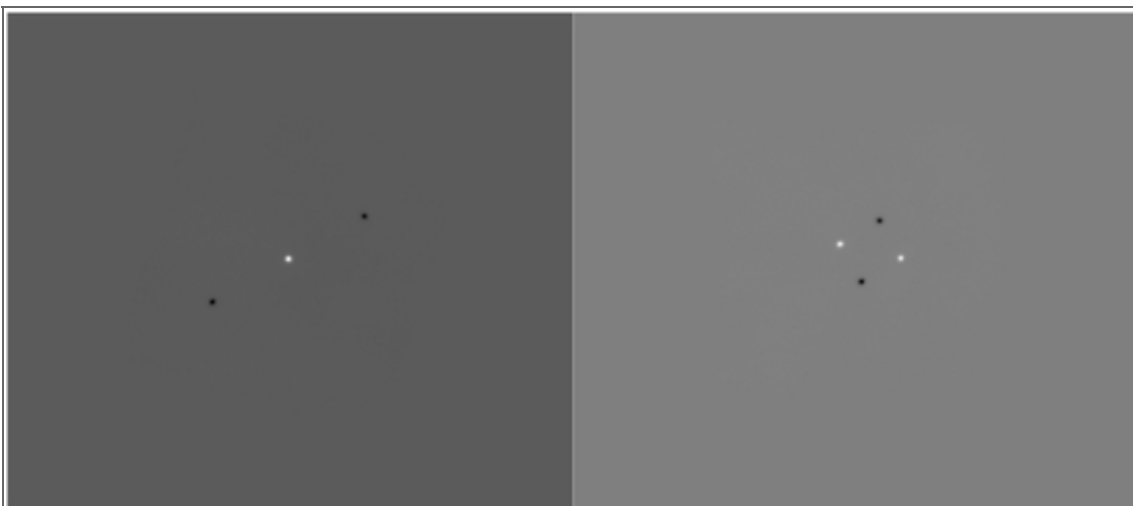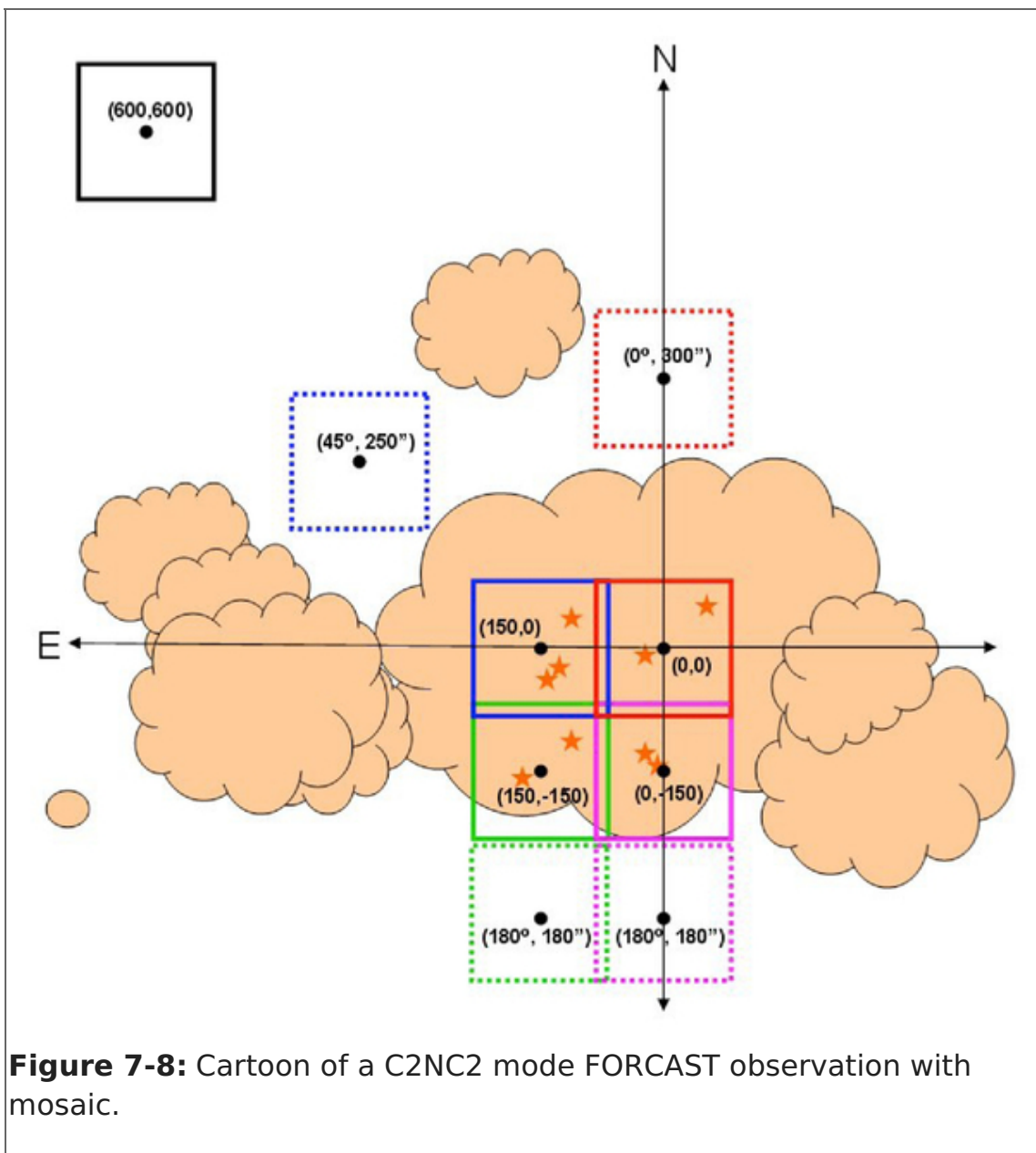

Figure 7-7: *Left:* FORCAST image of β And taken in Nod-Match-Chop (NMC) mode. *Right:* FORCAST image of α Boo taken in Nod-Perp-Chop (NPC) mode.

Figure 7-8: Cartoon of a C2NC2 mode FORCAST observation with mosaic.

Once a proposal has been accepted, the GI, in collaboration with the SMO instrument scientist, will specify the details of chopping and nodding for each observation using the SOFIA observation preparation tool (SSPOT). Experienced GIs are encouraged to design their observations using SSPOT *before* writing their proposals to prevent the loss of observing time that might occur if, during Phase II, the observations are discovered to be more challenging than expected.

Following are a few of the most important issues that GIs should consider when preparing a proposal.

- It is recommended that a near-IR or mid-IR database (e.g., 2MASS, *Spitzer*, *WISE*, MSX or IRAS) be checked to see if the target of interest is near other IR sources of emission. In the case of extended sources, where on-chip chop and nod is not possible, it is necessary to pick areas free of IR emission for the chop and nod positions to get proper background subtracted images.
- If the IR emission from the region surrounding the source is restricted to a region smaller than half the FORCAST field of view (i.e. ~1.6′) then the chop and nod can be done "on-chip". Observations performed in NMC mode either "on-chip" or "off-chip" yield a S/N equal to or slightly better than that obtained in NPC mode. For additional

discussion of this point, see the calculations of S/N for various FORCAST chop-nod scenarios provided here.

- The chop throw is defined as the distance between the two chop positions in either symmetric or asymmetric chopping modes. When using a symmetric chop, e.g., in C2N mode, chopping and nodding can be performed in any direction for chop throws less than 584″ .
- When observing in one of the symmetric chop modes, large chop amplitudes may degrade the image quality due to the introduction of coma. This effect causes asymmetric smearing of the PSF parallel to the direction of the chop at a level of 2″ per 1′ of chop amplitude.
- When using an asymmetric chop, the maximum possible chop throw is 420''. However, some chop angles (as measured in the instrument reference frame) are not allowed for asymmetric chop throws between 250'' and 420''. Since the orientation of the instrument relative to the sky will not be known until the flight plan is generated, GIs requesting chop throws between 250 - 420'' are required to specify a range of possible chop angles from which the instrument scientists can choose when the flight plan is finalized.
- For large, extended objects, it may not be possible to obtain clean background positions due to these limitations on the chop throw.

There are some additional considerations for observations of faint targets.

- Currently, the longest nod dwell time (that is, the time spent in either the nod A or nod B position) for FORCAST is 30 sec in the SWC-only and dual channel modes and up to 120 sec in the LWC-only modes (depending on the filter). Proposers should run the exposure time estimator to determine if the object will be visible in a single A-B chop-subtracted, nod-subtracted pair, with an exposure time of 30 sec in each nod position. If the object is bright enough to be detectable with S/N greater than a few, it is recommended that dithering be used when observing in C2N mode. The dithering will mitigate the effects of bad pixels when the individual exposures are co-added.
- If the object is not visible in a single A-B chop-subtracted, nod-subtracted pair, with an exposure time of 30 sec in each nod position, dithering should NOT be used." --> "If the object is not visible in a single A-B chop/nod-subtracted pair, with a nod dwell time of 30 sec in each nod position (60 sec integration), then dithering should NOT be used.

7.2.2 Mosaicking

If the source has an angular extent large enough that multiple pointings are required, the central position of each FORCAST field must be specified, with due consideration of the desired overlap of the individual frames. Mosaicking can be performed in each of the three available observing modes, NMC, NPC, and C2NC2. A sample mosaic using C2NC2 mode is demonstrated in Figure 7-8. One should keep in mind that for fields requiring large chop amplitudes, the effects of coma may compromise the image severely when in symmetric chopping mode (NMC and NPC).

7.3 Planning FORCAST Spectroscopic Observations

During Cycle 4, grism spectroscopy with FORCAST will only be available in single channel mode. By default, observations will be set up using NMC aligned along the slit in long-slit mode and perpendicular to the slit in XD mode. Due to the size of the PSF, neither chopping or nodding along the slit nor dithering are possible for high-resolution XD

observations. For long-slit observations, it is possible to use NPC, either chopping or nodding along the slit, but GIs are discouraged from doing so unless they provide adequate justification for doing so. Those wishing to use NPC should discuss the possibility with their SMO Support Scientist. GIs should also bear in mind that for sources smaller than the slit length, NMC yields slightly improved efficiency over NPC. For larger sources and for targets embedded in crowded fields, GIs are advised to use C2NC2 mode.

The observing efficiency for FORCAST spectroscopic observations is currently unknown, but is expected to be of order 25 -- 50%, depending on the chosen observing mode. These efficiency estimates are built-in to the SPT and do not need to be specified.

It is important to note that due to the fixed position of the grisms/slits in the filter/aperture wheels, the orientation of the slit on the sky will be dependent on the flight plan and will not be able to be predetermined. Further, the slit orientation rotates on the sky with each telescope Line-of-Sight (LOS) rewind. These limitations may be especially important to consider when proposing observations of extended objects.

7.4 Estimation of Exposure Times

7.4.1 Estimation of Exposure Times for Imaging Observations

The exposure times for FORCAST imaging observations should be estimated using the on-line exposure time calculator, SITE. SITE can be used to calculate the signal-to-noise ratio (S/N) for a given "total integration time", or to calculate the total integration time required to achieve a specified S/N. The total integration time used by SITE corresponds to the time for a single chop/nod pair, without overheads. The format of the S/N values output by SITE depends on the source type. For Point Sources, the reported S/N is per resolution element, but for Extended Sources, it is the S/N per pixel.

For mosaic observations the total integration time required for a single field should be multiplied by the number of fields in the mosaic to obtain the total time, which is to be entered in SPT.

An important consideration in planning observations is whether FORCAST should be used in single channel mode, or in dual channel mode, since one gains the extra filter observation at the cost of lower system throughput in the individual bands. On the SITE form, the single channel mode is specified by selecting the filter of interest for one channel and "Ignore" on the other channel in the "Instrument properties" section.

7.4.2 Estimation of Exposure Times for Spectroscopic Observations

The exposure times for FORCAST grism mode spectroscopic observations should be estimated using the FORCAST on-line grism exposure time calculator. This calculator can be used to calculate the signal-to-noise ratio (S/N) for a given "total integration time", to calculate the total integration time required to achieve a specified S/N, or to estimate the limiting flux for a desired S/N.

In either case, **overheads should not be included**, as SPT calculates them independently.

8. Instruments V: FPI+

8.1 Instrument: FPI+

The Focal Plane Imager (FPI) is the standard tracking camera for the SOFIA telescope. Since an imager upgrade in 2013, the FPI uses a science grade CCD sensor and is referred to as FPI+ (FPI_PLUS). Since the FPI+ is a subsystem of the SOFIA tracking system, it is permanently installed on the telescope. Therefore, it can be operated on every observing flight, either stand-alone or in parallel with any science instrument that is mounted on the telescope's SI flange.

As a science instrument, the FPI+ is intended to be used as a fast framerate imaging photometer in the visual wavelength range. The highly configurable readout modes of the camera can be adapted to the proposed observation needs. Examples for the scientific use of the FPI+ include observations of stellar occultations and exo-planet transits. The observations of stellar occultations benefit from SOFIA's mobility, e.g. the abilities to fly into the shadow path and to avoid cloud cover. The observation of exo-planet transits benefit from the much reduced scintillation noise at flight altitude, resulting in higher signal-to-noise ratios in the light curves compared to ground based measurements.

8.1.1 Instrument Overview

In this document, the instrument sensitivity and resolution is provided to allow estimation of the feasibility of scientific investigations. The performance summaries show the expected system performance based on data collected prior to Cycle 3. The values listed will be updated during further commissioning work indented to be performed during Cycle 3 and 4 SOFIA observations.

8.1.2 Instrument Design

Most of the visual light passes SOFIA's tertiary beam splitter (M3-1) before it is reflected into the Nasmyth tube by the fully-reflective tertiary (M3-2). A significant amount of visual light is not transmitted, but rather absorbed or reflected along with the longer, infrared wavelengths. However, in the range between 480 nm to 800 nm, where the visual-light CCD cameras are most sensitive, more than 50% of the light is transmitted to the FPI+. The visual light continues through a set of four silver-coated folding mirrors inside the so called "delay line assembly" of the telescope. This setup allows focusing the FPI+ independently from the instrument at the telescope science instrument flange. A pair of windows is installed between the Nasmyth tube and the delay line that create the boundary between the stratospheric conditions in the telescope cavity and cabin conditions inside the delay line assembly. Two "eyepiece" lenses are used to collimate the telescope beam. Close to the camera is a pellicle beam splitter made of a nitrocellulose membrane with 85% transmission. The beam splitter can be used to reflect a reticle into the light path for camera alignment purposes. The last optical element in front of the camera is an industrial ZEISS 1.4/85 mm Planar T* IR photo lens.

A double-carousel, filter wheel with six positions on each carousel is installed between the reticle beam splitter and the ZEISS lens.

8.1.3 Angular Resolution

The CCD sensor of the FPI+ is an e2v CCD201-20 1024 x 1024 pixel frame transfer EMCCD with a plate scale of 0.51''/pix and a square field of view (FOV) of 8.7'x8.7'. The unvignetted FOV is a circular beam of approx. 9' diameter centered on the FPI+ sensor.

Pixel binning of 2x2, 4x4, etc. is available and can be used to increase the frame rate and reduce the effective readout noise. In flight, the seeing blur size of the observatory is at about 4'' diameter. Therefore, a reduction of the angular resolution by binning up to 4x4 (2x2 arcsec2) still provides critical sampling of the seeing element.

The image quality in visible wavelengths on SOFIA is dominated by seeing and image motion effects. A wavelength dependent analysis of the image quality for the visual wavelength range has been done by the HIPO team.

8.1.4 Filter Suite

The wavelength range of the FPI+ is 360 nm to 1100 nm. Six spectral filters are available within this range. These are five Sloan Digital Sky Survey filters u'g'r'i'z' and a Schott RG1000 near-IR cut-on filter. Additionally, three neutral density (ND) filters can be used to attenuate bright stars. The ND filters are required for the tracking function of the FPI+ and the optical densities are chosen in such a way that stars within the brightness range of 0 < V mag < 16 can be imaged with an exposure time of 1 second. The "daylight" filter is also a requirement for telescope tracking to be able to acquire bright guide stars in twilight.

Table 8-1: FPI+ filter wheel configuration for the two filter wheel carousels

FPI+ filter wheel configuration for the two filter wheel carousels

Carousel 1	Carousel 2
OPEN	OPEN
Sloan u'	ND 1
Sloan g'	ND 2
Sloan r'	ND 3
Sloan I'	Daylight
Sloan z'	Blocked

Table 8-1 shows the configuration of the FPI+ double filter wheel. Filters from carousel one and two can be combined freely with a few exceptions. The daylight tracking filter from carousel two can only be used with the OPEN position of carousel one to avoid non-overlapping wavelength bands. The "blocked" position cannot be selected for observations, but instead is used for taking calibration data (bias frames, dark frames).

Filter Throughput

Figure 8-1 shows a plot of the FPI+ total system throughput, which includes a model for atmospheric extinction, the calculated SOFIA telescope throughput, and the instrument quantum efficiency. The filter spectral response has been measured and is added to the plot. At the wavelengths where the Sloan u' filter is transparent, other elements in the FPI+ light path (dichroic tertiary mirror, protected silver coatings, ZEISS lens) are nearly

opaque. This results in a very low throughput (~0.5%) for the selection of the FPI+ with the Sloan u' filter.
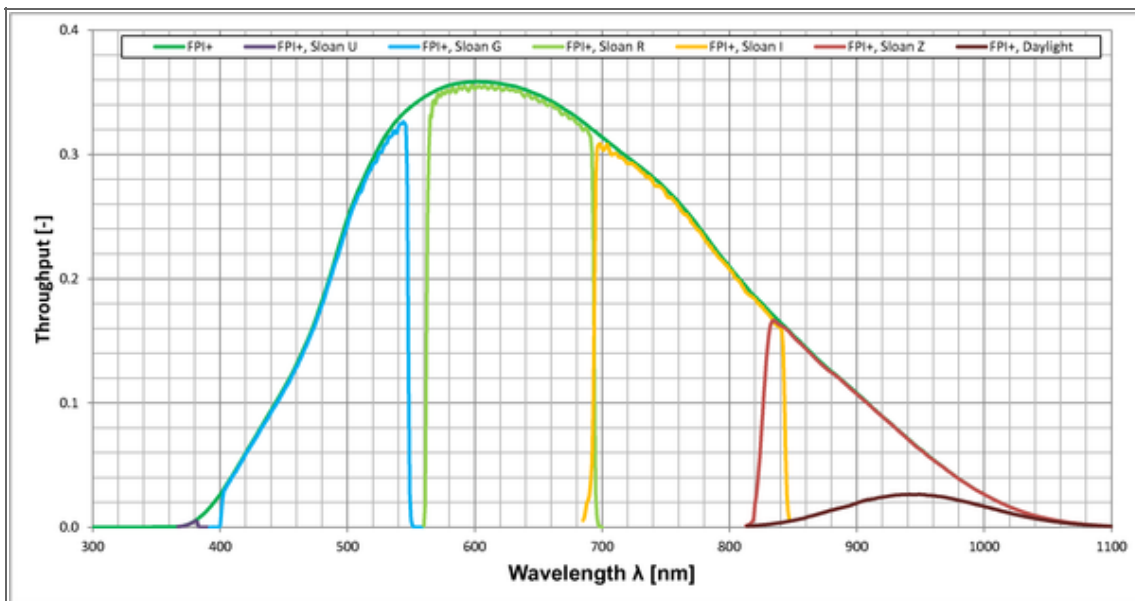

Figure 8-1: Total system throughput for Sloan filters, the Schott RG1000 (daylight) filter and the "OPEN" FPI+ configuration.

Figure 8-2 is a plot of the neutral density filter transmittance vs. wavelength for the three installed ND filters. Over the entire wavelength range of the FPI+, the ND filters have the average optical density listed in Table 8-1. However, there is a wavelength dependence of the optical density of all ND filters that has to be considered when using the ND filters in conjunction with the Sloan filters. All filters are par focal despite their different thicknesses, because they are installed in the parallel beam in front of the Zeiss lens.
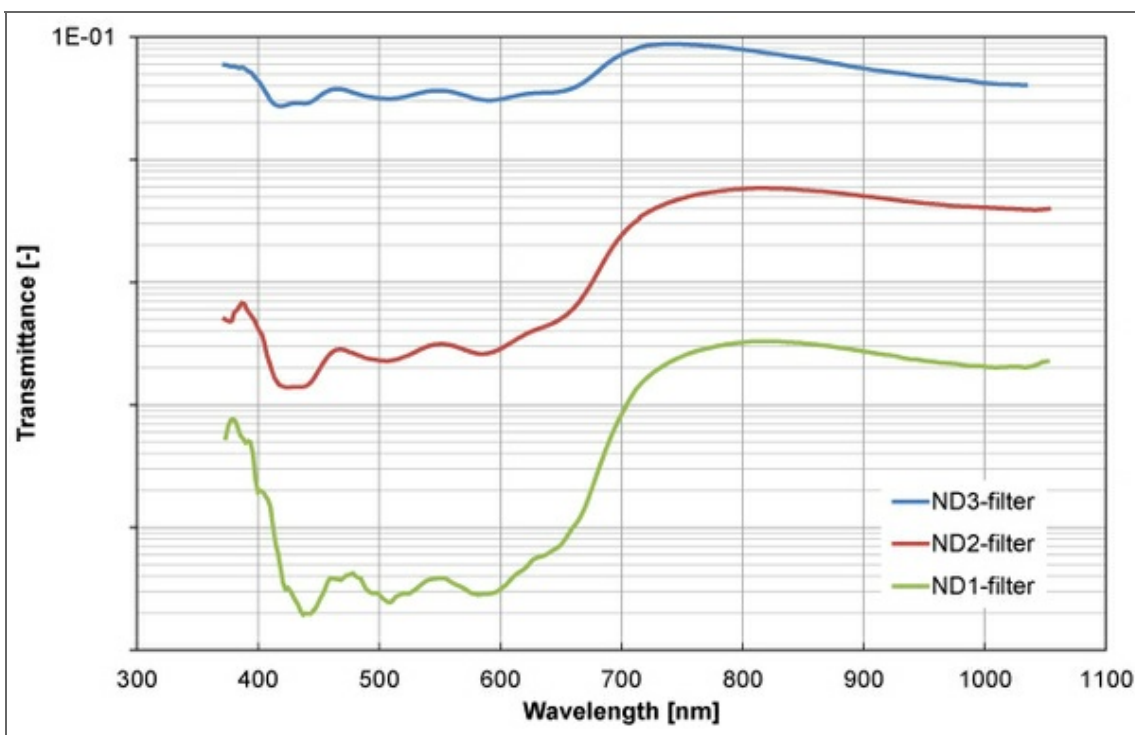
Figure 8-2: Transmittance curves of the FPI+ neutral density filters.

Table 8-2: FPI+ Neutral density filter properties

FPI+ Neutral density filter properties

Filter name	Glass Type	Thickness	Average Optical Density
ND1	Schott NG9	4.0mm	4
ND2	Schott NG3	3.5mm	2.6
ND3	Schott NG4	2.8mm	1.3

8.1.5 Imaging Sensitivities

The sensitivity of the FPI+ in its different Sloan filters was measured in-flight as part of the camera upgrade verification. The selected star field had targets with a wide range in V mag brightness (11.1 < V mag < 16.7). The full-frame images were acquired with an exposure time of one second without pixel binning. The SNR values in Figure 3 are the result of aperture photometry with an exponential fit in the logarithmic plot. Displayed are the results of the OPEN configuration and the Sloan filters g', r', i', and z'. The plot for the "daylight" filter is a calculation based on a filter transmission measurement done in the lab. The Sloan u' filter is not displayed in this plot because it requires much brighter stars due to the low system throughput at the corresponding wavelengths. To achieve significant SNR values in the Sloan u' filter, stars should be brighter than V mag=6.5.
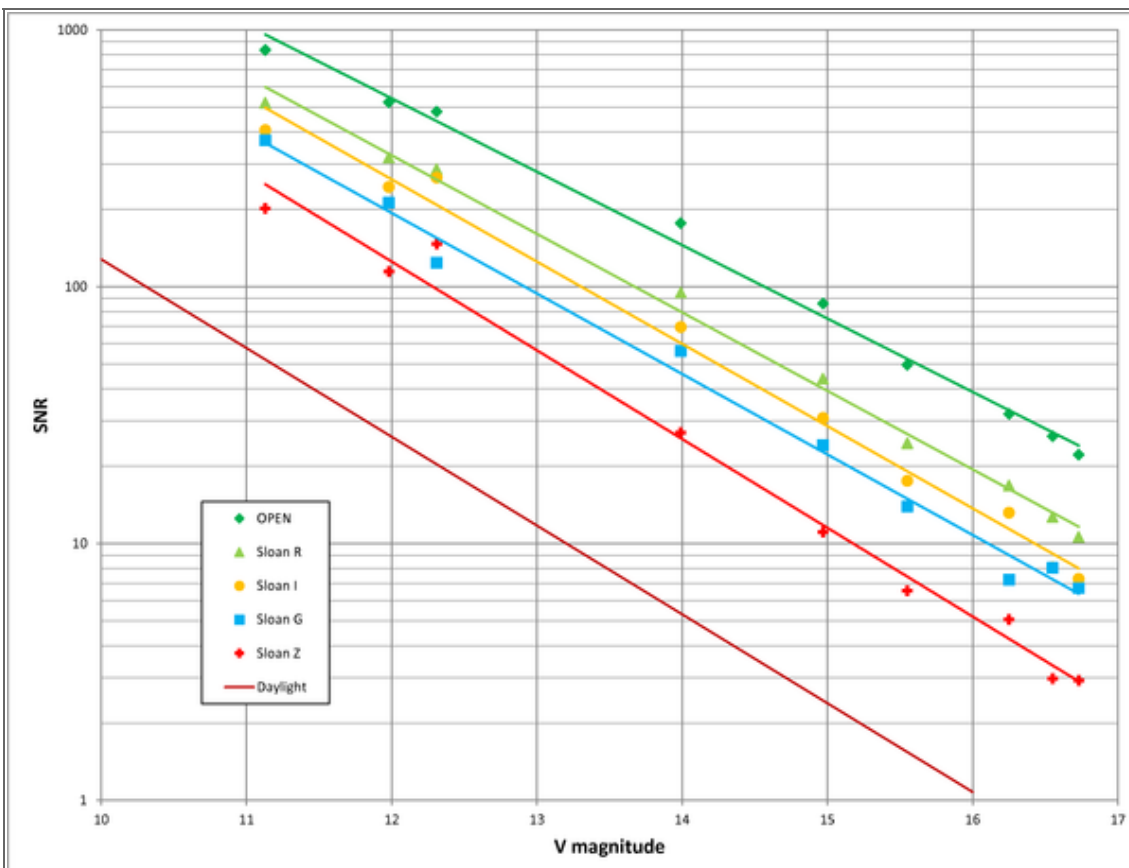

Figure 8-3: Signal to Noise Ratio (SNR) for point sources imaged with FPI+ at tEXP = 1 sec. Displayed is the OPEN broadband configuration

as well as the spectral Sloan filters g', r', i', and z'.

8.1.6 Camera Performance

Table 8-3: FPI+ Camera Modes and Performance

FPI+ Camera Modes and Performance

FPI+ Observing Mode	Horizontal Clock Rate	Bit Depth	Gain [e-/DU]	Minimum Read Noise	FPI+ Tracking Possible
FAST_STARE	10 MHz	14 bit	10.7	45.9 e-rms	No
FPI_TRACK_MEDIUM_STARE	5 MHz	14 bit	8.9	36.1 e-rms	Yes
FPI_TRACK_SLOW_STARE	1 MHz	16 bit	0.7	6.0 e- rms	Yes

Dark Current:

With the camera's multi-stage thermo-electric cooler, it is possible to achieve sensor temperatures of 100° C below ambient temperature. The measured dark current rate at a sensor temperature of -85° C, the recommended setting, is 0.001 e-/pixel/second.

Frame Rates:

The frame rates listed in Table 8-4 are for the full frame. When sub-frames are used (without FPI+ tracking) the achievable rates can be increased. The frame rate then depends on the sub-frame size and its position on the sensor.

Table 8-4: FPI+ frame rates in frames per second for the acquisition of full frames in the three observing modes

FPI+ frame rates in frames per second for the acquisition of full frames in the three observing modes

Size	FAST_STARE	MEDIUM_STARE	SLOW_STARE
1x1	8.9	3.8	0.9
2x2	17.5	6.9	1.7
4x4	33.6	11	3.2

8.2 Planning FPI+ Observations

8.2.1 Observing Modes

The FPI+ science instrument offers one imaging configuration with three observing modes. The modes are labeled FPI_TRACK_SLOW_STARE, FPI_TRACK_MEDIUM_STARE and FAST_STARE. There is no slit for spectroscopy available. The two slower observing modes

offer, but don't require, tracking in the FPI+ in parallel to the acquisition of science data. However, simultaneous FPI+ tracking does impose certain restrictions on the camera acquisition setting.

Acquisition setting restrictions for simultaneous FPI+ tracking are as follows:

- Image frame size: Full frame
- Pixel binning: 1x1, 2x2, 4x4
- Exposure time: between 100 and 4,000 ms for best tracking performance
- Target:Track star available in FPI+ field of view

With simultaneous FPI+ tracking, a target position accuracy of 0.17'' rms has been measured over a two hour time period. There is no positional drift of the target evident.

Alternatively, all of the three observing modes can be used with tracking in the Fine Field Imager (FFI; the tracking camera on the telescope front ring) or without any tracking at all. This allows the selection of an arbitrary sub-frame and binning factors along with the choice of very short (or longer) exposure times in the FPI+. With FFI tracking, positional drifts of the target of 3.9 arcsec per hour have been observed.

8.2.2 Estimation of Exposure Times

The sensitivities of the FPI+ with all spectral filter options have been implemented into the SOFIA Instrument Time Estimator (SITE). This online tool allows the estimation of exposure times to achieve a desired signal to noise ratio.

8.2.3 Overheads

Values for the observation overheads will be determined during the commissioning of the FPI+. Generally, observations can be set up very efficiently and overheads are small. For each observation, bias frames and dark frames will be acquired for image calibration. These calibration acquisitions will result in additional overheads.

9. Instruments VI: GREAT

9.1 GREAT Instrument Overview

GREAT is a dual channel heterodyne instrument that will provide high resolution spectra (up to $R=10^8$) in several frequency windows in the 1.5 – 5 THz range. The front-end unit consists of two independent dewars, each containing a set of mixers, labeled L1, L2, M_a, M_b, and H, sensitive to ''**L**ow'', ''**M**edium'' and **H**igh'' frequencies.

L1 operates in the range 1.262 – 1.396 THz (237.7 – 214.9 µm) and 1.432 – 1.523 THz (209.5 – 197.0 µm). The gap matches frequencies blocked by the atmosphere. L2 operates in the range 1.800 – 1.910 THz (166.7 – 157.1 µm). The M channel requires two local oscillators. M_a in the range 2.495 – 2.519 THz (120.2 – 119.1 µm) and M_b in the range 2.67 – 2.68 THz (112.28 – 111.86 µm). The H channel operates at 4.745 THz (63.18 µm).

The upGreat Low Frequency Array (LFA) is the first of two second-generation receivers for the GREAT instrument. The LFA is a 14-pixel array (2 polarizations × 7 pixels) arranged in a hexagonal geometry with a central beam. The current tuning range of the LFA is restricted to within several GHz of the [CII] transition at 1900.536 GHz.

During Cycle 4, L1, L2, H, and the LFA will be configurations L1-LFA and L2-H. The H channel range is currently limited by the tuning range of the quantum cascade laser local oscillator and, therefore, only the velocity range -25 − +90 km/s around the 4744.77749 GHz [O I] line will be available for Cycle 4. With the negative velocity setup, the useable velocity range is -140 − -30 km/s.

The GREAT instrument uses Fast Fourier Transform (FFT) spectrometers as backends. Each XFFTS spectrometer has a bandwidth of 2.5 GHz and 64,000 channels, providing a resolution of 44 kHz. The beam size is close to the diffraction limit - about 16' at 160 µm.

9.1.1 Observing Modes

Four observing modes are supported by GREAT.

- **Position switching (PSW):** In this mode the telescope nods between a target and nearby emission-free reference position. This mode should be used for observing one or more positions on an extended source. The reference position should ideally be less than 30' away from the source positions.
- **Beam switching (BMSW):** In this mode, the secondary mirror chops between the source and a reference position less than 10' away at a rate of about 1 − 2 Hz. The telescope nods between these positions at a slower rate. This mode results in better sky cancellation than position switching, but can be used only for compact targets, where the chop/nod throw would move the beam off-source.
- **Raster mapping:** In this mode, the telescope points to an off position, followed by several on-position observations. The user must specify the map positions, the off-position for a PSW observation or the chopper set-up for a BMSW observation, and the totl integration time per map position. This mode is ideally used for small maps or strips, where relatively long exposure times (> 30 s) per map point are required.
- **On-the-fly mapping (OTF):** In this mode the telescope scans along a line of constant latitude (a row) with the backends continuously integrating the incoming signal and recording an average after the telescope has moved a fraction (typically 1/3) the beam size. Once the end of the row is reached, the telescope moves off-source to a reference position. Then, the telescope steps half a beam width in longitude and scans the next row. This process continues until a map of the desired size has been observed. The whole map is repeated until the required sensitivity is reached.

9.2 Planning GREAT Observations

The Guide to Observation Planning with GREAT (GOPG) describes the GREAT instrument and the available observing modes. The information required to estimate observing times in each mode, along with examples on how to do so, are also contained in the GOPG.

Note that the sensitivity calculations for PSW and BMSW modes are the same. In the case of OTF mapping, the sensitivity reached depends on the scan rate and the overlap between successive rows.

If the frequency of interest has not already been used by GREAT, please contact the GREAT team to ensure that the line is feasible. There may be gaps where the broadband Local Oscillators do not provide enough power to pump the mixers.

9.2.1 Estimating Exposure Time

The exposure times for GREAT observations may be estimated using the Online Calculator.

10. Instruments VII: HAWC+

The High-resolution Airborne Wideband Camera is a multi-wavelength far-infrared camera and imaging polarimeter with continuum bandpasses from 40 μm to 300 μm. HAWC consists of two 64x40 bolometer arrays that simultaneously measure both orthogonal states of linear polarization. With one exception, each passband is diffraction limited with pixel spacing that Nyquist samples the beam, yielding spatial resolutions of 5 to 20 arcsecond and instantaneous fields of view of 2 to 8 arcminutes. (The 63 μm band is optimized for mapping speed at the expense of sampling density.) HAWC+ can measure either total intensity only, or also polarized intensity, as determined by the usage of rotating half-wave plates.

10.1 Instrument Overview

10.1.1 Design

A schematic of the HAWC+ optical design is shown in Figure 10-1. Light enters the set of warm fore-optics mounted outside the cryostat, reflecting from a folding mirror and a field mirror that images the SOFIA pupil at the cold pupil inside the HAWC cryostat. After the fore-optics, light enters the cryostat through a 7.6 cm (3.0 in) diameter HDPE window, followed by near-infrared blocking filters, then the cold pupil on a rotatable carousel. The pupil carousel contains eight aperture positions, four of which contain HWPs, one with a clear aperture whose diameter is matched to the SOFIA pupil, and three other aperture options meant only for instrument alignment tests. Light then passes through a stack of band-pass filters and plate-scale-defining lenses mounted on a six position movable carousel; filters and lenses for the five bandpasses are mounted here.

The pupil carousel and filter/lens wheel are at an approximate temperature of 10 K. After this point the light passes through a wire grid that reflects one component of linear polarization and transmits the orthogonal component. This grid is heat-sunk to the HAWC+ 1 Kelvin stage. The grid directs the two components (often referred to as the R and T components) to the two detector arrays.

Each of the two 64x40 HAWC+ detector arrays is composed of two co-mounted 32x40 subarrays from NASA/GSFC and NIST. The detectors are superconducting transition-edge sensor (TES) thermometers on membranes with wide-band absorber coating. The detector array is indium bump bonded to a matched array of superconducting quantum interference device (SQUID) amplifiers, all cooled to a base temperature of ~0.1- 0.2 K.

The optical design allows HAWC+ to measure solely the total unpolarized intensity, or simultaneously the polarized intensity. In both cases the incoming radiation is split into two orthogonal polarizations by the wire grid and measured simultaneously by the two detector arrays. In the case of polarimetry, the half-wave plate (HWP) matched to the band-pass is selected and rotated to modulate the incident polarization states. The total intensity is given simply by summing the signal in the two orthogonal arrays. Alternatively, unpolarized intensity can be measured without polarization by removing the HWPs from the optical path (utilizing the open pupil position). The resulting

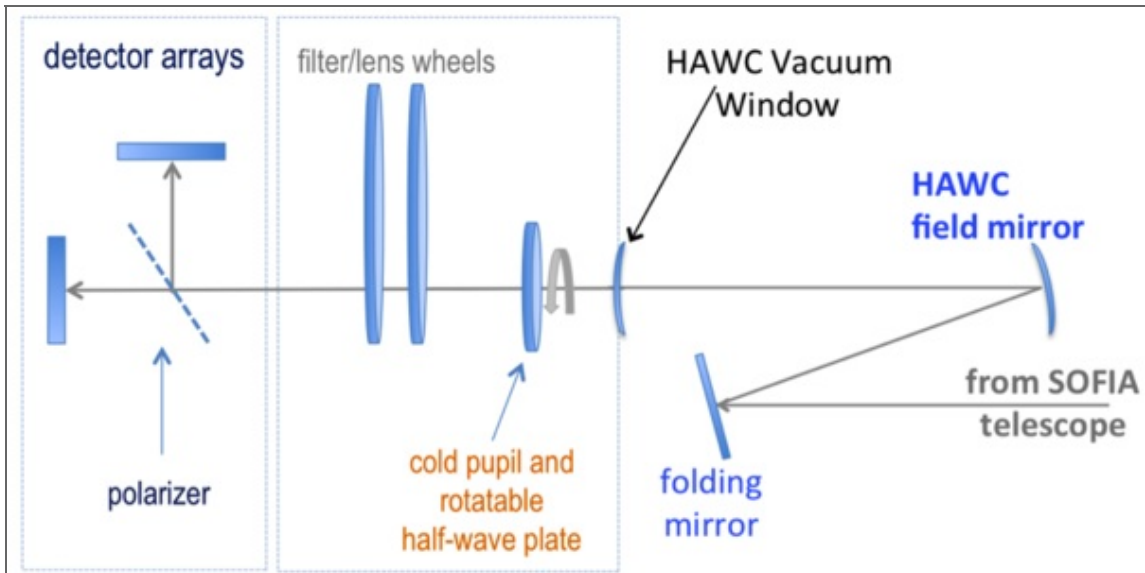sensitivity improvement is not yet measured, but is expected to be small.

Figure 10-1: Schematic of the HAWC+ optics. Light from the SOFIA telescope is incident from the right. The field and folding mirrors are mounted on the HAWC+ cryostat but extend into the SOFIA Nasmyth tube. At the polarizing grid the light is split into two orthogonal components of linear polarization and detected at the two separate arrays.

10.1.2 Performance

The absorbing coatings on the HAWC detector arrays were optimized to produce about 50% efficiency across the wide (40 - 300 µm) range of bandpasses. The TESs were designed to optimize the sensor time constants and background power at which they saturate, with the goal being operation at both laboratory and stratospheric background levels. The final design included a superconducting transition temperature of ~0.3 K and a detector yield of > 50%. Measurements of detector noise show that their contribution to total measurement uncertainties is negligible such that noise levels are dominated by background photons from the atmosphere.

Measurements of the HAWC optical system in the laboratory are consistent with optical models, confirming that the system should be diffraction limited on SOFIA. Table 10-1 lists the FWHM of Gaussian beams approximating the SOFIA/HAWC+ beams, taking into account the monochromatic diffraction limit, the finite size of the HAWC detectors, and a convolution across the measured filter bandpasses. The filter transmission curves (text tables) are available as a zip file or individually from Table 10-1.

Table 10-1: HAWC+ Instrument Characteristics

HAWC+ Instrument Characteristics

Parameter	Units	Band A	Band B	Band C	Band D	Band E
Mean Wavelenth (λ_0)	µm	53	63	89	154	214

Parameter	Units	Band A	Band B	Band C	Band D	Band E
Filter Width ($\Delta\lambda/\lambda_0$)	-	0.17	0.15	0.19	0.22	0.20
Resolution (FWHM)	arcsec	4.7	5.8	7.8	14	19
Pixel Pitch[f]	arcsec	2.6	4.0	4.0	6.8	9.1
Field of View	arcmin	2.7x1.7	4.2x2.6	4.2x2.6	7.3x4.5	8.0x6.1
NESB[a] (photo)	MJy sr^{-1} h$^{1/2}$	15	12	4.7	1.2	0.57
MDCF[b]	mJy	69	85	60	47	43
Mapping Speed[c]	See footnote c	0.016	0.059	0.39	18	110
MDCPF[d]	% Jy	11	13	9.5	7.3	6.7
MIfP[e]	MJy sr^{-1} h$^{1/2}$	24,000	20,000	7700	1900	940
		txt file	txt file	txt file	txt file	txt file

Note: All photometric sensitivity estimates assume 100% observing efficiency without chopping and nodding. These values are pre-flight estimates and subject to change after the HAWC+ instrument has been commissioned. The SPT time calculator will estimate the correct overhead values for C2N.

[a] Noise Equivalent Surface Brightness for S/N = 1 into a single HAWC+ beam (FWHM given here).

[b] Minimum Detectable Continuum Flux for a point source with S/N = 4 in a 900 second integration.

[c] Real scan rate required to achieve a given an NESB. Units: arcmin ^{2} h^{-1} (MJy sr^{-1})$^{-2}$

[d] Minimum Detectable Continuum Polarized Flux for a point source with a S/N = 4 in a 900 second integration. [e]Minimum total Intensity required to measure Polarization (MIfP) to an uncertainty level $\sigma_p \leq 0:3\%$. All chop/nod and polarization overhead values have been applied to this value.

[f] The center-to-center spacing of the pixels; pixel sizes (the space taken up by the photon sensitive area) are smaller by 0.21 arcsec at 53 μm and 0.75 arcsec at 215 μm.

10.1.3 Filters

Imaging with HAWC+ can be performed in either TOTAL INTENSITY or POLARIZED INTENSITY modes. The dual-beam nature of HAWC+ allows simultaneous measurement of both total and unpolarized intensity (Stokes parameters I, Q, and U) in the POLARIZED

mode since the total intensity is given simply by the sum of the signal in the two polarization beams (neglecting circular polarization). The HWPs that allow modulation of the polarization can also be removed from the optical path such that the beam passes through an open pupil for TOTAL mode. There is a slight gain in total sensitivity in this mode as the HWP transmission is < 100% and additional overhead is required to account for rotating the HWP.

Both observing modes can utilize any one of five optical filters. Each passband includes a bandpass filter and a number of low-pass cut-off filters. Figure 10-2 shows transmission profiles including all filters for all bandpasses. The effective wavelengths and bandwidths averaged over the total filter transmission are given in Table 10-1.
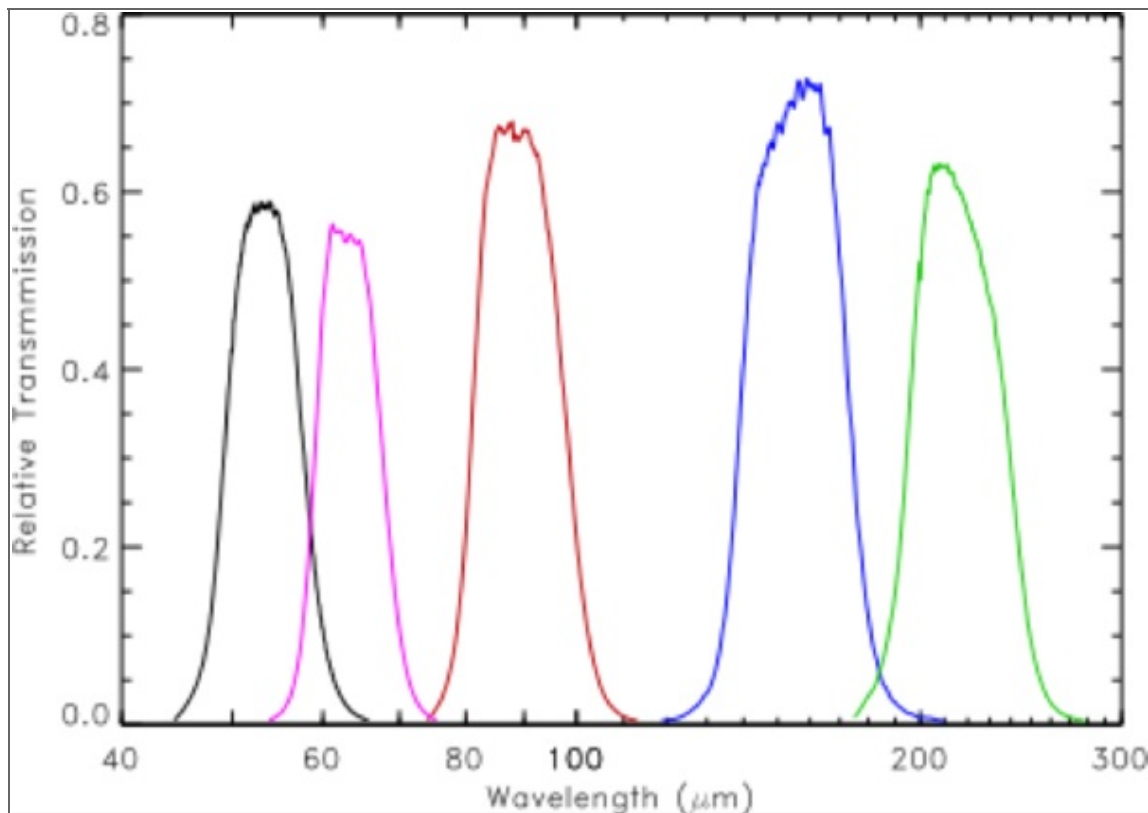
Figure 10-2: HAWC+ filter transmission profiles.

10.1.4 Imaging Sensitivities

Observations with HAWC+ for measurements of total (unpolarized) intensity can be performed using either on-the- fly scanning (where the telescope moves continuously at rates of ~10 - 100 arcsec/second without chopping of the secondary mirror) or using rapid modulation (chopping ~ 5 - 10 Hz) of the secondary accompanied by slow nodding of the telescope. The former mode is likely to be the more efficient mode but has not yet been tested by other imaging instruments on SOFIA. The chopping option consists only of a two-position chop, parallel to the nod direction where the chop amplitude matches the nod amplitude (C2N-NMC).

Figure 10-3 and Table 10-1 present HAWC+ imaging sensitivities for point sources, surface brightness, and mapping speed through each bandpass. Surface brightness is measured in units of MJy/sr and is the intensity required for a S/N=1 observation in a one-hour integration time averaged over a single HAWC+ beam. The Minimum Detectable Continuum Flux into a HAWC+ beam is that needed to obtain a S/N=4 in 900 seconds of on-source integration time. Figure 10-3 plots the MDCF for both observing

modes OTFMAP and C2N (NMC) where the latter follows from the former based on overheads related to chopping and nodding the telescope.
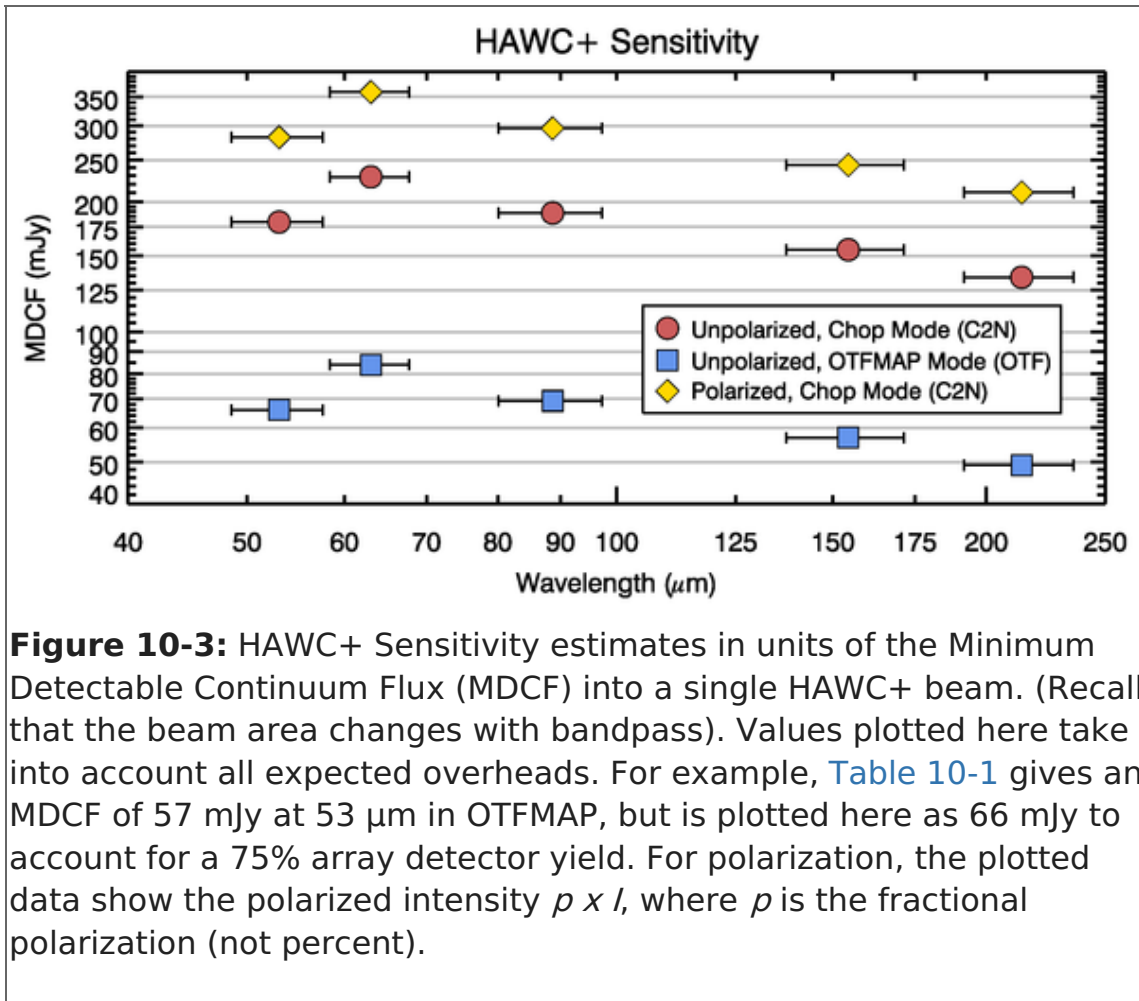

Figure 10-3: HAWC+ Sensitivity estimates in units of the Minimum Detectable Continuum Flux (MDCF) into a single HAWC+ beam. (Recall that the beam area changes with bandpass). Values plotted here take into account all expected overheads. For example, Table 10-1 gives an MDCF of 57 mJy at 53 μm in OTFMAP, but is plotted here as 66 mJy to account for a 75% array detector yield. For polarization, the plotted data show the polarized intensity *p x I*, where *p* is the fractional polarization (not percent).

HAWC time estimates should be made using the on-line exposure time calculator, SITE. Here we note that integration times scale in the following manner from the values in Table 10-1:

$$t = \left(\frac{\text{NESB}}{\sigma}\right)^2$$

or

$$t = (900 \text{ s}) \left(\frac{\text{MDCF}}{4\,\sigma}\right)^2,$$

where t is the integration time and σ is the desired sensitivity for S/N = 1, each in the appropriate units. For OTF mapping, a useful sensitivity value is the mapping speed

$$M = \frac{d\Omega}{dt} = \frac{\gamma\,\Omega_{\text{array}}}{s^2},$$

where γ is related to the filling factor, Ω_{array} is the solid angle of the HAWC detector array,

and s is some measure of the instrument sensitivity (e.g., MDCF or NESB). The values in Table 10-1 are given for S/N = 1 in a one-hour integration time assuming $\gamma = 1$, while SITE and Figure 10-3 use a more realistic value $\gamma = 0.75$. The time to map an area Ω ($\geq \Omega_{array}$) to a sensitivity level σ is given by

$$t = \frac{\Omega}{M\,\sigma^2},$$

Note that this scaling only applies to map areas larger than the array field of view.

Atmospheric transmission will affect sensitivity, depending on water vapor overburden as will telescope zenith angle and telescope emissivity. For the estimates in Table 10-1 and Figure 10-3 we use a precipitable water vapor of 7.3 µm, a 50° zenith angle, and a telescope emissivity of 15%.

10.1.5 Polarization Imaging Sensitivities

HAWC contains four monochromatic HWPs. For Bands C, D, and E, the HWP thicknesses are matched to the bandpass filters. The thickness of the "Band A" HWP is matched to a wavelength between those of Bands A (53 µm) and B (63 µm), approximately 58 µm. However, this slight mismatch should not introduce significant systematics into the system. For the pre-flight HAWC+ sensitivity estimate here, the total system polarization efficiency (HWP + polarizing grid + all other optics) is assumed to be 90% for all five passbands.

The polarization sensitivity σ_p follows from the imaging sensitivity σ_I so that

$$\sigma_p = \frac{\sigma_I \sqrt{2}}{\eta_p\,I} \times 100\%,$$

where I is the source intensity, η_p is the system polarization efficiency, and σ_p is measured in units of percent (%). The Minimum Detectable Continuum Polarized Flux (MDCPF) reported in Table 10-1 is the value σ_p x I above, and follows from the unpolarized MDCF. SPT will add overhead values appropriate to C2N mode for polarimetry.

For polarization imaging another useful quantity is the Minimum unpolarized Intensity required in order to measure polarization (MIfP) to a given depth in a given time interval. Choosing $\sigma_p = 0.3\%$ allows a polarization S/N = 3 for a source polarization of 1%, a value not atypical of bright Galactic clouds and a likely lower limit for HAWC+ systematic uncertainties. Table 10-1 lists these values for a one-hour integration time in units of surface brightness for an extended source where, unlike other values in Table 10-1, all appropriate overhead values have been added.

HAWC+ time estimates should be made using the on-line exposure time calculator, SITE. Here we note that integration times scale in the following manner from the values in Table 10-1:

$$t = (1\ \text{h}) \left(\frac{\text{MIfP}}{I}\right)^2 \left(\frac{0.3\%}{\sigma_p}\right)^2$$

or

$$t = (900\ \text{s}) \left(\frac{\text{MDCPF}}{4\ \sigma_p\ I}\right)^2 ,$$

where t is the integration time and σ_p is the desired sensitivity for S/N = 1, each in the appropriate units.

A simple estimate for the polarization angle uncertainty is given by:

$$\sigma_\phi = \frac{180}{\pi}\ \frac{\sigma_p}{2\ p}\ \text{[degrees]}$$

The above values assume only statistical uncertainties. Current best estimates for systematic uncertainties are no better than 0.3% in percent polarization and 2° in polarization position angle.

10.2 Planning HAWC+ Observations

10.2.1 Total Intensity Scan Mapping

HAWC+ imaging observations may be performed in on-the-fly (OTF) mode, sometimes referred to as scan-mapping. In this mode the secondary mirror remains stationary on the optical axis of the telescope while the telescope assembly itself slowly moves with respect to the sky. This scan motion modulates the celestial source with respect to the atmosphere in a manner similar to chopping the secondary mirror. Scan rates must reach (~2 Hz) x (HAWC beam width) in order to remove the source from the atmospheric background. This implies rates ~10 - 80 arcseconds per second depending on the band-pass.

In order to ensure absolute flux calibration in this mode, observers must carefully plan observations so that some of the mapped region contains no extended flux. Otherwise, one can only measure a differential flux with respect to the lowest measured intensity level. Further removal of residual atmospheric signal is performed by removing common-mode noise observed in all HAWC+ detectors. This averaging amounts to a spatial filter with size equal to the HAWC FOV. Therefore, while large maps may be necessary to reach a true zero-intensity level, users should be aware that one cannot also recover all spatial scales in a given region.

HAWC+ will offer two types of OTFMAP scan patterns (Figure 10-4). Lissajous scans are small and meant for sources smaller than the HAWC+ FOV while Linear Cross scans are more efficient at mapping large areas several times the FOV. The patterns in Figure 10-4 show the two-dimensional location of the array center where movement along any curve is movement in the time dimension. Two-dimensional scans are necessary in order to reconstruct all spatial scales in a map. The Lissajous scans are 2D by definition.

However, linear scans require multiple scans, even in the case where a source fits completely in the HAWC+ FOV. The secondary (or cross) scan direction should by rotated with respect to the initial scan (while orthogonal scans are best, they are not absolutely necessary).
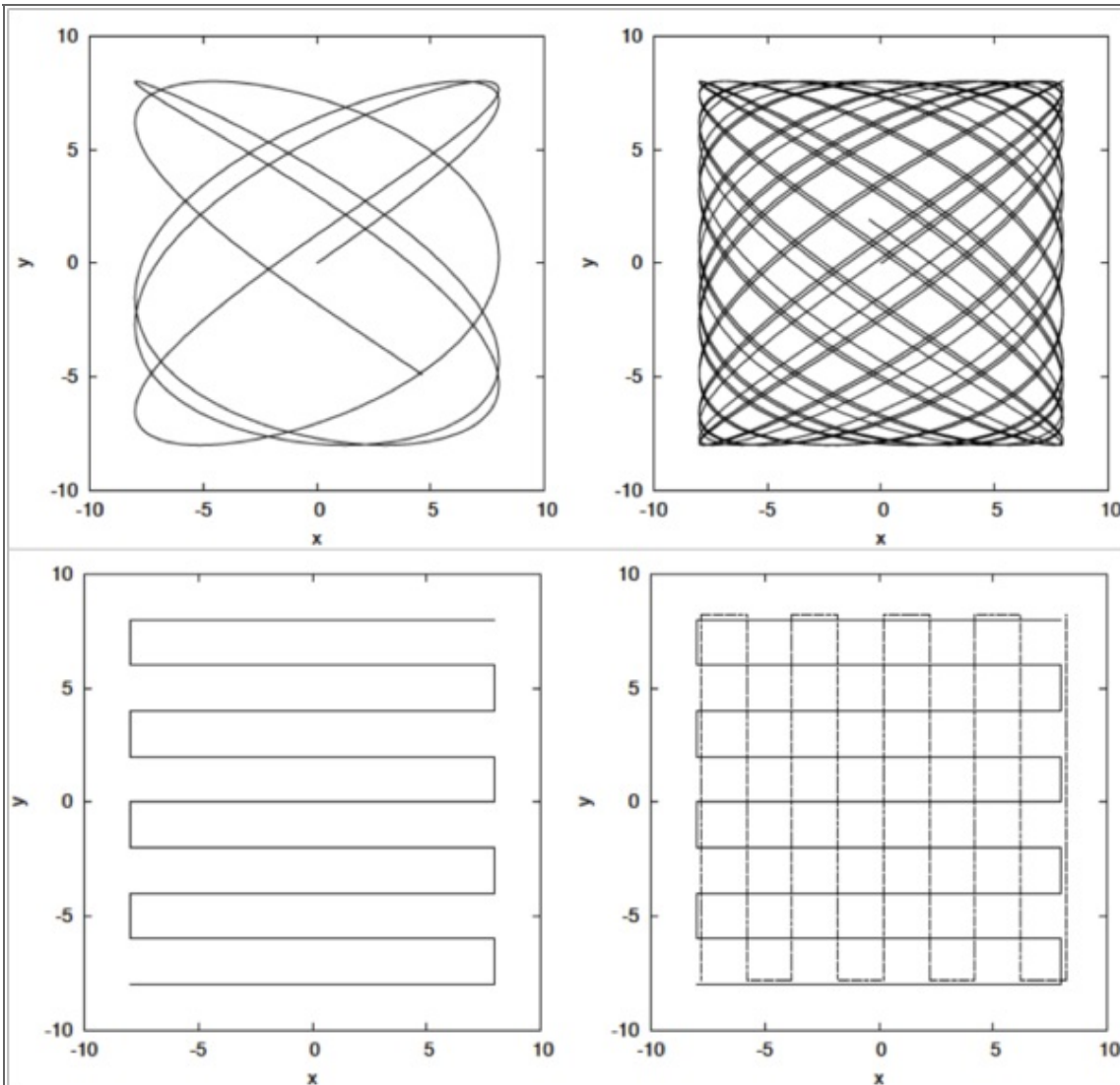

Figure 10-4: Example scan patterns for HAWC+ OTFMAP mode. These patterns show the location of the central array pixel, which moves along the paths at a user-defined rate. The upper panels are Lissajous patterns. The top-left panel is shortly after starting an integration, while the top-right panel is after a longer time period. The lower-left panel shows a series of linear scans used to cover a larger region. The lower-right panel also shows the required cross-scan in the case of linearly scanned areas. Plots taken from Kovács (2008).

While proposers must request an area for scan mapping, they do not need to specify any specific pattern in Phase I proposals. Successful proposers will work with a SOFIA Support Scientist to choose an optimal scan pattern and strategy for their observations. For the purposes of the proposal, scanmap time estimates should be made using the sensitivity estimates in Table 10-1. For sources smaller than the HAWC FOV use the MDCF or NESB. For larger maps one may use the Mapping Speed.

In order to avoid inefficiencies such as computer crashes and the like, we do not recommend scan durations longer than 10 minutes. If a given map area and sensitivity

cannot be achieved in that time, then multiple pointing positions should be used. This is an estimate based on previous ground-based experience and may differ once HAWC+ is commissioned on SOFIA.

10.2.2 Total Intensity while Chopping

HAWC+ imaging observations may be performed using a symmetric nod-match-chop (NMC), which is a variation of the standard two-position chop with nod (C2N) mode described in the FORCAST section of this manual (for further details see the FORCAST Observing Modes document).

The chop is symmetric about the optical axis of the telescope with one of the two chop positions centered on the target. The nod throw is oriented 180° from the chop, i.e. anti-parallel, such that when the telescope nods, the source is located in the opposite chop position. A standard ABBA position sequence lasting a total of ~1- 2 minutes is used for these observations. Users have a choice of chop/nod angle with respect to the sky, which can be useful if extended flux exists in some directions but not others.

- If the source of interest has little extended flux then a user may wish to choose a chop throw smaller than the HAWC FOV. In this case the chop/nod subtraction results in two negative beams on either side of the positive beam, which is the sum of the source intensity in both nod. An example of an observation taken in this mode is presented in the left panel of Figure 29 (FORCAST).
- If significant extended flux exists then a chop throw larger than the HAWC FOV should be chosen up to a maximum throw of 10'. In this case no negative beams will appear in the image as they are always outside the array FOV.
- When choosing chop throws and angles one should carefully inspect other observations to avoid chopping into extended flux. The Herschel Space Observatory and WISE mission archives are good places to examine extended regions at HAWC+ wavelengths.

The C2N mode also requires small dithers in order to mitigate the effects of bad and missing detector pixels. The baseline HAWC+ dithering mode will consist of a four-point dither at the corners of a square with size of ~1- 2 HAWC+ beams. Therefore, the minimum time for a single C2N observation with dithering is ~5 minutes.

10.2.3 Polarization while Chopping

For Cycle 4, HAWC+ polarization observations may only be performed using the C2N (NMC) observing mode (see Section 10.2.2 above). In this mode, four standard C2N (NMC) observations are taken, one at each of four angles of the HWP (relative angles 0, 22.5, 45, and 67.5 degrees). This is followed by dithering, where the HWP cycle is repeated again for a total of four dither positions. We currently estimate an additional overhead of 90% efficiency associated with moving the HWP between positions. This has been incorporated into polarization sensitivities in Figure 10-3. The minimum time for a single polarization C2N observation with dithering is ~20 minutes.

As in the case of TOTAL INTENSITY C2N, one must take care to avoid chopping into regions of bright, extended flux. Additionally one must consider the polarization state of that reference flux, in both percent polarization and angle. Typically, neither of these values will be known for HAWC+ observations (although users may want to consult the latest Planck data release). This "polarized reference" beam will produce additional

systematic uncertainties in the data. In the case where the source and reference beam have the same polarization level, the systematic polarization uncertainty is linearly proportional to the reference-to-source intensity ratio. For further discussion, see Schleuning et al. (1997) and Novak et al. (1997).

10.2.4 Mosaic Maps

If the source has an angular extent larger than the HAWC+ FOV in C2N mode, or larger than can be accommodated in a 10 minute OTFMAP, the central position of each HAWC+ field must be specified, with due consideration of the desired overlap of the individual frames. For mosaic observations, proposers should ensure that they request the total integration time required for all fields.

10.3 References

1. Kovács, A. 2008, in SPIE Conf. Ser. 7020, Millimeter and Submillimeter Detectors and Instrumentation for Astronomy, IV. Eds. W. D. Duncan, W. S. Holland, S. Withington, & J. Zmuidzinas, 7, astroph/0806.4888

2. Novak, G., Dodson, J. L., Dowell, C. D., et al. 1997, ApJ, 487, 320

3. Schleuning, D. A., Dowell, C. D., Hildebrand, R. H., Platt, S. R., & Novak, G. 1997, PASP, 109, 307

11. Instruments VIII: HIPO

The **H**igh **S**peed **I**maging **P**hotometer for **O**ccultations (HIPO) is a special-purpose science instrument for SOFIA that is designed to provide simultaneous high-speed time resolved imaging photometry at two optical wavelengths. It is possible to mount HIPO and FLITECAM on the SOFIA telescope simultaneously, called the FLIPO configuration, to allow data acquisition at two optical wavelengths and one near-IR wavelength. HIPO has a flexible optical system and numerous readout modes, allowing many specialized observations to be made. The instrument characteristics required for our proposed scientific pursuits are closely aligned to those needed for critical tests of the completed SOFIA Observatory, and HIPO has been used heavily for these tests. The general design and performance goals of the instrument are described in Dunham et al. (2004, SPIE, 5492, 592). Additional references are available on the HIPO web page.

The primary scientific use of HIPO is for observing stellar occultations. In a stellar occultation, a star serves as a small probe of the atmospheric structure of a solar system object or the surface density structure of a planetary ring or comet. Such observations provide information at high spatial resolution that would otherwise require a space mission to obtain. This work makes use of SOFIA's mobility, freedom from clouds, and near-absence of scintillation noise to provide the best possible occultation data.

The low atmospheric scintillation in airborne photometry gives HIPO the potential to detect P-mode stellar oscillations in sunlike stars and will provide excellent photometry of stellar transits by extrasolar planets. HIPO will be available for Guest Investigator use on a collaborative basis, and potential Guest Investigators should contact the PI prior to proposing to ensure that the proposed observations are feasible, that they make the best use of HIPO's capabilities, and that the proposal is as strong as possible.

11.1 Instrument Overview

The instrument sensitivity and resolution summaries are provided to permit estimating feasibility of scientific investigations. The HIPO performance summaries show the expected system performance for Full Operational Capability, which may differ from that during commissioning.

11.1.1 Instrument Design

The HIPO optical system is reconfigurable to meet its varied requirements. It incorporates two dichroic beamsplitters, one to divert the infrared beam to FLITECAM (if mounted) and one to split the red and blue sides of the HIPO optical paths. Either or both of these may be removed if desired. It is also possible to move either CCD so it is placed directly at the optimal SOFIA focal plane for highest spatial resolution and throughput. The optical design is described in detail in Dunham (2003, SPIE, 4857 62).

The 8-position filter wheels are located near the pupil image formed by the collimator optics. Two positions in the red CCD's filter wheel are normally used for Shack-Hartmann lenslet arrays, but these may be replaced if necessary for a particular observation. We have contemplated adding grism capability to HIPO but have not yet carried this out.

The region between the mounting flange and the gate valve on the telescope can be evacuated to reduce image degradation due to density fluctuations in this region of the optical path. When this is done a window is installed at the location of the gate valve.

HIPO provides a number of CCD readout modes as described in Dunham et al. (2008, SPIE, 7014, 70144Z). The most commonly used are the single frame mode and a frame transfer time series (basic occultation) mode with readout frequency up to 50 Hz. A variety of readout rates are available allowing the observer to optimize the subframe size, speed, noise, full well, and linearity tradeoff for a particular event. This is also discussed together with HIPO data format details in the "HIPO Data Cycle System Software Interface" document.

11.1.2 Angular Resolution

The primary HIPO detectors are e2v CCD47-20 1024x1024 pixel frame transfer CCDs with plate scales of 0.33''x0.33'' pixels at low resolution and 0.05''x0.05'' pixels at high resolution. The HIPO field of view (FOV) is a 5.6' square, the 8' diagonal of which corresponds to the 8' diameter SOFIA FOV. Pixels will normally be binned to best match the seeing blur size and to reduce the effect of read noise. The high resolution mode includes no re-imaging optics. It is possible to replace one or both of the CCD47's with CCD67's having half the field of view, twice the pixel size, and much faster imaging operation.

The HIPO image quality is dominated by seeing and image motion effects. The red curve in Figure 11-1 is the nominal image quality expected at first light for SOFIA, based on the expected shear layer seeing, the as-built optical performance, and 2'' rms image motion. The blue curve represents the ultimate combined optical quality and image motion requirement (80% encircled energy in a 1.6'' diameter circle) convolved with the expected shear layer seeing. Also plotted are representative photometry aperture diameters likely to be used for processing occultation frames under both conditions described above. The image motion assumed is larger than will be experienced when

observing at high frame rates. Occultation photometry will be extracted from data frames using effective aperture sizes comparable to the 80% enclosed light diameter plotted here.
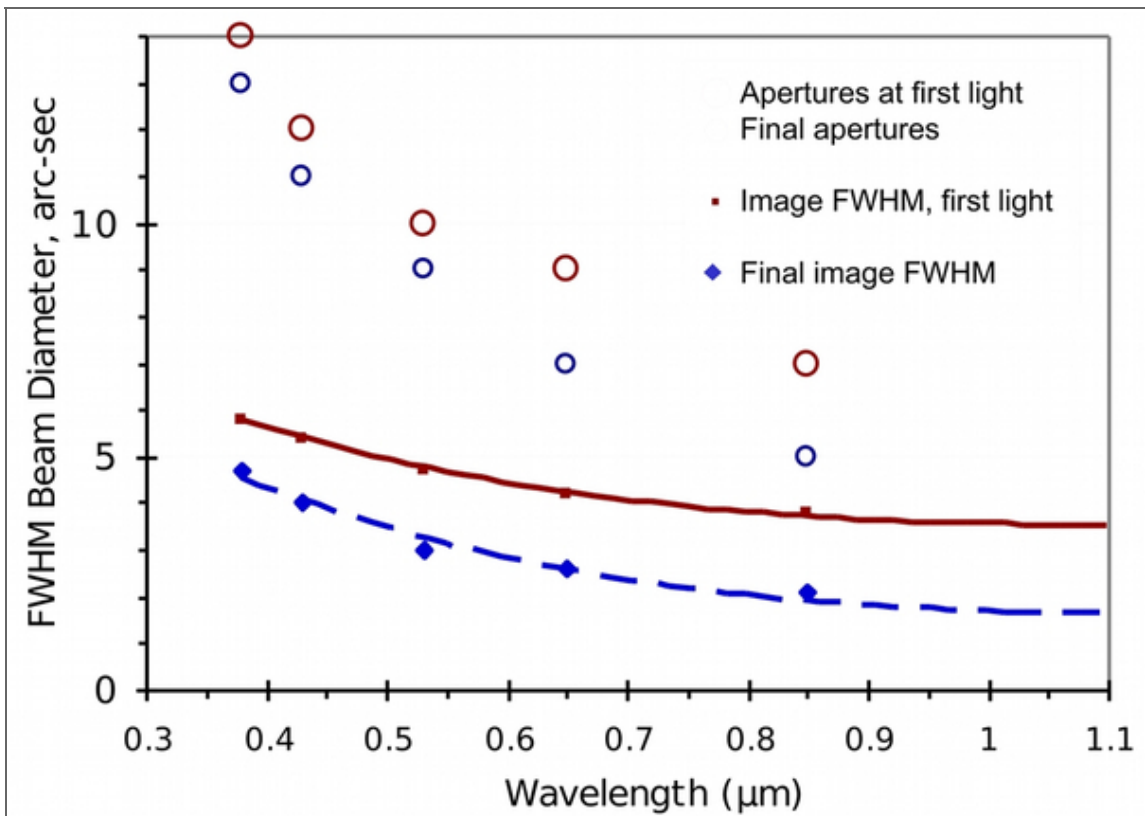

Figure 11-1: Plotted here is the expected instrument FWHM beam diameter as a function of wavelength.

11.1.3 Filter Suite

Wavelength range: 0.3 - 1.1 µm. HIPO currently includes standard Johnson UBVRI and Sloan Digital Sky Survey u' g' r' i' z' filters. Occultation observations will normally be unfiltered for events involving faint stars or will use specialized filters such as the narrow-band methane filter ($\lambda c \sim 0.89$ µm) for events with bright stars. Additional custom filters will be added as needed for specific events.

HIPO uses a dichroic reflector to separate its blue and red channels. Two dichroics are currently available with transition wavelengths of 0.575 and 0.675 µm respectively. Other dichroics will be added as necessary for specific events. The 0.575 µm dichroic transition wavelength is close to the boundary between the Sloan g' and r' filters and the 0.675 µm transition is close to the boundary between the Sloan r' and i' filters.

HIPO has been upgraded recently with the addition of deep depletion CCDs having a multi-layer antireflection coating. This provides higher quantum efficiency across the board with much higher quantum efficiency at longer wavelengths. It also nearly eliminates fringing at longer wavelengths. The figures below reflect this improvement.

Below are two plots (Figures 11-2 and 11-3) of the HIPO total system throughput including atmospheric extinction, SOFIA telescope throughput, and instrument throughput for each of the available bandpasses. The first figure shows the total system throughput for the Johnson and methane filters with the 0.575 µm dichroic. The second

figure shows the Sloan filters with the 0.675 µm dichroic. These figures assume that the FLITECAM dichroic beamsplitter is not installed. The very low total system throughput for HIPO is due to the dichroic tertiary mirror in the telescope. The long-planned aluminized tertiary will increase our throughput by a factor of nearly 3, on average, when it becomes available. The corresponding throughputs are presented in Figures 11-4 and 11-5.
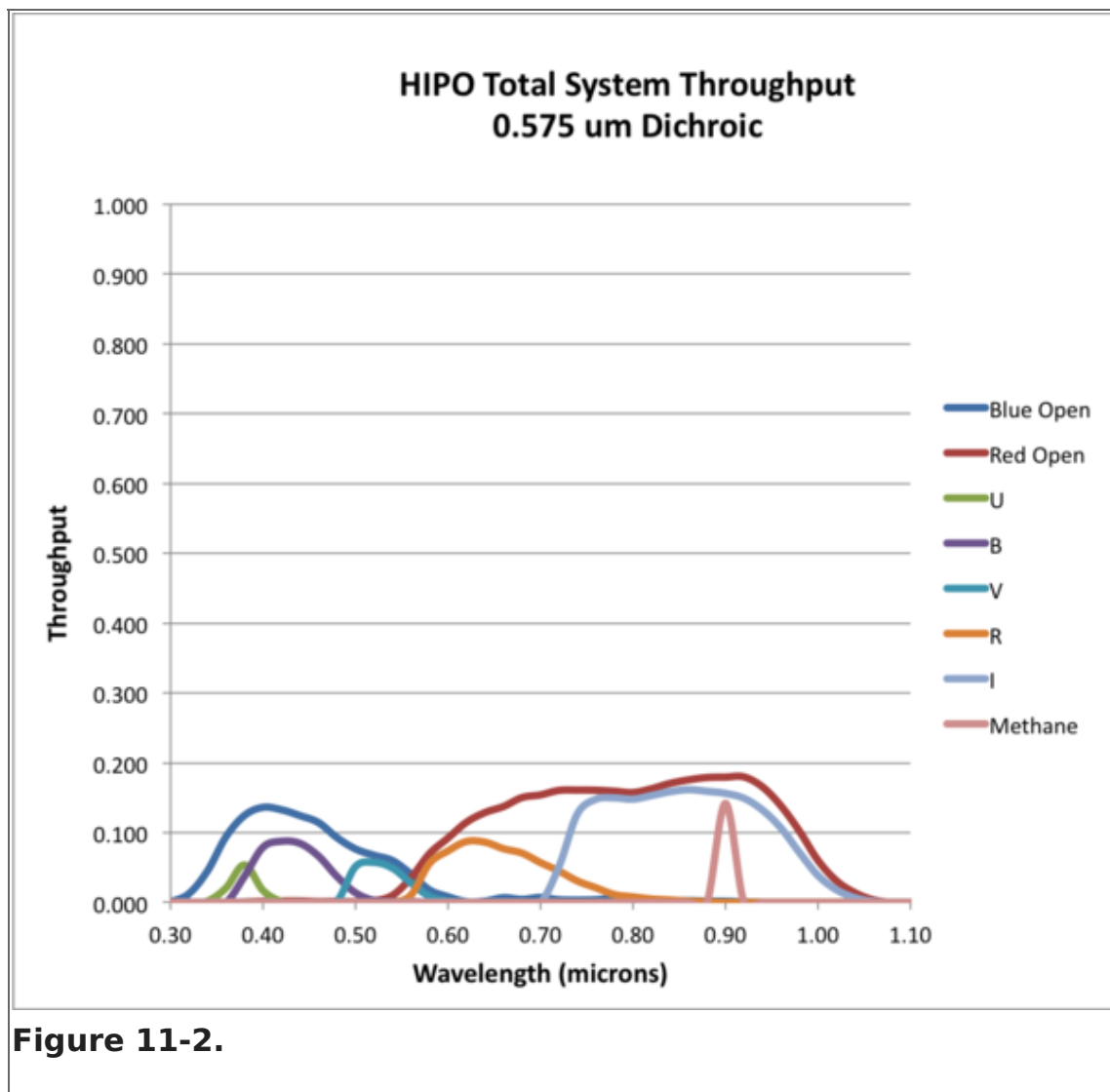

Figure 11-2.

HIPO Total System Throughput
0.675 um Dichroic

Legend:
- Blue Open
- Red Open
- SDSS u'
- SDSS g'
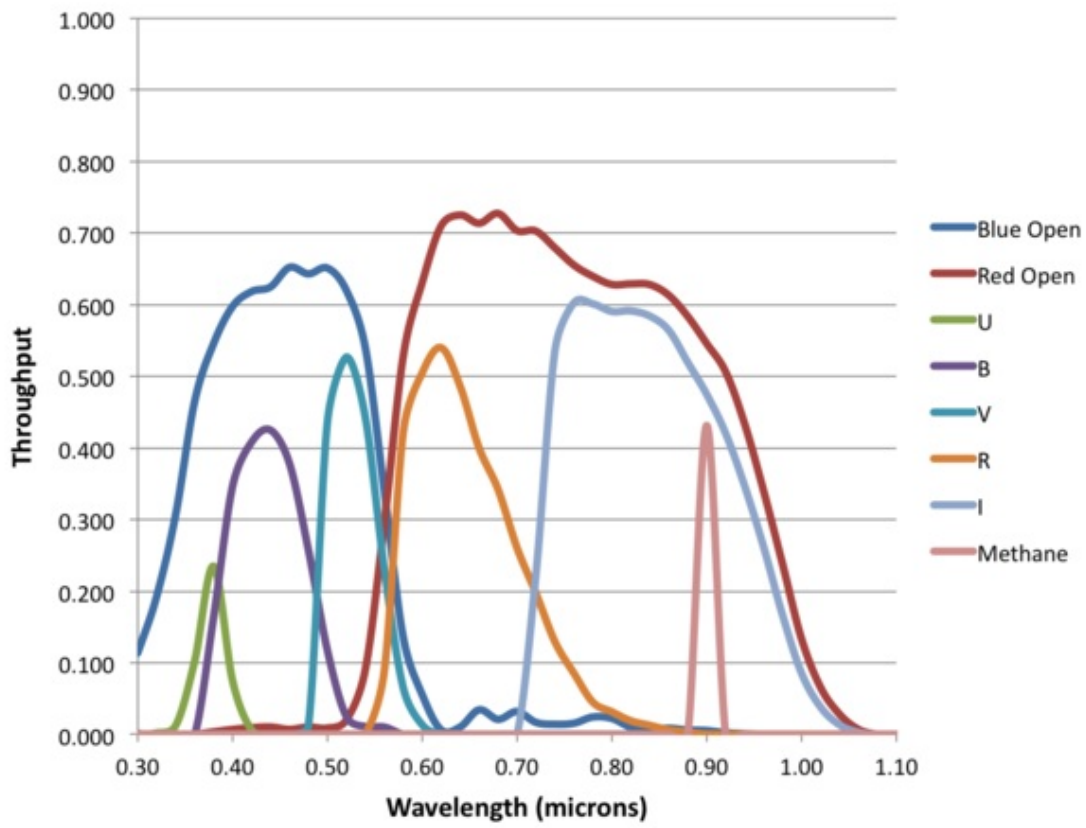- SDSS r'
- SDSS i'
- SDSS z'
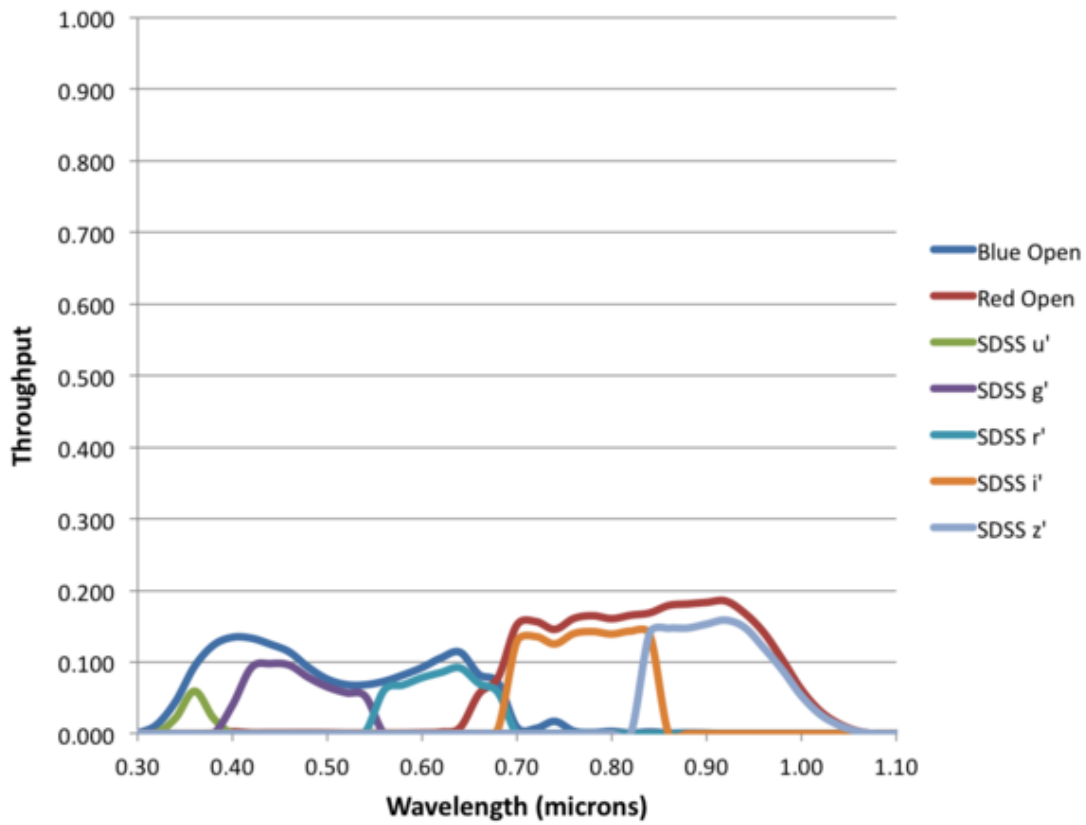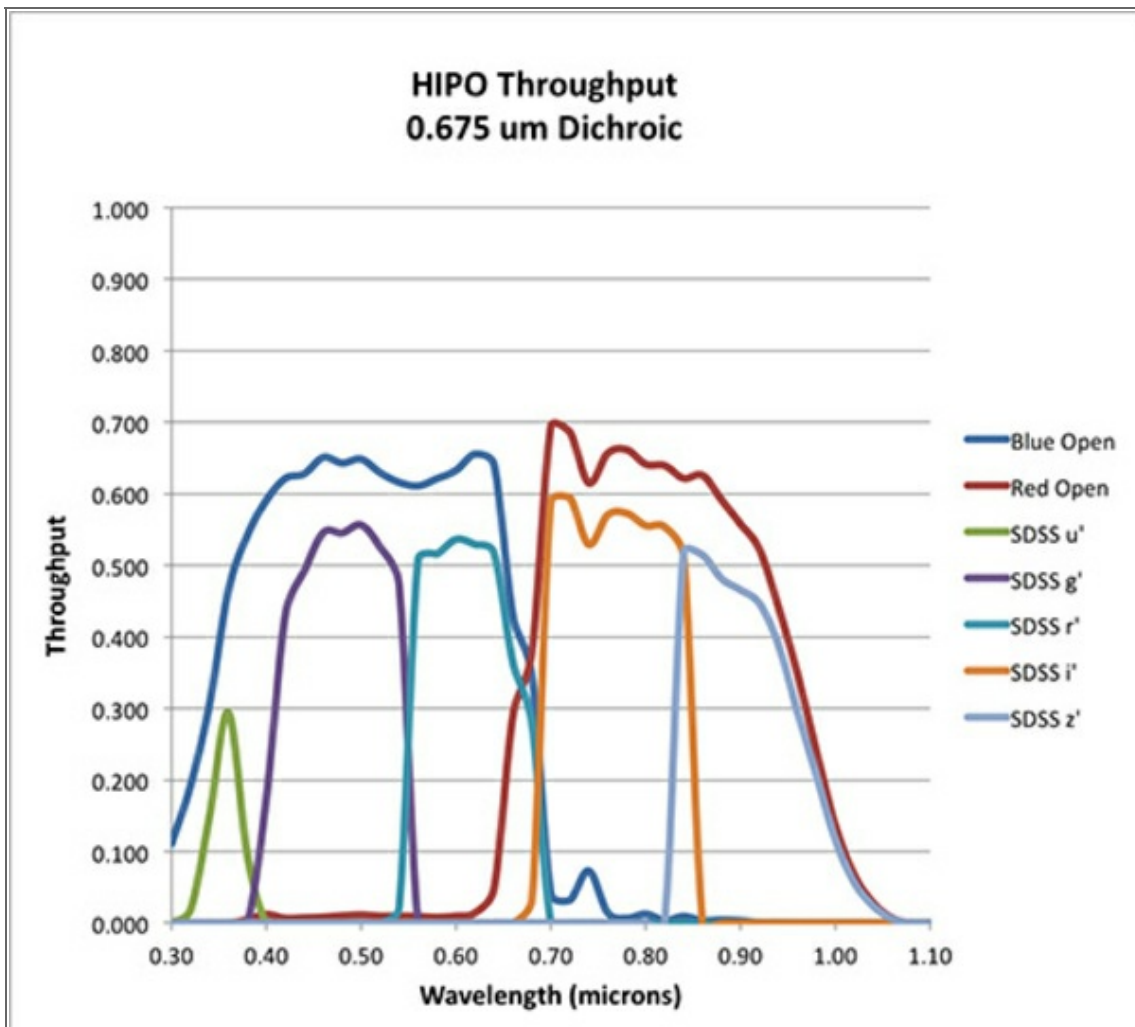
Figure 11-3.

Figure 11-4

Figure 11-5

11.1.4 Imaging Sensitivities

Plotted in Figure 11-6 below are HIPO first-light sensitivities for several representative cases. These figures assume that the FLITECAM dichroic beamsplitter is not installed. The upper figures correspond to occultations by Pluto or Triton while the lower two are for the case of a very faint occulting object. The left and right figures are for 0.5 sec and 50 ms integrations, respectively.Each figure shows S/N for no filter (dichroic only) and for the 0.675 um dichroic plus standard Sloan filters. The dichroic transition is assumed to occur from 0.57 and 0.67 μm.
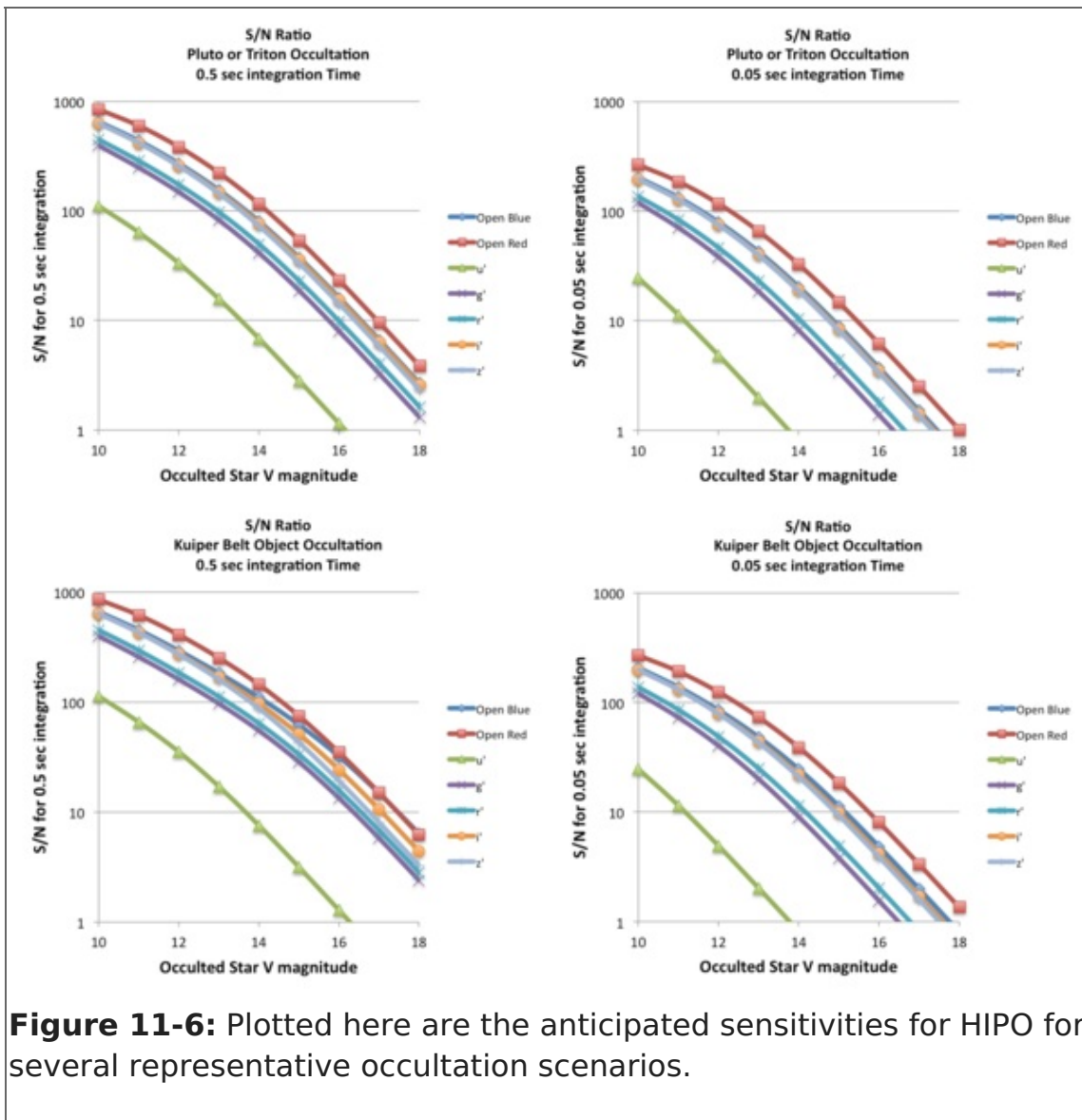
Figure 11-6: Plotted here are the anticipated sensitivities for HIPO for several representative occultation scenarios.

The deviation of S/N from a square root dependence is mostly due to shot noise on the occulting object in the upper left figure, about equally shot noise on the occulting object and read noise in the upper right figure, about equally shot noise on the sky and read noise in the lower left figure, and read noise in the lower right figure. Once the aluminized tertiary mirror is available read noise will only be significant in the lower right figure. The improved final SOFIA pointing stability will increase sensitivity for sky-limited events and improve discrimination from nearby bright objects (e.g. Neptune for a Triton occultation).

11.1.5 HIPO Sensitivity Spreadsheet

A spreadsheet exposure time and SNR estimator for HIPO is available here. This spreadsheet accounts for transmission of all optical components from the atmosphere through the telescope, and inside HIPO, ending with the quantum efficiency of the detectors. It accounts for shot noise on the target, a possible background object (important for occultation work), and sky brightness as well as read noise. The wavelength dependence of the stellar flux is simply modeled as blackbody radiation, with the effect that there are systematic errors in the predictions that vary with wavelength and spectral type. The spreadsheet has been checked against a number of spectrophotometric standard stars with calibrations traceable through Vega to blackbody sources. Observed signals of these standards with the deep depletion CCDs is typically ~10% higher than predicted but in the Johnson I and Sloan i' bands the observed signals

are ~30% higher than predicted.

THE SPREADSHEET SNR ESTIMATION DOES NOT ACCOUNT FOR SYSTEMATICS THAT DOMINATE AT HIGH SNR VALUES (~500 OR HIGHER) ON TIMESCALES OF ~10 MINUTES OR LONGER. THIS REMAINS A RESEARCH AREA! PLEASE CONTACT THE PI IF YOU HAVE QUESTIONS ALONG THESE LINES!

The spreadsheet is operated from its first tab, the Control Sheet. The next four tabs deal with optics that are common to both sides of HIPO (e.g. the atmosphere and telescope optics), optics peculiar to the blue or red sides, and the special case of the bare CCD. The last two tabs deal with blackbody and sky fluxes and the final combination of all the previous calculations that eventually appear back on the Control Sheet.

The spreadsheet is operated by filling in the yellow (most commonly used) and orange (less commonly used) cells to account for the star brightness and effective temperature, observing circumstances, CCD operations (integration time, binning, photometric aperture diameter), optics selections, and CCD choices. Results are returned in the light green cells. The main results are the signal levels from target, sky, and background object and the various noise contributions modeled by the spreadsheet. Scintillation noise is very difficult to measure and its value is not well determined yet. Finally the overall S/N ratio and fractional error are given. An estimate of the peak pixel signal in a star image is given in cells G34-H36. This is highly dependent on focus state and image jitter, and somewhat dependent on altitude so should be only used as a guide. The peak signal for the target star is also given in units of full well (assumed to be 100,000 electrons) in cells G35-H35. Note that full well is not affected by binning in a CCD47-20 since this CCD has no summing well. It is sometimes convenient to know the flux-weighted effective wavelength of a given filter/star combination. These are returned near the top center of the Control Sheet for the blue and red sides. For convenience the names of the beamsplitters, filters, and windows, or an indication if they have been removed, is given in the green cell above the selection cell for each optical element. The same applies to the CCD selection cells.

The optical elements modeled, in order, follow:

- Atmosphere: Atmospheric extinction is a combination of ozone (assumed to be 300 Dobson units) and Rayleigh scattering appropriate for 41,000 foot altitude. This matches observations quite closely. The usual sec(Z) airmass correction is applied.
- Telescope: The condition of the aluminum coatings on the telescope optics can be changed using cells J43-L43. At present the only tertiary mirror available is the dichroic tertiary and cell L43 has no effect. Cell B26 allows selection of either the dichroic tertiary or the not-yet-available aluminized one. If the aluminized tertiary is selected the aluminum coating condition in L43 does have an effect. The SOFIA coatings are maintained in excellent condition so cases 0 and 1 are the only reasonable ones to use.
- Fore optics: If the tub is to be evacuated the gate valve window must be installed. Whether this window is installed or not is modeled by selecting 1 or 0 in cell C26. The dichroic reflector used in the FLIPO configuration is controlled by cell D26. It can be left out (0), be the new Reynard dichroic (1), or the old Lick dichroic (2). The Reynard dichroic has about half the emissivity of the Lick one and similar optical performance

so is likely to be preferred in most cases.

- The dichroic beamsplitter internal to HIPO is controlled by cell E26 and can be left out (0) or be one of the two presently available ones (1 or 2). If it is left out no light reaches the blue side CCD.
- Filters for the blue, red, and bare CCD cases are controlled by cells F26-H26. There is a short explanation of what the various codes mean to the right of the cells used to select the various optics. New filters are certain to be added from time to time.
- CCD selection is made using cells F30-H30 with 0 being the original standard silicon CCDs and 1 being the newer deep depletion CCDs.The deep depletion CCDs have substantially higher QE and will be preferred in most cases in spite of their greater cosmic ray sensitivity. For UV work the thin blue CCD has better sensitivity than the deep depletion CCD.

A helpful figure showing the total signal per micron of bandwidth as a function of wavelength is shown in the upper right of the Control Sheet. It gives a graphical representation of the total signal accounting for everything from the star and sky through the CCD. The vertical axis on this graph autoscales.

An informational box related to the systematic error introduced by the blackbody approximation for stellar fluxes is given in the lower right of the control sheet. Errors at the ends of the wavelength range for very red stars can be ~50% but are 30% or less for most cases.

Another informational box at bottom center provides a crude estimate of effective temperature given either spectral class or B-V for a target object.

Finally the revision list is given at bottom left. This spreadsheet will be updated from time to time as optics or detector selections change, or as additional information becomes available. The sky brightness estimate is currently a weak area and may be changed relatively soon.

11.2 Planning HIPO Observations

HIPO is a special purpose instrument, and the material included here is suitable for getting an initial idea of its capabilities. In order to propose to use HIPO, or the combination of HIPO and FLITECAM it is necessary to consult with the Instrument Principal Investigator, Dr. E. W. Dunham. It is expected that the details of observation planning will be a central part of the discussions. HIPO (and HIPO+FLITECAM) proposals require the endorsement of the instrument PI.

Dr. E.W. Dunham
Email: dunham@lowell.edu
Phone: 928-233-3221

12. The Data Cycle System

SOFIA proposals and observation data are managed by the SOFIA Data Cycle System (DCS). The DCS is designed primarily to support Science and Mission Operations activities associated with Guest Investigator (GI) programs for the observatory. From a GI point of view, observatory data flow is cyclic in nature (see Figure 12-1). The GI first develops and submits a proposal to the SOFIA Science Mission Operations (SMO). Once

approved, the proposal becomes an observing plan that the GI uses to create and update astronomical observation requests (AORs) that are used in both flight planning and on-aircraft execution. After execution of the observations in-flight, the resulting data are archived and, for Facility Science Instruments (FSIs), automatically processed (pipelined) to produce the final data products, which are then served back to the original GI via a simple user-interface -- thus completing the cycle begun by the original proposal and perhaps driving new proposals. The data products are made available to the astronomical community for archival research purposes after an appropriate proprietary period.
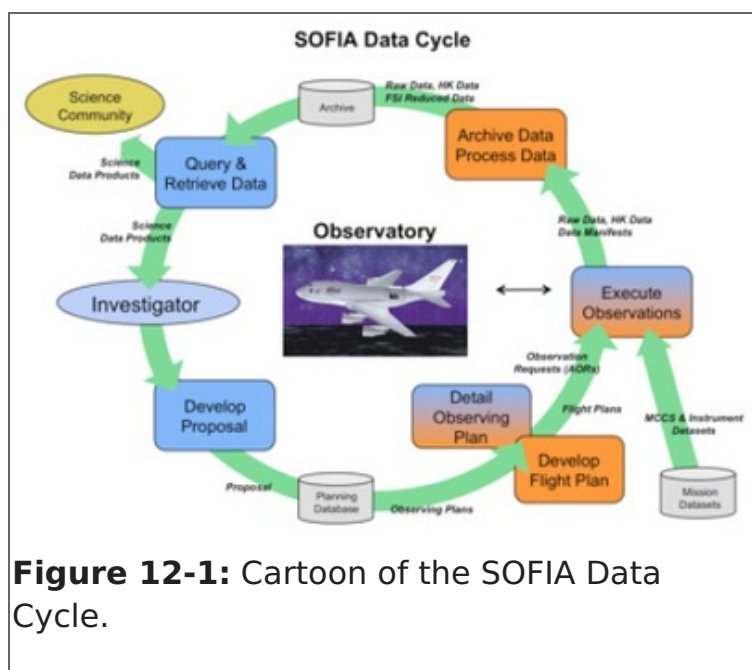

Figure 12-1: Cartoon of the SOFIA Data Cycle.

The goal of the SOFIA DCS is to maximize the scientific productivity and efficiency of the observatory by providing a suite of easy-to-use tools and infrastructure that are integrated with each other as well as other applications (e.g. Flight Management Infrastructure) at each step in the data cycle.

The DCS Archive is the permanent repository for all raw scientific and housekeeping data accumulated during SOFIA flights and any pipeline products produced thereafter (for example, pipeline reduced data for FSIs). Access to the SOFIA Data Archive is via the DCS web pages. GIs are able to retrieve their data from the archive during the proprietary period using an assigned DCS login username and password. The proprietary period for Cycle 3 will be 1-year from the date of ingestion into the DCS Archive. Once the proprietary period expires, the data becomes public and can be accessed by anyone in the general community.

In order to make use of most of the features of the DCS website, users must register by clicking on the ''Register with DCS'' link on the DCS home page. After the registration form has been submitted, the user will be notified by e-mail when the account has been created. (Users should verify that mail from ''sofia.usra.edu'' is not blocked by any spam filters.) After logging in, a registered user can change his/her profile and password at any time using the View Profile link displayed next to the login name at the top of the DCS pages.

The DCS includes a suite of software tools to archive data and to assist GIs in preparing

and submitting proposals:

- **SOFIA Proposal Tool (SPT):** SOFIA proposals are created and modified using the SPT, a stand-alone Java application available for a wide variety of platforms. The Download SPT page'' includes links to download the Java application and installation instructions for all supported platforms. Complete help files are included with the application distribution and can be accessed via the Help menu options with the SPT.
- **Time Estimators:** In order to assist in the creation of SOFIA observing proposals, the DCS web site provides an online SOFIA Instrument Time Estimator that calculates the total observation time required or signal-to-noise achieved for FLITECAM and FORCAST imaging modes. The DCS also maintains the on-line FLITECAM Grism Exposure Time Calculator and the online FORCAST Grism Exposure Time Calculator. Exposure time calculators for GREAT and EXES are also available, and links may be found on the SITE page.
- **Atmospheric Transmission Estimator (ATRAN):** To allow proposers to estimate the effects of atmospheric transmission on potential observations and exposure times with SOFIA instruments, the DCS provides access to a web-based version of the ATRAN program written by Steve Lord. For a specified observing altitude and wavelength range, the web page will run ATRAN and generate an output file and plot of the atmospheric transmission as a function of wavelength. Both the output file and plot can be downloaded to the user's desktop. A brief description of the input parameters and how to run ATRAN is given at the top of the web page.
- **Visibility Tool (VT):** The Target Visibility Tool provides the capability to estimate what date, time, and aircraft heading are required to observe an astronomical target. The tool is a Java applet that is accessible on the Visibility Tool page. Details of which operating systems and browsers are compatible with VT are provided on the Visibility Tool page. A stand-alone version of VT is available for download.
  To find the visibility of a given target, the user enters its co-ordinates (J2000 RA and DEC), the estimated latitude and longitude of the observation (which defaults to the SOFIA take-off location of Palmdale, CA), the start date and time, and the duration of interest. The application plots the target elevation for the period of interest. A target is visible to SOFIA if the elevation is in the range 20° to 60°.

  The nominal period of observations for Cycle 3 is 1 March, 2015 to 31 January, 2016. GIs should use VT to ensure that the proposed targets are in the allowed elevation range for visibility. For flights that take off from and return to Palmdale, the southernmost observable declination is -36\arcdeg. However, there will be up to two Southern Hemisphere Deployments during Cycle 3.

  Instructions on how to use VT and help on specific topics are available as part of the tool, using either the ''Help'' pull-down menu or the ''?'' button, both at the top, left of the applet window.

In addition, the DCS provides users with a variety of search options for proposals, data, and observing plans.

- **Proposal Search:** All proposals submitted via SPT are stored in the DCS observation planning database and can be accessed from the DCS web pages. Users can retrieve summary data for available proposals by using the Proposal Search page and entering the relevant search criteria for the proposal(s) of interest. Summary information will

be displayed for each proposal (appropriate to the permissions of the user).

- **Archive Search:** Summary information is available for all public data in the DCS archive. From the Science Archive Search page, MCS Archive Search page, or the Ancillary Files Search page, users can specify search criteria to identify data of interest. Summary info for resulting matches is shown in a table with appropriate links based upon user permissions. Data that are still proprietary are available only to the GIs on the associated observing plan. Hence, \textit{users must log in using a DCS username to view any proprietary data}. Proprietary data can only be seen by the program GIs and selected SMO staff members. From the Summary Information table for science data, users can click through to a list of all data products associated with a particular observation (e.g., raw or pipelined data), or identify data to be downloaded.
- **Observing Plans Search:** Once a proposal is approved, it becomes an observing plan, which can be accessed and modified as needed to support science and mission requirements by the proposal GI and selected SMO staff members. Observing plans can be accessed from the planning database using the Search Observing Plans link on the DCS web page. Summary information will be displayed for each observing plan along with links to the Observing Plan Details page. The Observing Plan Details page provides all the information available for a plan and corresponding links to the editor functions to make changes (for users with appropriate permissions).
- **Data Retrieval:** Data can be retrieved by identifying desired data in the summary table and then clicking the ''Retrieve Data'' button. In order to retrieve any data, the user must be logged in. Only GIs with appropriate permissions and SMO staff are able to retrieve data that is still within the proprietary period. Once designated for retrieval, the files are staged to a public FTP server and a direct link is e-mailed to the user. All science data products are available in their original format (e.g., FITS). The same retrieval process is used for the MCCS and Ancillary data files.

12.1 Data Rights and Availability

All scientific data from SOFIA observations will be distributed via the SOFIA Data Cycle System's Science Archive. All data will be archived as Level 1 data (raw). Where appropriate, Level 2 (corrected for instrumental and atmospheric effects) and Level 3 (flux calibrated) will also be archived. These data will be accessible to the general community after a proprietary period of twelve months, starting at the ingestion of the calibrated data into the archive.

In order to query the archive and retrieve data, it is necessary to register with the DCS. This can be done by following the appropriate link ("Register With DCS") on the main DCS page. Registration is not required for using the proposal preparation and submission tools.